FEDERAL UNIVERSITY OF SANTA CATARINA
SCHOOL OF TECHNOLOGY
GRADUATE PROGRAM IN CHEMICAL ENGINEERING

Victor de Aguiar Pedott

Hierarchical Y Zeolite Green Synthesis Using Rhamnolipid and Sophorolipid Biosurfactants as Structure Directing Agents

Florianópolis - SC
2023

Victor de Aguiar Pedott

Hierarchical Y Zeolite Green Synthesis Using Rhamnolipid and Sophorolipid Biosurfactants as Structure Directing Agents

Dissertation presented to the Graduate Program in Chemical Engineering of the Federal University of Santa Catarina to obtain the Master of Science degree in Chemical Engineering.

Supervisor: Cristiano José de Andrade, Prof. Dr

Co-supervisors: Cíntia Soares, Prof. Dr.; Natan Padoin, Prof. Dr.

Florianópolis - SC

2023

Ficha de identificação da obra elaborada pelo autor,
através do Programa de Geração Automática da Biblioteca Universitária da UFSC.

de Aguiar Pedott, Victor
Hierarchical Y zeolite green synthesis using rhamnolipid and sophorolipid biosurfactants as structure directing agents / Victor de Aguiar Pedott ; orientador, Cristiano José de Andrade, coorientadora, Cíntia Soares, coorientador, Natan Padoin, 2023.
96 p.

Dissertação (mestrado) - Universidade Federal de Santa Catarina, Centro Tecnológico, Programa de Pós-Graduação em Engenharia Química, Florianópolis, 2023.

Inclui referências.

1. Engenharia Química. 2. Green Synthesis. 3. Hierarchical Zeolite. 4. Biosurfactants. 5. Pores. I. de Andrade, Cristiano José. II. Soares, Cíntia . III. Padoin, Natan IV. Universidade Federal de Santa Catarina. Programa de Pós-Graduação em Engenharia Química. V. Título.

Victor de Aguiar Pedott

Hierarchical Y Zeolite Green Synthesis Using
Rhamnolipid and Sophorolipid Biosurfactants as Structure Directing Agents

Síntese verde de zeólita Y hierárquica de usando biossurfactantes ramnolipídicos e soforolipídicos como agentes diretores de estrutura

This Master's Dissertation will be presented before an examining board composed of the following members:

Prof.(a) Dachamir Hotza Dr.(a)
Federal University of Santa Catarina - UFSC

Prof.(a) Marcelo Luis Mignoni Dr.(a)
Integrated Regional University of Alto Uruguai and Missões - URI

We certify that this is the original and final version of the final work that was considered suitable for obtaining a master's degree in chemical engineering.

Documento assinado digitalmente
Debora de Oliveira
Data: 06/11/2023 13:12:02-0300
CPF: ***.453.929-**
Verifique as assinaturas em https://v.ufsc.br

Coordination of the Graduate Program

Documento assinado digitalmente
Cristiano Jose de Andrade
Data: 06/11/2023 13:10:27-0300
CPF: ***.875.168-**
Verifique as assinaturas em https://v.ufsc.br

Supervisor Cristiano José de Andrade Prof. Dr.

Florianópolis – SC
2023

Este trabalho é dedicado à minha namorada, Julia Michelin Barichello (*in memoriam*), por toda a importância que teve em minha vida.

AGRADECIMENTOS

Aos meus pais, Jussara, Joel, e à minha irmã Valentina, que me formaram como pessoa através de seus ensinamentos e por sempre estarem presentes nesta caminhada, apoiando-me e incentivando-me em todos os momentos.

Ao meu orientador, Prof. Dr. Cristiano José de Andrade, e aos coorientadores, Prof.ª Dr.ª Cíntia Soares e Prof. Dr. Natan Padoin, por todos os ensinamentos, momentos compartilhados e parceria na elaboração deste projeto.

A todos os meus amigos que sempre se mostraram disponíveis em todos os momentos, em especial aos meus amigos do LabMAC, com os quais compartilhei a rotina diária de trabalho durante o desenvolvimento desse projeto, rendendo ótimas discussões e trocas de conhecimento no famoso "café científico".

A todos os professores que transmitiram seus conhecimentos durante toda a minha vida acadêmica, tornando possível este momento.

À UFSC, ao Departamento de Engenharia Química e Engenharia de Alimentos e ao Programa de Pós-graduação (PósENQ), onde tive a oportunidade de iniciar a construção da minha carreira acadêmica, que se tornou de extrema importância em minha vida.

Aos membros da banca examinadora pelas contribuições.

Ao LabMAC e à Central de Análises do Departamento de Engenharia Química, pela infraestrutura para a realização do trabalho proposto, e aos técnicos Dr. Leandro Guarezi Nandi e Msc. Fernanda Volpatto, pela prestatividade.

Ao Programa de Recursos Humanos (PRH 11.1) da Agência Nacional do Petróleo, Gás Natural e Biocombustíveis (ANP) pelo suporte financeiro que me proporcionou a oportunidade de realizar este trabalho.

A todos que, de alguma forma, contribuíram e torceram por mim.

“Por vezes sentimos que aquilo que fazemos não é senão uma gota de água no mar. Mas o mar seria menor se lhe faltasse uma gota.” (Madre Teresa de Calcutá)

RESUMO

A utilização de biossurfactantes como agentes direcionadores de estrutura no processo de síntese representa um avanço significativo em direção à química verde na síntese de materiais porosos. Os biossurfactantes possuem estruturas únicas de autoagregação que podem induzir formas e organizações de poros nos materiais sintetizados. No entanto, a natureza aniônica/não-iônica dos biossurfactantes dificulta sua aplicação nesse campo. Entre os biossurfactantes comercialmente disponíveis, os ramnolipídios e soforolipídios têm recebido considerável atenção, tornando-se uma alternativa promissora aos surfactantes sintéticos utilizados atualmente. A aplicação de biossurfactantes como indutores de mesoporos foi demonstrada por meio da síntese sol-gel por via ácida, resultando em materiais que exibem isotermas do tipo I e curvas de histerese H4, indicativas da formação de mesoporos. A análise de FT-IR confirmou a presença de ligações eletrostáticas e covalentes entre biossurfactantes e moléculas de (3-Aminopropil)trietoxisilano (APTES), levando à formação dos compostos APTES-ramnolipídio e APTES-soforolipídio. Na síntese da zeólita Y com hierarquia de poros, inicialmente, a fase microporosa foi obtida e confirmada por meio da análise de difração de raios X. Posteriormente, a adição de biossurfactantes e dos compostos biossurfactantes-APTES no processo de síntese induziu a formação de mesoporos, o que não impactou significativamente a cristalinidade dos materiais. A influência dos biossurfactantes pôde ser observada no tamanho de partículas e poros, sendo o APTES fator crucial na redução do tamanho de partícula. A introdução de mesoporos foi confirmada por meio de análise de adsorção e dessorção de N_2, sendo observada a formação de histereses e comprovada pela distribuição de tamanho de poros. As áreas de superfície dos materiais hierárquicos sintetizados foram afetadas pela concentração de mesoporos, exibindo uma diminuição conforme a concentração de mesoporos aumenta. Além disso, a adição de APTES aos biossurfactantes promoveu uma maior concentração de mesoporos na faixa de 3,0 nm a 5,5 nm, enquanto os biossurfactantes puros resultaram em mesoporos mais estreitos, na faixa de 2,0 nm a 3,0 nm. Portanto, o uso de ramnolipídios e soforolipídios como agentes direcionadores de estrutura na síntese da zeólita Y com estrutura hierárquica de poros mostrou-se bem-sucedida. Essa abordagem oferece uma alternativa verde às rotas de síntese convencionais, abrindo novas possibilidades para a aplicação de biossurfactantes no campo de materiais porosos.

Palavras-chave: Biossurfactantes. Materiais hierárquicos. Zeólitas. Poros. APTES.

RESUMO EXPANDIDO

Introdução

As zeólitas são materiais de estrutura microporosa de ocorrência natural, podendo também ser sintetizadas. Desde sua descoberta, no ano de 1756, pelo mineralogista Friedrich Axel Cronstedt, 251 novas estruturas foram registradas pela Associação Internacional de Zeólitas (do inglês *International Zeolite Association* – IZA). Porém, apenas algumas são comercialmente viáveis, sendo estas aplicadas, principalmente, pela indústria de petróleo como catalisadores, adsorventes, trocadores iônicos etc. O motivo de sua aplicação são suas propriedades únicas, como alta área de superfície, estabilidade térmica, acidez e seletividade (FELICZAK-GUZIK, 2018; VERMEIREN; GILSON, 2009).

A maior limitação para aplicação de zeólitas microporosas é sua limitação no transporte de moléculas com dimensões maiores que seus poros (> 2 nm), causando, assim, a desativação do catalisador, tornando necessária sua ativação por processos de reativação, principalmente os térmicos (JIA *et al.*, 2019). Uma maneira de contornar esse problema é introduzir mesoporosidade na estrutura desses materiais, aumentando, assim, a transferência de massa pela sua estrutura porosa. Existem diferentes maneiras de atribuir mesoporosidade em estruturas zeolíticas, podendo essa ser realizada pela utilização de agentes direcionadores de estrutura durante a síntese do material, por processo pós-sintéticos ou pela combinação de ambos os processos. A utilização de agentes direcionadores de estrutura é preferível pois induz a formação de uma rede de mesoporos com maior grau de organização, tornando a transferência de massa pela estrutura mais eficiente (JIA *et al.*, 2019).

Os agentes direcionadores de estrutura (SDA, na sigla em inglês) utilizados atualmente são geralmente surfactantes, polímeros e líquidos/sólidos iônicos, normalmente de origem catiônica, que interagem com as espécies de silício e alumínio para induzir a formação de diferentes estruturas zeolíticas. Entretanto, os surfactantes comumente utilizados apresentam algumas limitações em seu uso, como alto custo, toxicidade, dificuldade de obtenção e descarte, podendo causar problemas ambientais (EJKA; MORRIS; NACHTIGALL, 2017). Nesse sentido, uma alternativa sustentável é através do uso de biossurfactantes, considerado um avanço importante em direção à química verde de materiais porosos, além de aplicar as estruturas de autoagregação únicas induzidas por eles, o que pode promover formas e organizações únicas de poros nos materiais sintetizados. O principal desafio na aplicação de biossurfactantes é a sua natureza aniônica/não-iônica, que dificulta a interação direta com as

espécies de sílica (VARJANI; UPASANI, 2017). Para melhorar a interação dos biossurfactantes na síntese de materiais porosos, é necessário o desenvolvimento de rotas e mecanismos de interação inovadores, visando adaptar parâmetros de síntese e utilizar ligantes orgânicos, que se mostram alternativas promissoras.

Ramnolipídeos e soforolipídeos são biossurfactantes glicolipídicos comercialmente disponíveis. Extensas pesquisas têm sido desenvolvidas em relação à caracterização das estruturas moleculares e de autoagregação, tornando-se uma alternativa promissora para substituir surfactantes sintéticos na síntese de materiais porosos. Portanto, a investigação de novas rotas de síntese e melhor interação entre biossurfactantes e as espécies inorgânicas na síntese de zeólitas com estrutura hierárquica de poros é essencial para a aplicação dessas moléculas neste campo, possibilitando a síntese "verde" destes materiais.

Objetivo

Desenvolver uma nova rota de síntese para a obtenção de zeólitas com estruturas hierárquicas de poros utilizando os biossurfactantes soforolipídeo e ramnolipídeo como agentes direcionadores de estrutura.

Objetivos específicos

- ✓ Investigar as interações dos biossurfactantes puros e funcionalizados com as espécies inorgânicas de silício, para a síntese de sílicas mesoporosas.
- ✓ Avaliar a melhor composição de SiO_2, Al_2O_3, Na_2O e H_2O para a formação da estrutura da zeólita Y.
- ✓ Empregar a abordagem "*bottom-up*" para a síntese da zeólitas Y com hierarquia de poros.
- ✓ Identificar a influência dos biossurfactantes na síntese da zeólita Y com hierarquia de poros.

Metodologia

Como primeiro passo para a síntese da zeólita com estrutura hierárquica de poros, a interação dos biossurfactantes com as espécies de silício foi realizada através da síntese de sílicas mesoporosas. Para tanto, fez-se uso dos biossurfactantes como direcionadores de fase mesoporosa por meio da técnica sol-gel utilizando hidrólise ácida do precursor de silício. Em seguida, a zeólita Y foi obtida sem a utilização de biossurfactantes, sendo a melhor composição molar entre os reagentes e o tempo de síntese avaliados.

Com o objetivo de melhorar a interação entre os biossurfactantes e as espécies de silício, a molécula de 3-aminopropil)trietoxisilano foi acoplada aos diferentes surfactantes e sua ligação caracterizada por FT-IR. Após a obtenção das fases microporosa (0 a 2 nm) e mesoporosa (2 a 50 nm), os testes de síntese das zeólitas Y com hierarquia de poros foram realizados. Utilizou-se o gel de composição molar $4SiO_2$:$1Al_2O_3$:$10.6Na_2O$:$220H_2O$, introduziu-se os biossurfactantes e suas combinações com APTES durante o processo de formação do gel, sendo este submetido a cristalização em autoclave a 100 °C por 24 h. Os materiais obtidos foram caracterizados por meio das técnicas de Difração de Raios X (DRX), Microscopia Eletrônica de Varredura (MEV), Microscopia Eletrônica de Transmissão (MET) e adsorção/dessorção de N_2.

Resultados

A aplicação de biossurfactantes como indutores de mesoporos foi comprovada por meio da síntese sol-gel por via ácida, resultando em materiais com isotermas do tipo I e laços de histerese H4, indicando a formação de mesoporos. Em relação à síntese de compostos de biossurfactante-APTES, a análise de FT-IR confirmou a presença de ligações eletrostáticas e covalentes entre os biossurfactantes de ramnolipídio e soforolipídio e a molécula de APTES, levando à formação dos compostos APTES-ramnolipídio e APTES-soforolipídio.

Como primeiro passo na síntese de zeólita Y hierárquica, a fase microporosa foi obtida sem a adição de agentes direcionadores de estrutura no processo de síntese, sendo a formação da estrutura confirmada pela análise de DRX utilizando o padrão da zeólita Y (código #416357) do *Inorganic Crystal Structure Database* (ICSD) como parâmetro estrutural. Após a obtenção da estrutura microporosa, os biossurfactantes puros e sua combinação com moléculas de APTES foram adicionados ao processo de síntese, atuando como indutores de mesoporos. O uso de biossurfactantes não demonstra uma influência significativa na cristalinidade dos materiais. A cristalinidade do material HYZ-R não foi afetada pela adição do biossurfactante de ramnolipídio, enquanto para os outros materiais sintetizados observou-se uma leve diminuição na cristalinidade. Uma influência significativa dos biossurfactantes nos materiais sintetizados finais pôde ser observada por meio de imagens de MEV, onde as partículas dos materiais foram afetadas, resultando em uma diminuição em seu tamanho, sendo a adição de APTES às moléculas de biossurfactante um fator crucial na diminuição do tamanho das partículas dos materiais. Em relação às propriedades texturais dos materiais hierárquicos sintetizados, a introdução de mesoporos na estrutura dos materiais foi confirmada por meio da

análise de adsorção e dessorção de N_2, pela formação de laços de histerese e pela Distribuição de Tamanho de Partícula (PSD) dos materiais hierárquicos. As áreas específicas de superfície dos materiais hierárquicos foram afetadas pela introdução de mesoporos, sendo que, para as concentrações mais altas de mesoporos, maior foi a diminuição na área específica de superfície. A introdução de APTES às moléculas de biossurfactante contribuiu para um aumento na formação de mesoporos na faixa de 3,0 nm a 5,5 nm. Quando foram utilizados biossurfactantes puros, a maior concentração de mesoporos pôde ser observada na faixa estreita de mesoporos, entre 2,0 nm e 3,0 nm.

Portanto, o uso de ramnolipídeos e soforolipídios como agentes direcionadores de estrutura na síntese de zeólita Y hierárquica foi comprovado. Ambos os biossurfactantes demonstraram a propriedade em induzir à formação de mesoporos, tornando-se uma alternativa "verde" às rotas clássicas de síntese de zeólitas hierárquicas, ou seja, um novo campo de aplicação para os ramnolipídeos e soforolipídios.

Considerações finais

Os resultados obtidos fornecem bases teórico/práticas para o desenvolvimento de novos materiais através da utilização de biossurfactantes. Isso influencia positivamente novas pesquisas sobre o assunto, além de potencializar a aplicação de biossurfactantes em uma nova área.

Palavras-chave: Biossurfactantes, Materiais, Zeólitas, Zeólitas Hierárquicas.

ABSTRACT

The utilization of biosurfactants as Structure Directing Agents (SDAs) in the synthesis process represents a significant advancement toward green chemistry in porous materials. Biosurfactants possess unique self-aggregation structures that can induce diverse porous shapes and organizations in synthesized materials. However, the biosurfactants anionic/nonionic nature hinders their application in this field. Among commercially available glycolipid biosurfactants, rhamnolipids and sophorolipids have gained considerable attention, becoming a promising alternative to synthetic surfactants in porous materials synthesis. The application of biosurfactants as mesopore inducers has been demonstrated through acid sol-gel synthesis, resulting in materials exhibiting type I isotherms and H4 hysteresis loops, indicative of mesopore formation. Fourier transform infrared (FT-IR) analysis confirmed the presence of electrostatic and covalent bonds between biosurfactants (rhamnolipids and sophorolipids) and (3-Aminopropyl)triethoxysilane (APTES) molecules, leading to the formation of APTES-rhamnolipid and APTES-sophorolipid compounds. In the synthesis of hierarchical Y zeolite materials, initially the microporous phase was obtained and verified through XRD analysis. Subsequently, the addition of biosurfactants and biosurfactants-APTES compounds in the synthesis process induced mesopore formation, which did not significantly impact the crystallinity of the materials. The biosurfactants influence could be observed on particle and pore sizes, with the incorporation of APTES playing a crucial role in reducing the material particle size. The introduction of mesopores was confirmed through N_2 adsorption and desorption analysis, by hysteresis loop formation, and pore size distribution. The specific surface areas of the synthesized hierarchical materials were affected by the mesopore concentration, exhibiting a decrease with higher mesopore concentrations. Furthermore, the addition of APTES to biosurfactants promoted a higher concentration of mesopores in the range of 3.0 to 5.5 nm, while pure biosurfactants resulted in narrower mesopores in the range of 2.0 to 3.0 nm. In conclusion, the use of rhamnolipids and sophorolipids as structure-directing agents in the synthesis of hierarchical Y zeolite has proven successful in inducing mesopore formation. This approach offers a green alternative to conventional synthesis routes, opening new possibilities for the application of biosurfactants in the field of porous materials.

Keywords: Biosurfactants. Hierarchical materials. Zeolites. Pores. APTES.

FIGURES LIST

TABLES LIST

LIST OF ABBREVIATIONS

APS	Amino Pure Silica
APTES	(3-Aminopropyl)triethoxysilane
CMC	Critical Micelle Concentration
CTAB	Cetyl-Trimethyl Ammonium Bromide
FT-IR	Fourier-transform infrared spectroscopy
ICSD	Inorganic Crystallography Structure Database
IZA	International Zeolite Association
PS	Pure Silica
PSD	Porous Size Distribution
RA-HYZ	Rhamnolipid-APTES – Hierarchical Y Zeolite
R-HYZ	Rhamnolipid – Hierarchical Y Zeolite
R-MS	Mesoporous Silica Rhamnolipid
SA-HYZ	Sophorolipid-APTES -Hierarchical Y Zeolite
SDA	Structure Directing Agent
SEM	Scanning Electron Microscopy
S-HYZ	Sophorolipid – Hierarchical Y Zeolite
S-MS	Mesoporous Silica Sophorolipid
TEM	Transmission Electron Microscopy
TEOS	Tetraethyl orthosilicate
XRD	X-Ray Diffraction

TABLE OF CONTENTS

CHAPTER I

This chapter presents a brief introduction to the research developed and its general and specific objectives.

1 INTRODUCTION

Zeolites are formed by aluminum and silicon atoms, which can organize themselves in different structural conformations, attributing unique chemical and physical properties to these materials, which direct their application. High acidity, specific area, thermal stability, selectivity, and ion exchangeability are the main properties of zeolites, being these properties adjusted by modifying the reagents ratios and structure organization (FELICZAK-GUZIK, 2018; VERMEIREN; GILSON, 2009). Usually, zeolites present a microporous structure, which limits their application, mainly in mass transport, causing surface accumulation of molecules with dimensions greater than 2 nm (JIA *et al.*, 2019).

To maintain the properties of zeolites and improve mass transport, zeolites with hierarchical pore structure are a promising alternative, since the introduction of mesoporous or macroporous to its structure reduces diffusional limitations and keeps its initial properties (CHEN *et al.*, 2012). The use of Structure Directing Agents (SDAs) is a crucial factor in the synthesis of hierarchical materials, inducing the formation of an enhanced structure by controlling SDA type and/or concentration (MOLINER; MARTÍNEZ; CORMA, 2015). SDAs are surfactants composed of polar and non-polar moieties, forming different types of self-aggregation structures (e.g. micelles) in solution, where these structures interact with the inorganic species of silicon and aluminum in the zeolite synthesis process, leading to a porous structure based on the self-aggregation form shape, which can induce the formation of the microporous or mesoporous phases (SACHSE; GARCÍA-MARTÍNEZ, 2017).

Usually, the SDAs used to induce the formation of microporous (0 to 2 nm) and mesoporous (2 to 50 nm) materials have a synthetic nature, characterized as surfactants, polymers, and ionic liquids/solids. Several SDAs have already proven their efficiency in obtaining microporous and hierarchical zeolite structures, allowing fine control of structure formation and pore sizes (EJKA; MORRIS; NACHTIGALL, 2017). However, commonly used SDAs have some limitations on their application as high cost, toxicity, isolation complexity, and difficulties with proper disposal, being a step back towards “green chemistry” (JIA *et al.*,

2019). Thus, biosurfactants are an alternative to commonly used SDAs, presenting both hydrophilic and hydrophobic moieties which induce the formation of unique self-aggregation structures, in addition to their green properties as renewable sources, environmental compatibility, nontoxicity, and biodegradability in water and soil (MONTONERI *et al.*, 2009; VARJANI; UPASANI, 2017).

The research related to biosurfactants and silica-based materials, such as porous silicas and zeolites, is still poorly investigated, since just a few research articles have been published. In order to illustrate the bibliometric data on the synthesis and modification of silica-based materials using biosurfactants, a Scopus database search has been made, and the result is shown in Figure 1.

Figure 1 – Occurrence of scientific publications regarding zeolites, silica and biosurfactants (Scopus database)

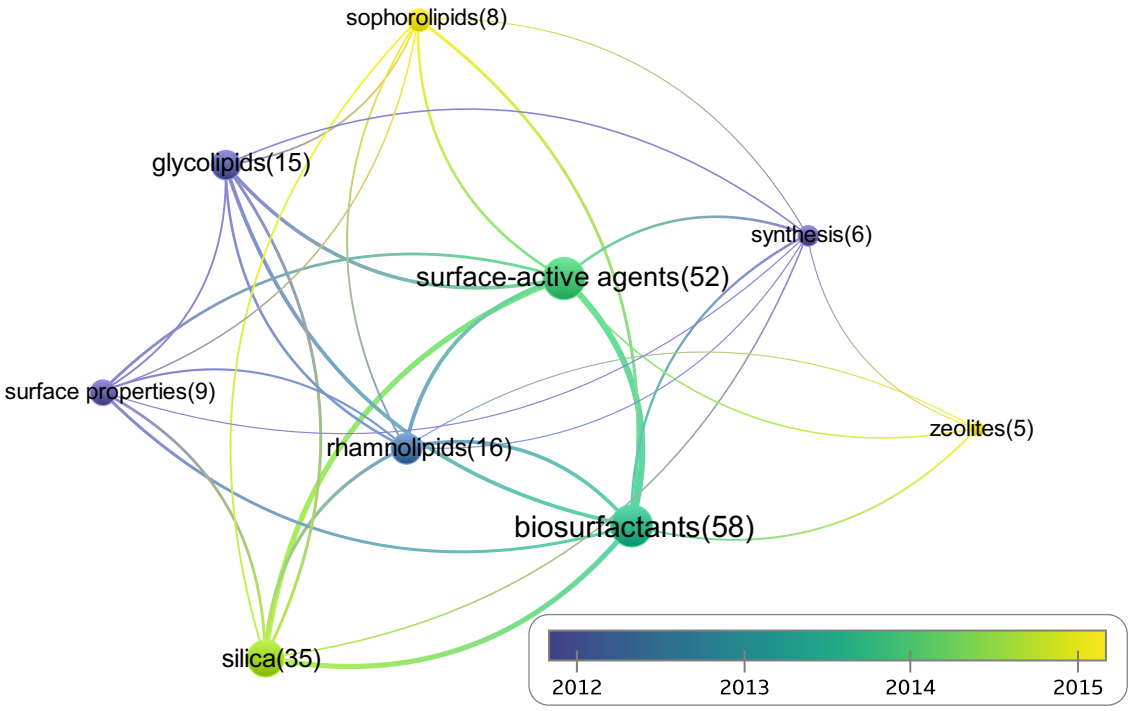

Source: elaborated by the author using VOSviewer software (2023)

From the data shown in Figure 1, it is possible to notice that the research involving biosurfactants on silica-based materials started in 2012. Since then, just 76 articles have been published, using zeolites, silica, and biosurfactants as keywords. When biosurfactants are involved in materials synthesis, rhamnolipids, and sophorolipids are the most used, when

comparing pure silica and zeolites. To date, pure silica materials have been the most explored field of application.

The main challenge in biosurfactants application as SDAs in microporous and hierarchical zeolite synthesis is their anionic/nonionic nature, which hinders their direct interaction with silica species. For better utilization of biosurfactants in materials synthesis, novel synthesis routes are necessary, aiming to improve the interaction between biosurfactants and inorganic species, allowing their organization in the solution and inducing the formation of ordered crystalline materials. Biosurfactant interactions could be improved by tailoring their structure or utilizing organic linkers that will behave as a bridge between the biosurfactant and the inorganic species.

Therefore, the investigation of new synthesis routes and better interaction between biosurfactants and inorganic species in microporous and hierarchical zeolite synthesis is essential to understand the novel application of these molecules in the material field, giving a step forward to the "green chemistry."

1.1 OBJECTIVES

1.1.1 General Objective

Develop novel synthesis routes for the synthesis of hierarchical pore structure zeolites using sophorolipid and rhamnolipid biosurfactants as structure-directing agents.

1.1.2 Specific Objectives

- ✓ Investigate silica interactions with pure biosurfactants and functionalized biosurfactants in the synthesis of mesoporous silicas.
- ✓ Evaluate the best molar ratios of SiO_2, Al_2O_3, Na_2O, and H_2O for the formation of Y zeolite structures.
- ✓ Utilize the bottom-up approach in the synthesis of hierarchical Y zeolite.
- ✓ Identify the influence of biosurfactants in the synthesis of hierarchical Y zeolite.

1.1.3 Conceptual diagram

What?
✓ Develop hierarchical zeolites through bottom-up strategy using biosurfactants as structure directing agents, which improve mass transport through the material porous structures, aiming it application in oils industry
Why?
✓ Zeolites are widely used in the petroleum industry. ✓ The search for materials with improved properties for application in different fields has been growing with technological advances. ✓ High research potential in the production and application of biosurfactants. ✓ Unique biosurfactants self-aggregation structures could lead to new zeolite materials. ✓ The substitution of synthetic surfactants by biosurfactants in hierarchical zeolite synthesis is a step forward to greener materials. ✓ There is little scientific data on the application of biosurfactants as structure-directing agents in conventional and hierarchical zeolites synthesis.
State of art
✓ Hierarchical zeolites could be synthesized though bottom-up and top-down techniques, where bottom-up strategies lead to higher degree of interconnected pores. ✓ Rhamnolipids and sophorolipids are commercially available biosurfactants, being constantly investigated by the research field. ✓ The anionic/non-ionic nature of biosurfactants hinders their interaction with silica species. ✓ Improvements in the interaction of biosurfactants with silica species were accomplished by controlling the pH and through biosurfactants functionalization with amine functional groups. ✓ Some biosurfactants have already been used to induce the formation of mesoporous in amorphous silicas.
Hypothesis
✓ The interaction of biosurfactants with silica species could be improved in acid media? ✓ Biosurfactants functionalization with APTES molecule will improve mesopore formation? ✓ Rhamnolipids and sophorolipids could be used as structure directing agents in the synthesis of hierarchical zeolites?
Phases
✓ Synthesize mesoporous silicas using rhamnolipids and sophorolipids biosurfactants as mesopore inducers. ✓ Functionalize rhamnolipids and sophorolipids with APTES molecule. ✓ Synthesize conventional Y zeolite without the use of biosurfactants.

✓ Induce the formation of mesopores on conventional Y zeolite using rhamnolipids, sophorolipids and their combination with APTES molecules as structure directing agents.
Expected results
✓ Obtain mesoporous silicas using the sol-gel method in acid environment. ✓ Confirm the formation of biosurfactant-APTES compound. ✓ Synthesize Y zeolite microporous phase without the use of biosurfactants. ✓ Obtain hierarchical Y zeolite using rhamnolipids and sophorolipids as structure directing agents.

1.1.4 Dissertation outline

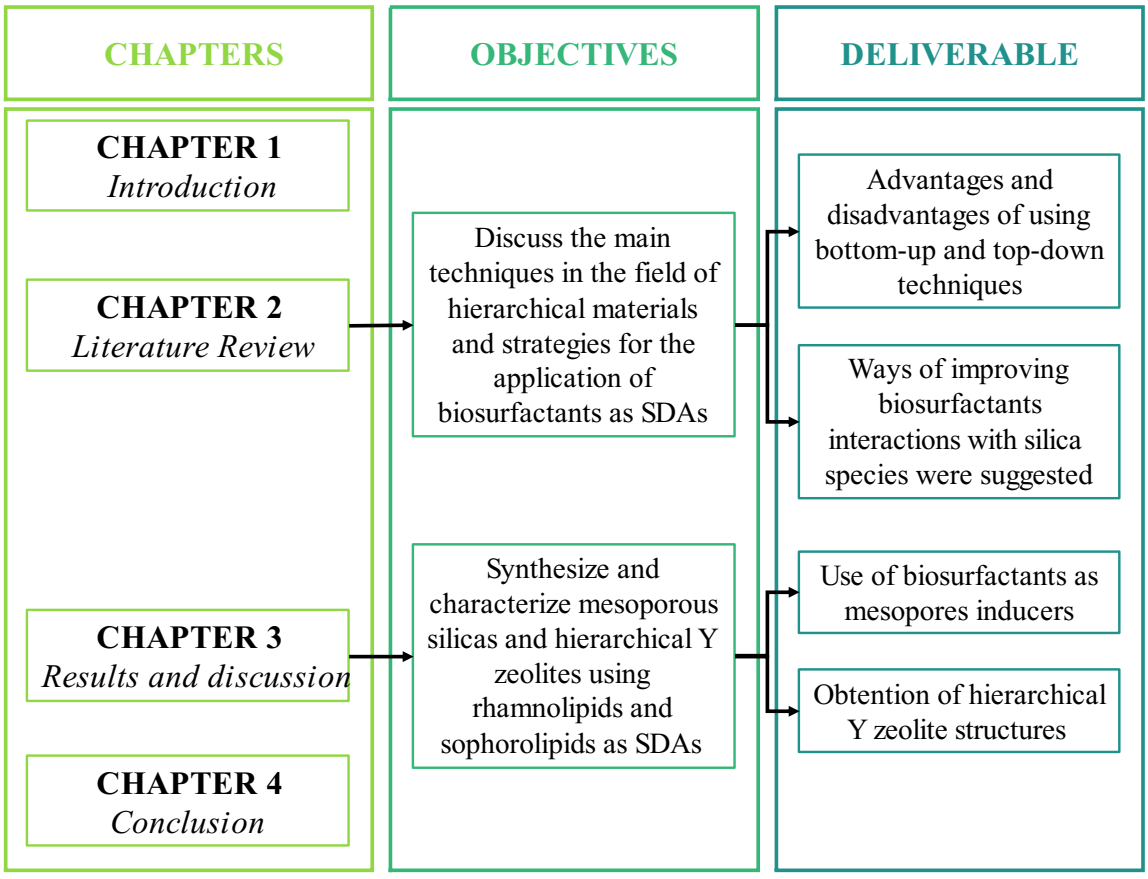

CHAPTER II – BIOSURFACTANTS AS STRUCTURE DIRECTING AGENTS OF POROUS SILICEOUS MATERIALS

In this section, a literature review was carried out, along with the publication of a review article, "Biosurfactants as Structure Directing Agents of Porous Siliceous Materials," which aims to discuss about the current pathways in the application of biosurfactants in materials synthesis and argue about different techniques used to achieve materials with different porosity levels, and the possible application of biosurfactants as structure directing agents in the porous silicious materials synthesis. This review article is linked to the journal "Microporous and Mesoporous Materials," published in October 2022 (doi: https://doi.org/10.1016/j.micromeso.2022.112279).

2 INTRODUCTION

Considering the discovery of zeolites catalytic properties in the oil industry by Union Carbide® and Mobil® companies (1963), the research on novel zeolitic structures and materials with improved properties has been investigated worldwide. Since then, 251 different zeolite structures have been registered by the International Zeolites Association (IZA). However, only a few are commercially available, playing a crucial role in petroleum refining, acting as catalysts, adsorbents, and ion exchangers, being essential to ensure high efficiency in the production process. Zeolite structures are formed by aluminum and silicon atoms, which can organize themselves in different structural conformations, attributing unique chemical and physical properties to these materials, which direct their application. High acidity, specific area, thermal stability, selectivity, and ion exchangeability are the main properties of zeolites, being these properties adjusted by modifying the reagents ratios and structure organization (FELICZAK-GUZIK, 2018; VERMEIREN; GILSON, 2009).

In order to maintain the properties of zeolites and improve the mass transport through the material structure, zeolites with hierarchical pore structure are a promising alternative, since the introduction of mesoporosity or macroporosity to its structure reduces diffusional limitations and keeps its initial properties (CHEN et al., 2012). Two approaches can be used to induce hierarchical pore structures formation: top-down or bottom-up. The first one is related to post-synthetic material treatment, and the second is related to the modification of synthesis parameters to induce the formation of microporous and mesoporous simultaneously, which is

normally induce by the use of surfactants as SDAs, being the bottom-up approach advantageous in terms of interconnected pore systems, where the different porous phases (microporous and mesoporous) organized itself in an ordered way (JIA et al., 2019; ZHU et al., 2014).

Several SDAs have already proven their efficiency in obtaining microporous and hierarchical zeolite structures, allowing fine control of structure formation and pore sizes (EJKA; MORRIS; NACHTIGALL, 2017). However, commonly used SDAs have some limitations on their application as high cost, toxicity, isolation complexity, and difficulties with proper disposal, being a step back towards "green chemistry" (JIA et al., 2019). In this sense, biosurfactants have properties, such as significant surface tension reduction, high thermal and pH stability and chemical resistance to high salt concentration. Thus, biosurfactants are a promising alternative as new SDAs in the synthesis of zeolites and mesoporous materials. The advantages of using biosurfactants as SDAs are their properties analogous to synthetic surfactants, and their main feature: biodegradability in water and soil, which can be metabolized by microorganisms for energy production (ZANOTTO *et al.*, 2019).

Therefore, the aim of this review was to critically discuss the current state of the art and future trends on the synthesis of siliceous porous materials, in particular the replacement of SDA by biosurfactants.

2.1 ZEOLITES

Zeolites are naturally occurring materials, mostly formed by volcanic and sedimentary rocks, such as chabazite, clinoptilolite, and mordenite (WANG *et al.*, 2009). Therefore, their unique structure was only reported in 1756 by the Swedish mineralogist Friedrich Axel Cronstedt. Since then, numerous natural zeolites have been discovered, and new zeolite structures have been achieved through synthetic methods, using different sources of silica and alumina (EJKA; MORRIS; NACHTIGALL, 2017; ISMAIL *et al.*, 2006; WANG *et al.*, 2009).

This class of materials is constituted by hydrated aluminosilicates as primary building blocks, made from silicon (Si^{4+}) and aluminum (Al^{3+}) as central atoms, linked by oxygen atoms (O^{2-}), which lead to tetrahedral structures (CORMA, 2003). The secondary zeolite building blocks are classified as an arrangement of zeolite primary building blocks whereby bridging through oxygen-oxygen atoms, forming rings, prisms, hexagons, and other arrangements. Each of the oxygen ions found in the zeolite structure is connected with two cations that are shared between two tetrahedron arrangements, resulting in tetravalent Si and trivalent negatively

charged Al (MEYNEN; COOL; VANSANT, 2009). The negative charge and the pores of zeolites can be occupied by group I A or II A metal ions and water molecules as it is denoted via the general equation.

$$M_{x/n}\ \{(Al_2O)_x\ (SiO_2)_y.zH_2O\} \quad (1)$$

Where M represents an alkali or alkaline earth cation, n represents the valence of the cation, z is the number of water molecules per unit cell, and x and y are the total numbers of tetrahedral per a unit cell. Figure 2 shows the tetrahedral zeolite structures, which will induce different zeolite structures.

Figure 2 – Zeolite tetrahedral structure

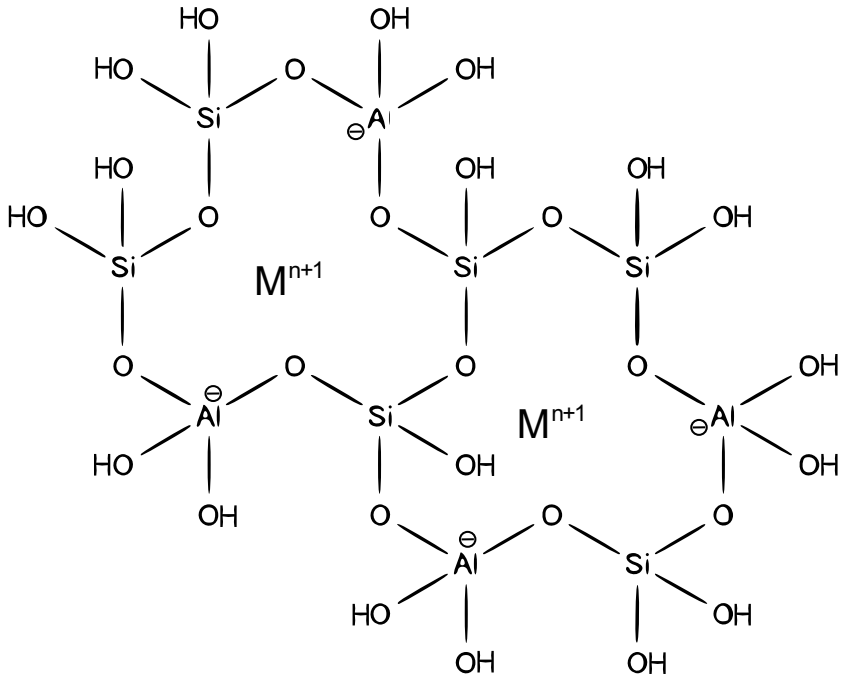

Source: elaborated by the author (2023)

In general, zeolites present a microporous structure with high surface area, ion exchange capacity and Bronsted/Lewis acid sites which allow their application in different fields acting as catalysts, adsorbents or ions exchangers.

2.2 HIERARCHICAL ZEOLITES

Limitations in the diffusional transport of zeolites could cause problems for it application, where their microporous structure fail to affect molecules with dimensions greater than zeolite pore sizes, reducing transport efficiency due to the long diffusion paths and negatively influencing catalytic rates (LI; VALLA; GARCIA-MARTINEZ, 2014). To overcome such problems, zeolite synthesis with hierarchical pore structures is a promising alternative, maintaining the original zeolite acidity, selectivity, and thermal stability (CHRISTENSEN *et al.*, 2007). The zeolite structure is fundamental for its application since it affects the mass transfer into or from zeolites (CHEN *et al.*, 2012).

The synthesis of zeolites with hierarchical pore structure provides advantages such as reduction in steric limitations of bulky molecules, increase in the rate of intra-crystalline diffusion, decrease in coke deactivation, increase in catalyst efficiency, and selectivity towards target products (HARTMANN; MACHOKE; SCHWIEGER, 2016; SUN; XIE; YU, 2018; VERBOEKEND; MITCHELL; PÉREZ-RAMÍREZ, 2013).

To achieve zeolites with hierarchical pore structures, different approaches could be used, being classified as top-down and bottom-up, where the top-down strategy is related to the post-synthetic treatment of the zeolite, whereas the bottom-up consists of the modification of synthesis parameters during the structure formation.

2.2.1 Top-down approach

The top-down approach is an easier way to achieve hierarchical structures, being the pioneer way of micro-mesoporous zeolites, consisting of a post-synthetic procedure, in which fractions of the zeolitic crystals are removed through destructive and extractive processes. The partial destruction of the zeolite structure could be carried out by well-known acid/basic or thermal treatments. The principal procedures in post-synthetic treatments can be classified as the removal of framework atoms, delamination (layered zeolites), and dissolution/recrystallization. Figure 3 shows the main top-down techniques applied to mesoporous in zeolites.

Figure 3 – Top-down techniques

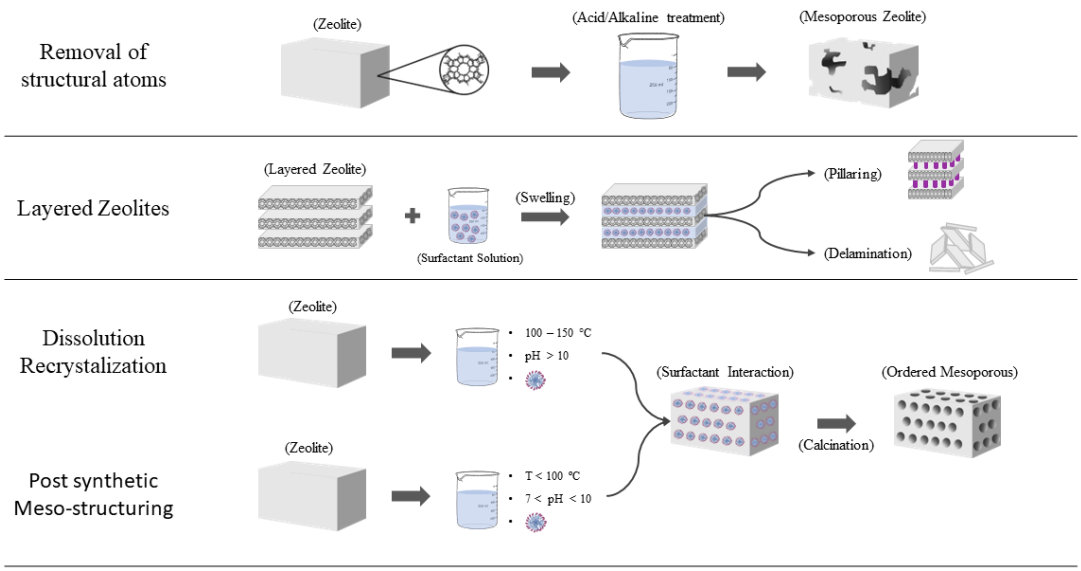

Source: elaborated by the author (2023)

2.2.1.1 Removal of framework atoms

Generally, zeolites are composed of Si, Al, and O, therefore, other atoms could be introduced into their structure. The removal of framework atoms from the zeolitic structure induces the formation of non-ordered meso/macroporous systems (JIA *et al.*, 2019). Chemical treatments using alkali, acid, H_2O_2 environments, or physical procedures such as hydrothermal treatment and radiation directly interact with framework atoms removing them from the zeolite structure. Normally, Si and Al form the major zeolitic structures, thus, desilication and dealumination processes are the most used procedures to attribute mesoporosity in zeolites (FELICZAK-GUZIK, 2018).

The desilication procedure create meso or macroporosity in zeolites maintaining their acidic properties created by the charge mismatch between Si and Al atoms (CORMA *et al.*, 1999). The silicon is removed by treatments with low concentration alkaline solutions at high temperatures, generating interconnected pore channels with tunable size and volume (EJKA; MORRIS; NACHTIGALL, 2017). The Si/Al ratio influences the desilication, affecting the pore size of the mesoporous phase (GROEN; PEFFER; PÉREZ-RAMÍREZ, 2003). For a lower Si/Al ratio (< 20), mesopores with small pore sizes (60 – 70 Å) are obtained, due to the high Al content, which prevents the removal of Si atoms from the zeolite structure. For Si/Al ration between 20 and 50, silicon is extracted in a controlled manner, leading to a mesoporous phase

with medium pore sizes (90 – 100 Å). For a higher Si/Al ratio (> 50), larger pore sizes are generated (200 – 500 Å) (EJKA; MORRIS; NACHTIGALL, 2017; FELICZAK-GUZIK, 2018).

The desilication process decreases the micropore phase surface, which is undesirable due to the presence of active acid sites in micropores, in this way, the desilication process should allow the formation of the mesoporous phase and minimize the loss in microporous surface area (ABELLÓ; BONILLA; PÉREZ-RAMÍREZ, 2009).

In the dealumination process, the removal of Al atoms normally occurs through acid treatments at high temperatures, which generates vacancies in the zeolite structure to which mesoporosity is attributed (SULIKOWSKI, 1993). However, the extraction of Al atoms changes the Si/Al ratio, decreasing the acid properties of zeolites (VAN OERS *et al.*, 2009). Generally, zeolites present more silica atoms than alumina, therefore, the dealumination process cannot be applied. However, in aluminum-rich zeolites, the removal of atoms does not change the acid properties, as example, the dealumination of zeolite Y forms a more stable material (USY zeolite) which is already used in industry in the fluid cracking catalyst (GARCÍA-MARTÍNEZ *et al.*, 2012).

2.2.1.2 Layered Zeolites

Some zeolitic structures have their lamellar structure form such as UTL, AFO, MWW, HEU, OKO, SOD, MFI, CDO, NSI, RRO, RWR, MTF, CAS, and PCR (ROTH *et al.*, 2016). It is possible to modify layered zeolites through intercalation or pillaring processes, generating mesoporosity between zeolite layers.(SELVAM; INAYAT; SCHWIEGER, 2014; XU *et al.*, 2009).

The pillaring process consists of two steps; (1) the expansion of the interlayer space; (2) the pillar formation between the expanded sheets using inorganic materials, as silica source, forming SiO_2 networks (CHOI *et al.*, 2008; GIL *et al.*, 2014; ROTH *et al.*, 1995). In the delamination process, the original form of the layered material is destabilized by intercalation of surfactants under alkaline conditions, separating the material sheets, and then, reorganizing the sheets in a way that the spaces between the sheets are in the mesoporous range (CORMA *et al.*, 1999; ROTH *et al.*, 2015). However, the delamination process can decrease crystallinity and porosity due to the high alkaline conditions.

2.2.1.3 Dissolution/Recrystallization

This technique is related to both top-down and bottom-up techniques, where the material is first submitted to a destructive alkaline treatment, followed by a recrystallization step (EJKA; MORRIS; NACHTIGALL, 2017). The steps to attribute mesoporosity through this technique are the partial solubilization of the zeolite crystal, using surfactants under mild alkaline conditions, followed by the formation of the mesophase by the surfactants under hydrothermal conditions (100 - 150 °C) using the dissolved zeolite crystals as building blocks, where the surfactant protects the zeolites from total dissolution, however, for zeolites with low Si/Al ratios i.e. high Al concentration, severe basic conditions hinder the hierarchical structure formation (SACHSE; GARCÍA-MARTÍNEZ, 2017). As an example, Ivanova et al (IVANOVA *et al.*, 2014) synthesized RZEO-1, -2, and -3 materials, using cetyltrimethylammonium (CTAB) as SDA, where initially the zeolite was exposed to a solution of NaOH, inducing a fast ion exchange between Na^{2+} with zeolite protons and breaks of silicon-oxygen bonds, leading to desilication. Secondly, the surfactant diffuses to the intracrystalline spaces, forming micelles inside the cavities, leading to the condensation of inorganic species dissolved from the zeolite framework, leading to the mesophase formation.

The Dissolution/Recrystallization process depends can lead to three different materials: (I) Zeolite coated with mesoporous silica; (II) A material consisting of co-crystallized zeolite and mesoporous material phase, and (III) Mesoporous material with zeolite fragments in the walls (IVANOVA; KNYAZEVA, 2013).

2.2.1.4 Post-synthetic meso-structuring

The post-synthetic strategy leads to an intracrystalline mesoporous phase in a wide range of zeolites (FAU, MFI, CHA, *BEA, MOR, among others) (SACHSE; GARCÍA-MARTÍNEZ, 2017). This process consists of the application of mild conditions, leading to the formation of the mesophase within the zeolite crystals, maintaining the original zeolite crystal morphology, through a short-scale rearrangement of the zeolite framework, that does not involve the dissolution of the zeolite species (CHAL *et al.*, 2010). The mild alkalinity breaks Si-O-Si bonds forming $Si\text{-}O^-$ species that interact with the positively charged surfactants, forming micelles in the materials voids, rearranging the zeolite framework, maintaining the

Si/Al ration constant due to desilication and dealumination does not occur in this process (GARCÍA-MARTÍNEZ *et al.*, 2012; PRASOMSRI *et al.*, 2015).

The surfactant structural properties influence the hierarchical pore structure formation. Surfactants with increasing aliphatic chain lengths, increases the pore diameters in almost a linear way, as observed by argon physisorption experiments (LI; VALLA; GARCIA-MARTINEZ, 2014). The employment of small tetraalkylammonium cations (such as tetrapropylammonium hydroxide) preserve the zeolite crystallinity, preventing the zeolite desilication (HOLM; HANSEN; CHRISTENSEN, 2009).

2.2.2 Bottom-up approach

In the bottom-up approach, both microporous and mesoporous phases are formed during the synthesis, being an *in-situ* process. The microporous and mesoporous phase are induced by different approaches, involving solids, surfactants, and polymers as templates, along with another strategy, approaching zeolite crystal growth rate.

2.2.2.1 Hard template

Hard templates are solid materials that are inserted into the material synthesis process, which occurs inside the material pore system or on its surface, being the hard template removed when the synthesis is completed, generating an additional pore system for the obtained material (HOLLAND; ABRAMS; STEIN, 1999). Carbonaceous, polymeric, and inorganic materials are commonly used as hard templates, which should be stable at the synthesis temperature, have surface properties that match with chemical properties of the synthesis mixture and the synthesized material inside it should be stable after the template removal. (CHAIKITTISILP *et al.*, 2013; DUTTA; BHAUMIK; WU, 2014; SCHWANKE; PERGHER, 2020; ZHU *et al.*, 2008; ZHU; EGEBLAD; CHRISTENSEN, 2007).

Numerous hierarchical zeolite structures could be achieved through a hard-templating approach, where the shape and size of the templates control the pore systems, leading to three-dimensionally ordered mesoporous structures with additional inter-crystalline pore system (MIAO *et al.*, 2008). Nevertheless, the application of hard templating is limited to the expensive and difficult preparation procedures, along with the laborious removal of the hard template after the synthesis process, damaging the zeolite framework (MACHOKE *et al.*, 2015).

2.2.2.2 Surfactant template

Surfactants act as porogens in the synthesis of hierarchical pore structures, leading to different pore structures and pore size distributions (SACHSE; GARCÍA-MARTÍNEZ, 2017). This technique has already been applied for a variety of metal oxides such as magnesium, aluminum, manganese, iron, cobalt, and nickel, among others, being also possible for their use for non-oxide compounds such as phosphates, sulfides, nitrides, carbides, and selenides (HUO *et al.*, 1994; ROBAK; HERBAGE; ELLMAN, 2010; SHI; WAN; ZHAO, 2011; SOLER-ILLIA *et al.*, 2002; WAN; ZHAO, 2007).

Surfactant-oriented technologies provide greater flexibility and enable the creation of different structural architectures with tailored properties, based on the interaction of surfactants and inorganic species (SACHSE; GARCÍA-MARTÍNEZ, 2017). The synthesis conditions have an impact on the structure organization mechanisms in the surfactant-templating, where the charges of the components involved in the synthesis pathway play a significant role in molecule organization (HUO *et al.*, 1994).

The surfactants (S) and inorganic species (I) found in the synthesis system, present an ionic behavior, which directly depends on pH, therefore, the mesophase formation is governed by columbic interactions between the surfactants and inorganic species. Four possibilities could be achieved in synthetic conditions of both inorganic moieties and surfactant molecules, which is presented in Figure 4. The first two possibilities involve only inorganic species and surfactant molecules. 1) interactions between positively charged surfactant (S+) and negatively charged inorganic species (I-) lead to the S+I- mesophase formation; 2) Interactions between negatively charged surfactant (S-) and positively charged inorganic species (I+) lead to the S-I+ mesophase formation. When both inorganic and surfactant species present the same charge in the synthesis system, additional anions (X) or cations (M) are introduced to the structure process, resulting in the last two possibilities. 3) S+X-I+ mechanism pathway and 4) S-M+I- mechanism pathway. Another pathway may exist if nonionic surfactants are used, where the path could be described as S_0I_0 and are based on hydrogen bond or dipolar interactions, where the hydrophilic/hydrophobic volume ratio is the main condition for the mesophase formation.

Figure 4 - Interactions between surfactants and silica

Pathways	Silica-Surfactant Interactions	Induced Structure

(1)S^+I^-	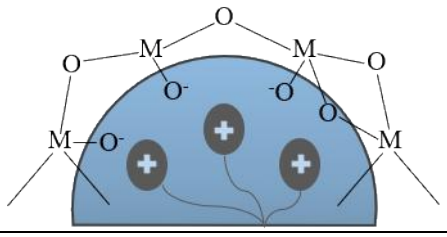	MCM-41, MCM-48, MCM-50 W oxide Sb Oxide
(2)S^-I^+	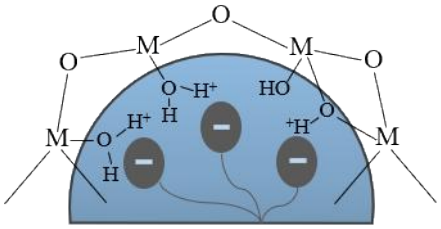	Mg, Al, Ga, Mn, Fe, Co, Ni, Ti and Zn Oxides Alumina
(3)$S^+X^-I^+$	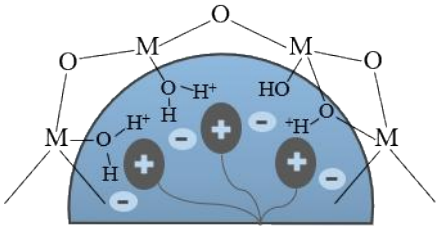	SBA-1 SBA-2 SBA-3 Zn Phosphate
(4)$S^-M^+I^-$	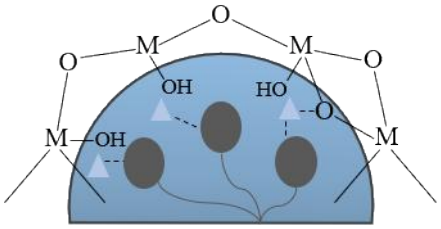	Zn Oxide Alumina
(5)S^0I^0	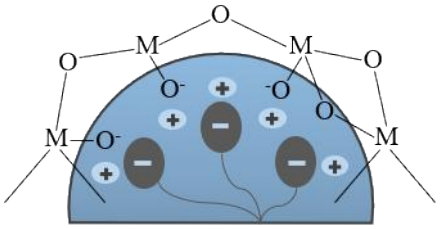	HMS and MSU-X Silica lamellar, cubic and, hexagonal

Source: elaborated by the author (2023)

The surfactants in the synthesis gel assemble the primary inorganic building units, inducing the formation of inter- or intra-crystalline mesopores (PARK *et al.*, 2011). The surfactant hydrophilic moiety acts as SDA for the zeolite formation or anchors the surfactant into zeolite (CHOI *et al.*, 2009), and the hydrophobic moiety act as a mesoporogen, generating the mesoporous phase (CHOI *et al.*, 2006; INAYAT *et al.*, 2012).

Different approaches could be used to generate mesoporosity into the zeolite structure using SDAs such as primary soft-templating and secondary soft-templating. The material originated from primary soft-templating, depends on the surfactant concentration and synthesis conditions, exhibiting a sponge-like or a layered-like morphology with inter-crystalline and

intra-crystalline additional porosity (CHOI *et al.*, 2006, 2009). Normally, the layered-like morphology is preferably due to its dimensions ranging from a few nanometers, and three-level porosity (EJKA; MORRIS; NACHTIGALL, 2017). However, just a few zeolites were reported presenting a layered morphology, being FAU and MFI structures as some examples (CHOI *et al.*, 2009; INAYAT *et al.*, 2012). In the secondary soft-templating, the surfactant is added to the synthesis gel, which contains the zeolite in its initial nucleation step, where the phase segregation is the leading process, yielding a microporous and crystalline phase and a mesoporous amorphous phase (SACHSE; GARCÍA-MARTÍNEZ, 2017). However, the materials obtained from this technique are not truly hierarchical, due to the very different mechanisms and kinetics between zeolite crystallization and mesophase formation. Amorphous mesostructures usually form fast and at low temperatures and zeolite synthesis requires longer crystallization times and often hydrothermal conditions (SACHSE; GARCÍA-MARTÍNEZ, 2017).

The soft templating method based on emulsion templating is another method to generate mesopores in zeolite structures, through a biphasic system containing an aqueous phase and an organic phase stabilized by surfactants, formed during the zeolite synthesis, where the zeolite precursor assembles at the interface between the organic and aqueous phases (LEE; SHANTZ, 2005). During the material formation, the droplets of the organic phase form voids between the zeolite precursors in the aqueous phase, where after drying, an amorphous silica phase is created, being this amorphous phase converted into the zeolite phase by steam-assisted crystallization, which could be tuned by adjusting the amount of organic solvent and surfactant (EJKA; MORRIS; NACHTIGALL, 2017).

Surfactant designing is a form of a soft template where surfactants are designed to interact with the inorganic species in the desired way as the surfactant used by Ryoo et al. based on amphiphilic silanes, which contains a hydrophobic tail and a headgroup covalently bounded to a trialkoxysilane moiety. Designed surfactants, based on amphiphilic silanes, direct the formation of the mesophase through self-assembly of the hydrophobic part, and the ammonium headgroup leads to the zeolite structure due to the ability of both parts to link with the inorganic species (SACHSE; GARCÍA-MARTÍNEZ, 2017).

Designed surfactants could contain multiple quaternary ammonium centers, which improves the organization of the zeolitic structure during crystallization. Ryoo and co-workers are the pioneers to achieve hierarchical MFI zeolite structures using surfactant C22-6-6 ($C_{22}H_{45}$-$N(CH_3)_2$-C_6H_{12}-$N(CH_3)_2$-$C_6H_{13}Br_2$), composed by two quaternary ammonium centers, spaced

by C6 alkyl chains, directing the formation of MFI structure, and the mesophase is formed by the hydrophobic micellar assemblies of the long hydrocarbon chain (SACHSE; GARCÍA-MARTÍNEZ, 2017). However, an increase in the number cationic centers in the designed surfactants lead to the loss of structural order, increasing the wall thickness (PARK *et al.*, 2011).

2.2.2.3 Zeolite seeds

Zeolites seeds could also be used as directing agents, acting as precursors of the crystalline phase through combination with surfactants, during hydrothermal treatments (MEI; DUAN; WANG, 2021). The used seeds are obtained through classical zeolite synthesis routes at shorter synthesis times and lower temperatures. The zeolite seeds show no X-ray diffraction peaks; however, the zeolite formation could be confirmed through typical vibrational bands observable by IT Raman spectroscopy. (STOJKOVIC; ADNADJEVIC, 1988).

The zeolite seeds approach does not achieve truly hierarchical structures, due to the lack of crystallinity, however, specific surfactants could be used to properly interact with the zeolite seeds to originate hierarchical zeolites (GU *et al.*, 2010). As an example, hierarchical FAU zeolites are achieved through the self-assembly of FAU seeds with CTAB in the presence of co-solvents and micelle swelling agents under hydrothermal conditions, using Trimethyl-Benzene (TMB) as a swelling agent and Tert-butyl Alcohol (TBA) as co-solvent, where TBA decrease the repulsive forces of the CTAB head groups, leading to an increase in the micelle packing and charge density and the TMB assembles zeolite crystals with CTAB by swelling the surfactant micelle to match with the large zeolite nanocrystals (SACHSE; GARCÍA-MARTÍNEZ, 2017).

The polar head groups of surfactants have a major influence in the assembly of zeolite seeds, as an example, imidazolium-based ionic liquids [C_{16}MIm]Cl, are employed as surfactants, where the imidazolium headgroup allows a stronger binding with the charged silica species, being important in the achievement of hierarchical structures (WANG *et al.*, 2007).

Another approach regarding zeolite seeds is the functionalization of zeolites for subsequent crystallization. As an example, Serrano et al. attached aromatic groups to the protonated zeolite seeds for further crystallization under hydrothermal conditions, generating a hierarchical zeolitic structure.

2.2.2.4 Non-templating

This method is carried on under hydrothermal conditions or by dry gel conversion, generating mesopores through a self–assembly effect of nanocrystals or by excessive crystal twinning during the synthesis step.

The main responsible for the formation of hierarchical structures through self-assembly is controlled nucleation and crystal growth (DING *et al.*, 2015). The synthesis conditions are chosen in a way that primary very small particles are generated during the aging of the synthesis gel, which aggregates during the crystallization process, forming open pores by an intense intergrowing procedure (AL-JUBOURI, 2020). Beside the hydrothermal crystallization, the dry-gel conversion technique can also be applied for the primary particle intergrowing crystallization procedure. Nevertheless, the mesoporosity generated through intergrowing particles is often unstable and may be lost under mechanical or thermal stress (EJKA; MORRIS; NACHTIGALL, 2017).

Combining two isostructural crystalline phases (structural twin) as MFI/MEL or FAU/EMT, enables the formation of pore hierarchy by forming inter-crystalline mesopores due to twining during the synthesis process. Each isostructural phases presents a crystal growth velocity in a specific direction, the differences between this two distinct phases induces the formation of intergrown layer-like zeolites, where an additional network of mesopores is formed between the layers (EJKA; MORRIS; NACHTIGALL, 2017). For the isostructural domains formation, SDAs as tetrabutylphosphonium, some organosilanes, and inorganic salts as lithium carbonate or zinc nitrate, induces the phase formation (SHVETS; KONYSHEVA; KURMACH, 2018). The application of this method is limited to zeolites with an isostructural phase.

Another technique applied for creating hierarchical MFI zeolites is a novel method, which consists of a two-temperature synthesis taking advantage of different growth processes that takes place at different temperatures, creating hierarchical pore structures through epitaxial growth (PAQUIN *et al.*, 2015). First, pre-crystalline clusters are formed by hydrolysis and precursor condensation at temperatures ranging from 20 to 80 °C. Second, at temperatures ranging from 100 to 140 °C, the first step clusters aggregate in an oriented manner, resulting in the formation of defects. These defects initiate epitaxial growth, resulting in increased porosity in the material. The resulting hierarchical zeolite has intra-crystalline pores and is composed of a purely microporous zeolite core surrounded by a shell of macro- and mesoporous zeolite.

2.3 BIOSURFACTANTS

Commonly used surfactants are usually derived from petroleum, being oil exploration dependent and causing environmental problems. Biosurfactants are a promising alternative to synthetic surfactants (SANTOS *et al.*, 2016) due to their biodegradable and nontoxic nature (VARJANI; UPASANI, 2017).

Biosurfactants are surface-active or bio-emulsifier molecules, synthesized by plants (saponins), microorganisms (bacteria, actinobacteria, yeasts, and filamentous fungi), and higher organisms (bile salts), showing antimicrobial, antitumor, and larvicidal or insecticidal potential (MARCELINO *et al.*, 2017; NITSCHKE; PASTORE, 2002; WU *et al.*, 2017). When compared with synthetic surfactants, biosurfactants are more efficient in reducing solutions surface tension at lower concentrations due to lower Critical Micelle Concentration (CMC) (COOPER; PADDOCK, 1984) which is defined as the minimum required to initiate the formation of auto-aggregation forms (e.g. micelles) (MULLIGAN, 2005). Some biosurfactants present high thermal, pH stability, and chemical resistance to high salt concentration, up to 10% (w/v) (BOGNOLO, 1999). Biosurfactants are easily degradable in water and soil and can be metabolized by microorganisms (FLASZ *et al.*, 1998; MULLIGAN; GIBBS, 1989).

Regarding biosurfactant production, these molecules could be derived from renewable resources such as sugarcane bagasse, hydrolysates, molasses, cassava meal, wheat bran, crude glycerol from biodiesel, and animal fat (BANAT *et al.*, 2014; DOMÍNGUEZ RIVERA; MARTÍNEZ URBINA; LÓPEZ Y LÓPEZ, 2019; MAKKAR; CAMEOTRA; BANAT, 2011).

Biosurfactants are mainly composed of unsaturated/saturated hydrocarbon chains or fatty acids in their hydrophobic moiety and composed of acid peptide cations, mono-, di- or polysaccharides anions, related to the hydrophilic part (BANAT, 1995; RAZA; KHALID; BANAT, 2009; YAN *et al.*, 2012). The classification of biosurfactants is based on their molecular weight. The first class is the low-molecular-weight compounds, such as glycolipids and some short-chain lipopeptides (BANAT, 1995; WHANG *et al.*, 2008; YAN *et al.*, 2012). The second classification is related to the high-molecular-weight compounds, known as bio-emulsifiers, such as lipopolysaccharides or lipoproteins (MARKANDE; ACHARYA; NERURKAR, 2013; UAD *et al.*, 2010).

Low-molecular-weight biosurfactants are more effective in reducing the surface and interfacial tension, whereas bio-emulsifiers are more effective in stabilizing emulsions of oil-

in-water (UAD *et al.*, 2010; WHANG *et al.*, 2008). Figure 5 shows a schematic view of biosurfactants arrangements.

Figure 5 – Main division of biosurfactants

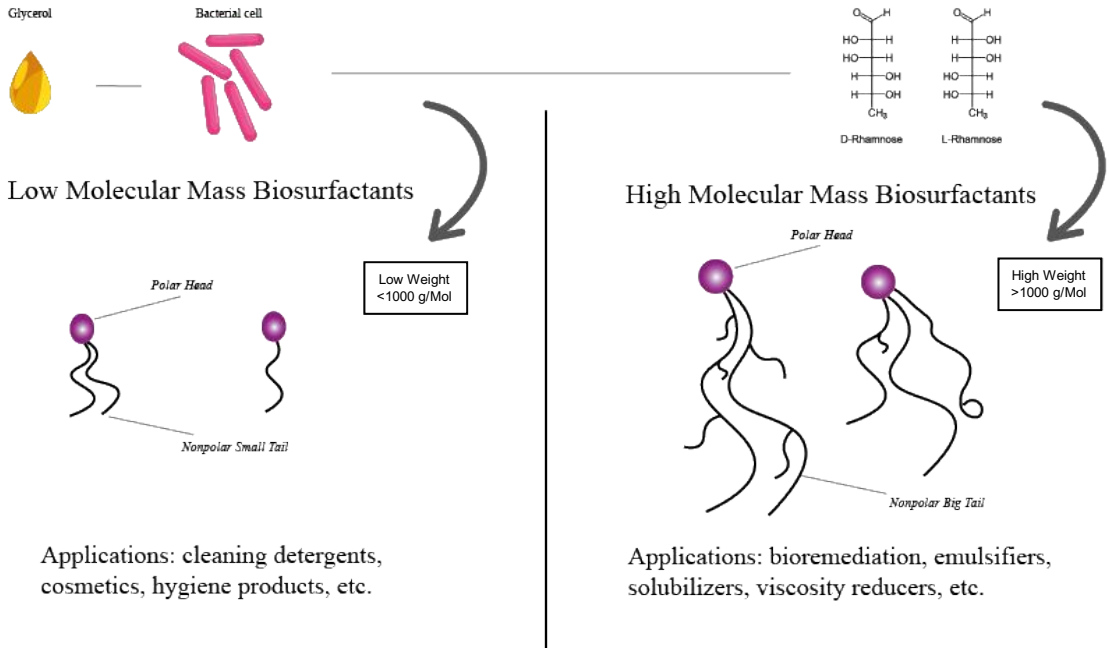

Source: elaborated by the author (2023)

2.3.1 Biosurfactant production and application

Biosurfactant production can be carried out in several ways through different microorganisms and substrates, being the obtained compounds promising bioactive molecules for the future of surfactants in research and industrial fields.

The bacterial biosurfactant production can either be natural or induced by some compounds, where the maximum production normally occurs during the exponential or stationary growth phase, where some factors such as pH, temperature, aeration, agitation speed, inoculum size, and stress, influence in the rate of biosurfactant production (JIMOH; LIN, 2019). Also, some specific elements such as carbon, nitrogen, iron, sulfur, phosphorus, and manganese have been showing a significant influence on biosurfactants production yields and their chemical structure (DARVISHI *et al.*, 2011; GUDIÑA *et al.*, 2015).

A better way of biosurfactant production is the use of industrial wastes as substrates, considering an environmentally friendly technique. Many industrial processing stages generate wastes that could be consumed by microorganisms such as molasses, corn steep liquors, animal

fat, starch, soap stock, cheese whey, curd whey, lactic whey, straw of sugar cane, wheat, straw of rice, bran, rice, bagasse of sugarcane, soy hull, corn, cassava flour, and waste-water products (DUBEY; JUWARKAR; SINGH, 2005; JOSHI *et al.*, 2008; MAKKAR; CAMEOTRA; BANAT, 2011; NITSCHKE; COSTA; CONTIERO, 2010; ONBASLI; ASLIM, 2009; RASHEDI *et al.*, 2005; RAZA; KHAN; KHALID, 2007), characterizing low-cost wastes which could improve the commercial availability of biosurfactants (KHOPADE *et al.*, 2012; SARAVANAN; VIJAYAKUMAR, 2013).

Oils are the most promising source of carbon and energy substrates for biosurfactant production, due to the different available kinds (JIMOH; LIN, 2019). As examples, is possible to obtain rhamnolipid biosurfactants by *Pseudomonas aeruginosa* LBI strain as reported by Nitschke, Costa, and Contiero (NITSCHKE; COSTA; CONTIERO, 2010) through the utilization of soybean oil as substrate, reaching rhamnolipid concentrations of 60 g/L after 144h of cultivation; the utilization of olive oil in the production of biosurfactants by marine *Nocardiopsis* sp. B4 was reported by Khopade *et. al.* (KHOPADE *et al.*, 2012) where the maximum productivity of the biosurfactant was determined by the decrease in the surface tension, reaching 29 mN/m after nine days.

It is worth noticing that the substrates sources are not the only factor that influences the biosurfactants production viability. The purification step of biosurfactant production can represent 70% - 80% of total production costs (ARAÚJO *et al.*, 2019; SANTOS *et al.*, 2016). Considering this factor for a viable large-scale production of biosurfactants, some improvements in the process are needed.

The biosurfactant application depends on their structural characteristic, where the major classification is between high molecular and low molecular weight biosurfactants. High molecular weight biosurfactants present a hydrophilic-lipophilic balance, which specifies a portion of hydrophilic and hydrophobic constituents in surface-active substances, indicating whether biosurfactant is related to water-in-oil or oil-in-water emulsion (SATPUTE *et al.*, 2010; SOUZA; VESSONI-PENNA; DE SOUZA OLIVEIRA, 2014). Considering a hydrophilic-lipophilic balance scale by assigning a value of 1 for oleic acid and 20 for sodium oleate and using a range of mixtures of these two components in different proportions to obtain the intermediated values products, biosurfactants could be classified as lipophilic for low hydrophilic-lipophilic balance (<6), stabilizing water in oil emulsification, or hydrophilic emulsifiers with high hydrophilic-lipophilic balance (10 – 18), being recommended for oil in water emulsification (DESAI; BANAT, 1997; PACWA-PŁOCINICZAK *et al.*, 2011; UAD *et*

al., 2010). Low molecular weight biosurfactants effectively reduce interfacial and surface tensions. Taking water surface tension (72 mN/m) as a parameter, the addition of low molecular weight biosurfactants reduces the surface tension to 25 - 38 mN/m, values close to or lower than those of synthetic surfactants (30 – 40 mN/m) (BAHRI *et al.*, 2006; DESAI; BANAT, 1997). Low molecular weight biosurfactants display an extensive variety of chemical structures, including phospholipids, glycolipids, lipopeptides, fatty acids, neutral lipids lipopeptides, polysaccharide complexes, flavolipids, lipids, and polymeric surfactants (DATTA; TIWARI; PANDEY, 2018).

Many studies have reported the applicability of biosurfactants for industrial processes. High molecular weight biosurfactants are often applied as an additive to stimulate the bioremediation and removal of oil from natural environments as shown by Bordoloi and Konwar (BORDOLOI; KONWAR, 2008) in the use of biosurfactants, produced by *Pseudomonas aeruginosa* strains, in the removal of 49 - 54% of crude oil from sand; Silva et. al. (SILVA *et al.*, 2010) also used a biosurfactant originated from *Pseudomonas aeruginosa* UCP-0992 strain, in the removal of diesel oil from sand, reaching removals rates above 85%; Araújo et. al. (ARAÚJO *et al.*, 2019) showed motor oil removal rates above 94% in the sand, using biosurfactant produced from by *S. marcescens* UCP-1549, while distilled water only removed 63%. Some biosurfactants also show antimicrobial activity, as reported by Nitschke et al. (NITSCHKE; COSTA; CONTIERO, 2010) the author used a rhamnolipid biosurfactant against *Bacillus cereus* (64 μg/mL) and *Mucor miehei* (64 μg/mL) and some inhibition of *Neurospora crassa*, *Staphylococcus aureus*, and *Micrococcus luteus* (256 μg/mL). Another important applicability of biosurfactants is in pollution control where these natural compounds could remove heavy metals from contaminated soil and water, as reported by da Rocha Junior et al. (DA ROCHA JUNIOR *et al.*, 2019) in the use of biosurfactants produced from *Candida tropicalis* yeast for removal of Cu and Zn from contaminated sand with rates ranging from 30 to 80%. Biosurfactants also have an important role in the petrochemical industry being applied in oil recovery, hydrocarbon bioremediation, oil-sludge cleaning, storage tanks, oil immobilization, or act as emulsifiers or de-emulsifiers on hydrophobic pollutants (DE ALMEIDA *et al.*, 2016; JHA; JOSHI; GEETHA, 2016).

2.3.2 Self-aggregation structures

Biosurfactants create self-aggregation structures in aqueous media via micellization at concentrations above the CMC, which is an equilibrium mechanism that induces the production of thermodynamically stable micellar structures (JAHAN *et al.*, 2020). Surfactant self-assembly is normally induced by hydrogen bonding or by hydrophobic and van der walls interactions, with the size, shape, and degree of ionization of generated structures being highly dependent on biosurfactant concentration, solvent, pH, temperature, pressure, and salt concentration. As a result, increasing the biosurfactant concentration over the CMC does not result in larger micelles, but rather increases the number of micelles (DELEU *et al.*, 2013; KITAMOTO *et al.*, 2009).

When compared to their hydrophobic regions, glycolipids biosurfactants have comparatively large hydrophilic head groups, resulting in spherical, disk-like, and rod-like micelles (SÖDERMAN; JOHANSSON, 1999). Increases in biosurfactant concentration cause liquid crystalline phases to develop in water solutions, resulting in a range of molecular assemblies such as cubic, hexagonal, lamellar, or sponge-like structures (IMURA *et al.*, 2007). The hydrophobic portion of glycolipids is made up of a range of fatty acids (short/medium chains; unsaturated/branched structures), which allows the biosurfactants to be in a fluid state at all times, making it easier to manage their liquid crystal forms (KITAMOTO *et al.*, 2009).

Innumerous factors influences the molecular assemblies formed by the biosurfactants molecules, however, controlling key hydroxyl groups in biosurfactants headgroups leads to desired molecular assemblies, different from conventional amphiphile/water systems where the interaction is simply repulsive in surfactants headgroups (HATO, 2001; KITAMOTO *et al.*, 2009).

For biosurfactants concentrations above CMC along with factors such as chemical structure, polarity, electrostatic interactions, ionic strength, and temperature, leads to different self-aggregation morphologies as micellar, micellar reverse, lamellar, hexagonal and hexagonal reverse (HOLMBERG *et al.*, 2002). The self-aggregation morphology of biosurfactants is particularly important in their applicability. Knowing how these compounds will behave in solution and interact with other molecules allows a better understanding of the behavior and different interactions with other molecules. The different chemical structures of biosurfactants lead to different self-aggregation structures, as can be seen in Figure 6.

Figure 6 – Biosurfactant self-aggregation structures

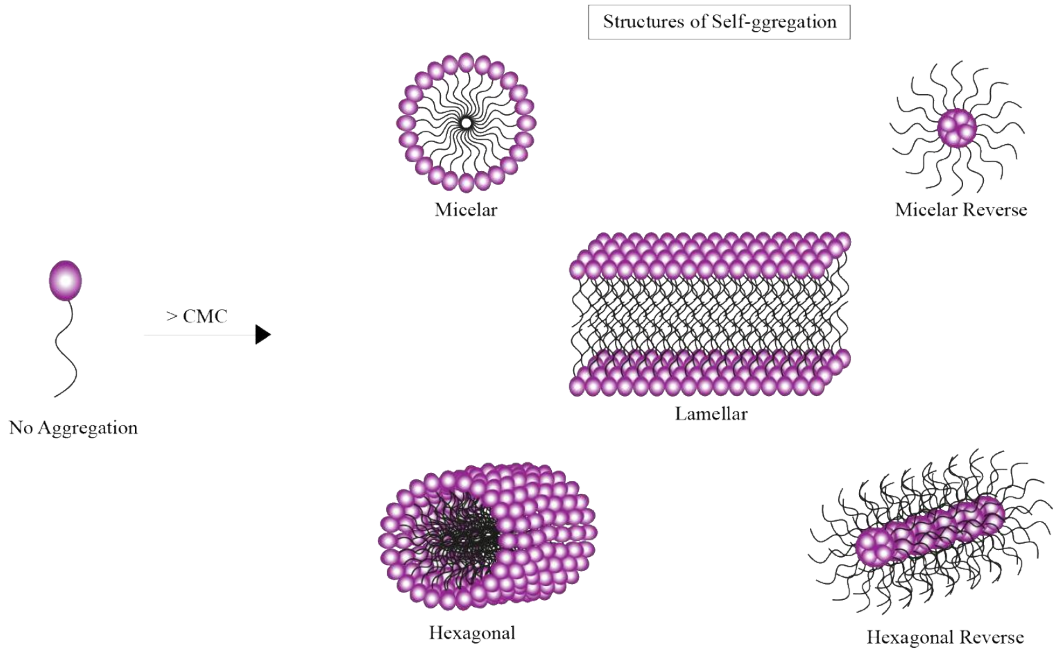

Source: elaborated by the author (2023)

Biosurfactant structure influences its CMC value, micelles, and molecular assemblies. Rhamnolipids biosurfactants have a microbial origin, mostly from *Pseudomonas aeruginosa*, where either one or two rhamnose molecules represent the hydrophilic moiety, which are linked to one or two β-hydroxylated fatty acid chains (hydrophobic region) (CHONG; LI, 2017). biosurfactants normally form spherical, vesicles or lamellar micelles, being dependent on solution ionic strength (LEBRÓN-PALER *et al.*, 2006; NITSCHKE; COSTA; CONTIERO, 2005). The pH has a major influence on the rhamnolipid micellar structure, where under pH < 5, the carboxyl group is protonated, being not sensitive to solution ionic strength, leading to reduced repulsion between rhamnosyl headgroups. Under pH > 5 the rhamnosyl headgroups are negatively charged, and the repulsive forces between the nearby hydrophilic rhamnosyl headgroups increase, resulting in larger spherical vesicles. (ABBASI *et al.*, 2013; PORNSUNTHORNTAWEE; CHAVADEJ; RUJIRAVANIT, 2009). For the surfactin biosurfactants, spherical micelles are formed, together with larger aggregates in an aqueous solution, being also dependent on pH, where alkaline environments lead to smaller micelles due to the deprotonation of surfactin carboxylic groups (DÉJUGNAT; DIAT; ZEMB, 2011; JAHAN *et al.*, 2020). The temperature also influences the surfactin molecule, where only the temperature is increased, the microviscosity of

surfactin micelles increases due to the formation of β-sheets in surfactin micelles (OSMAN; HØILAND; HOLMSEN, 1998). Mannosylerythritol is another class of biosurfactants, where its structure shows different conformations (MEL-A, MEL-B, MEL-C, and MEL-D) by varying their acetylation degree (GOOSSENS *et al.*, 2016). Mannosylerythritol lipids form lyotropic liquid crystalline phases in aqueous solutions, where lamellar conformations diffuse freely in the lateral direction in the bi-continuous cubic form, both solvent, and surfactant diffuse in three dimensions (JAHAN *et al.*, 2020). Changes in solution parameters also influence the mannosylerythritol structure, leading to the transformation of one self-aggregation structure into another (FUKUOKA *et al.*, 2012). Sophorolipids are glycolipid biosurfactants, produced yeast strains, made up of a hydrophilic sophorose moiety coupled with a hydroxylated fatty acid tail of 16 or 18 carbon atoms linked by a glycosidic bond (KULAKOVSKAYA; KULAKOVSKAYA, 2014). Sophorolipids concentration in solution has a major influence on their molecular characteristics, where above CMC values, sophorolipids form different structures, for pH < 5.5, acid sophorolipids self-assemble forming helical ribbons, due to strong hydrogen bonding between intermolecular disaccharide headgroups, and strong hydrophobic-hydrophobic interaction between hydrocarbon chains, and under pH > 5.5, the aggregates molecules are destabilized (KITAMOTO *et al.*, 2009). The source and producer microorganism also influence sophorolipid structure due to the presence, or not, of functional groups such as hydroxyl and CH_2 (ZHANG *et al.*, 2004).

Considering the classification of biosurfactants, high molecular weight biosurfactants are surface-active substances, which act as emulsifiers and present self-aggregation structures that effectively bind with non-polar substances, with high interface activity (PERFUMO *et al.*, 2010). Low molecular weight biosurfactants effectively reduce interfacial and surface tensions, where the addition of low molecular weight biosurfactants reduces the water surface tension to 25 - 38 mN/m, values close to or lower than those of synthetic surfactants (30 – 40 mN/m), taking water surface tension (72 mN/m) as a parameter (BAHRI *et al.*, 2006; DESAI; BANAT, 1997).

2.4 BIOSURFACTANTS AS STRUCTURE DIRECTING AGENTS

The idea of using bio-derived molecules in materials synthesis has been explored for some time. The starch was the first biological-derived molecule, used in materials synthesis,

and applied to mesoporous ceramics, hierarchically ordered porous silica monoliths, mesoporous silica films, and Titania 3-D networks (MIAO *et al.*, 2008; ZHANG; DAVIS; MANN, 2002). After the successful application of starch in materials synthesis, proteins, polynucleotides, and lipids were also used as templates for porous materials synthesis as demonstrated by Eglin et al. (EGLIN *et al.*, 2005) in the use of type I collagen at high concentrations (~100 mg/L); Modified DNA molecules could also be used as a template, as reported by Numata et al. (NUMATA *et al.*, 2004) which modified the DNA molecule with ammonium and guanidinium groups, changing the ionic character of the DNA molecule allowing it interaction with anionic silica molecules through the sol-gel method; Pawolski et al. (PAWOLSKI *et al.*, 2018) explored the synergism of soluble biomolecules by using organic components isolated from bio-silica of *Cyclotella cryptica* as templates for diatom-like porous silica; Dunphy et al. (DUNPHY *et al.*, 2009) reported the use of Diacyl phosphatidylcholines and Monoacyl phosphatidylcholines in the synthesis of mesoporous silica, where the Diacyl phosphatidylcholines molecules direct the formation of 2D hexagonal mesophases and Monoacyl phosphatidylcholines direct 3D micellular mesophases.

A large number of structures and properties are found in natural derived free fatty acids, which can be applied to direct the formation of mesoporous silicas, as reported by Canlas and Pinnavaia (CANLAS; PINNAVAIA, 2012) In the preparation of mesostructured silica materials using oleyl amine. Another possibility is the use of amino acids and sugars in the synthesis of porous materials as described by Thomas et al. (THOMAS *et al.*, 2011) in the synthesis of hybrid mesostructured silica using C12-glutamic-acid and C12-leucine-based surfactants. For sugar-derived biological surfactants, Botella et al. (BOTELLA; CORMA; QUESADA, 2012) used biocompatible alkyl maltoside surfactants to direct the formation of mesostructured silica under room temperature and physiological pH.

Biosurfactants have properties similar to commercial chemical surfactants, such as the formation of self-aggregation structures, which induces the formation of pores in materials structures. Low molecular weight biosurfactants, such as glycolipids and short-chain lipopeptides are more similar to commonly applied chemical surfactants (MARKANDE; ACHARYA; NERURKAR, 2013; WHANG *et al.*, 2008). The first application of biosurfactants in materials synthesis was in the sol-gel synthesis of porous materials by Montoneri and co-workers (BOFFA *et al.*, 2010). The authors obtained fats, polysaccharides, proteins, and lignin from urban refuses and produced a waste-derived high molecular weight biosurfactant through aerobic degradation, named BS110. The biosurfactant causes significant changes in the

molecular conformation of the mesoporous in the silica structure and controls the pore size distribution by varying the biosurfactant concentration in the synthesis medium.

Similarly, Boffa et al. (BOFFA *et al.*, 2014) and Hazra et al. (HAZRA *et al.*, 2014) applied biosurfactants in the synthesis of porous materials, titanium dioxide, and calcium sulfate particles. The authors used a waste-derived surfactant, named CVU90, for the synthesis of titanium dioxide particles through the sol-gel technique, where the biosurfactant, acts as structure directing agent under concentrations between 5 - 25 times its CMC, leading to a porous titanium dioxide, where the increase in the CVU90 concentration leads to the formation of a larger number of nucleation centers, however, in this case, the use of biosurfactant decrease the crystal size and increased the number of surface hydroxyl groups. In the synthesis of calcium sulfate material, the authors used low molecular weight biosurfactants (rhamnolipids and surfactin) isolated from *Pseudomonas aeruginosa* BS01 and *Bacillus clausii* BS02, through ultrasound-assisted methodology by adjusting the mass ratio of rhamnolipid/H2O, surfactin/H2O, and rhamnolipid/surfactin, showing a better energy efficiency, faster reactions, higher yields of material formation and better crystallization path (crystal shape and polymorph).

Another example is the use of high-molecular-weight biosurfactant, produced by *Bacillus subtilis* BBK006 in the synthesis of biological mesoporous silica nanoparticles, where the biosurfactant combines with the silica precursor and forms Si-O-biosurfactant complexed molecules, which bind with each other and produce a spherical molecule through condensation, presenting numerous Si-O-biosurfactant complexes (SHARMA *et al.*, 2021).

The combination of chemical surfactants/structure inducers with biosurfactants in porous materials synthesis allows better interactions between bio-molecules and inorganic species, as reported by Nie and co-workers (NIE *et al.*, 2021) in the synthesis of ZSM-5 zeolites, where the authors used N-methyl-2-pyrrolidone as structure inducer and the high molecular weight biosurfactant (JR-400) to induce the formation of ordered nano-ZSM-5 particles, which exhibits a hierarchical pore structure and a superior catalytic activity, high selectivity, and outstanding catalytic stability for benzene alkylation with bioethanol.

Nowadays, some biosurfactants have a large-scale production which allows their application in porous materials synthesis as structure-directing agents. The large-scale production of these biomolecules decreases their production cost, becoming an attractive alternative for porous materials synthesis. The large-scale low-molecular weight biosurfactants produced nowadays are listed in Table 1.

Table 1 – Commercially available biosurfactants

Rhamnolipids	**Surfactin**
Mono-Rhamnolipids 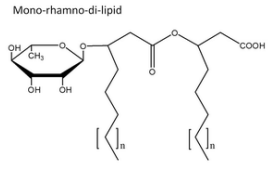 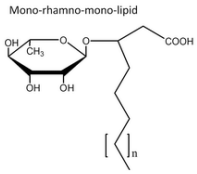 Di-Rhamnolipids 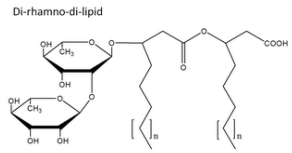 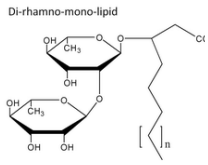	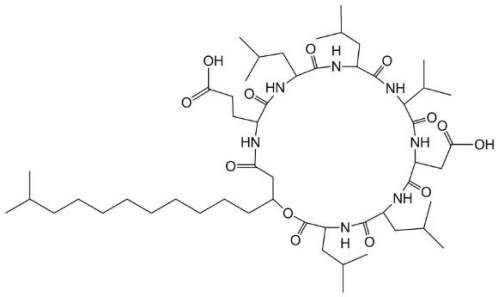
Sophorolipds	**Phospholipids**
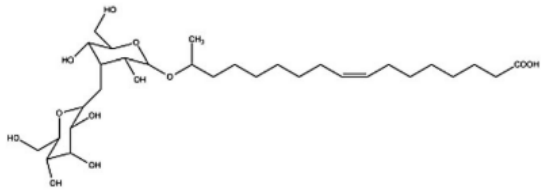	Monoacyl phosphatidylcholine 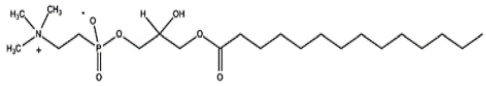 Lecithin 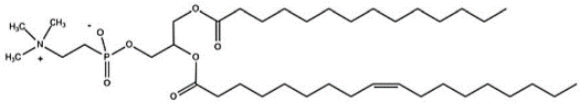
Mannosylerythritol lipids	
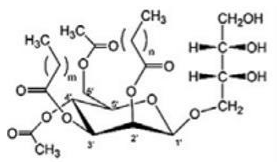 MEL - A 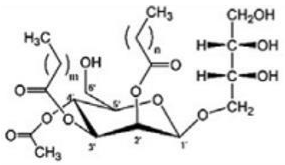 MEL - C	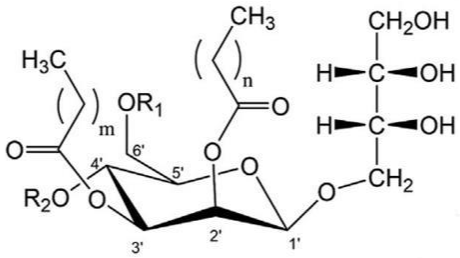 General MEL Strucutre	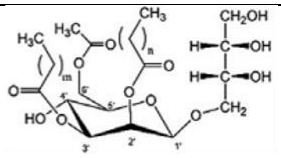 MEL - B 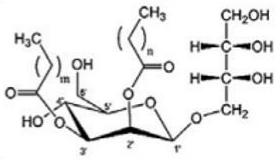 MEL - D

Source: elaborated by the author (2023)

The main challenge in the application of large-scale production biosurfactants in material synthesis, mainly in siliceous materials, is their anionic/non-ionic nature. Usually, materials synthesis happens in alkaline or mild acid conditions, where the silica molecules are in their anionic form, hindering the interaction between the biosurfactant and silica molecules. However, to induce an ordered porous silica structure using biosurfactants, it is necessary that silica molecules interact properly with the template molecules.

2.4.1 Biosurfactant Functionalization

The interactions between anionic/non-ionic biosurfactants with inorganic building blocks of porous materials do not naturally occur due to weak electrostatic interactions between them. One way to overcome such problems is by improving the interactions between biosurfactant templates and the inorganic species through organic linkers or by functionalizing biosurfactants in a way that the final product has cationic nature.

Regarding the functionalization of biosurfactants, some studies have been reported, aiming to improve the biosurfactant properties or promote a better interaction between molecules. Ramos da Silva et al. (RAMOS DA SILVA *et al.*, 2019) reported the functionalization of Mono- and Di-rhamnolipids with arginine and lysine by linking the free α-NH_2 group of these amino acids to the terminal carboxyl of the rhamnolipids generating a cationic biosurfactant with improved antimicrobial activity and are readily biodegradable. Another example was reported by LV *et al.* (LV *et al.*, 2020) in the tailoring of cationic biosurfactant through etherification reaction of C4 Alkyl polyglycosides (APG) with 3-Chloro-2-hydroxypropyl trimethyl ammonium chloride (CHPTAC), forming the CAPG biosurfactant, which was used as inhibitors in water-based drilling fluids, proving that the etherification of APG improved the inhibition property.

Another way of improving the interaction and properties of biosurfactants is the coupling of biosurfactants with cationic surfactants, where the synergistic effect between these molecules provides an enhancement of performance and functionality which cannot take place in single surfactant systems (KHAN; MARQUES, 1999; TONDRE; CAILLET, 2001). As an example, Jin *et al.* (JIN *et al.*, 2016) mixture surfactin biosurfactant with cationic gemini surfactant to evaluate their interaction in aqueous systems, the authors showed that the two amphiphilic moieties, present in the Gemini surfactant, are joined by a spacer group, which when a spacer group is short, are close to each other enhancing the

interaction between hydrophobic chains and decreasing the repulsion between hydrophilic groups, allowing lower CMCs, higher surface activity, and better wetting properties. However, this procedure could induce the precipitation of anionic/cationic surfactants and are not in agreement with "green chemistry" since it uses surfactants of synthetic origin.

Tailoring biosurfactants to induce a cationic behavior allows a better interaction between these molecules with anionic inorganic molecules such as silicas. Appling tailored cationic biosurfactants as SDAs for silica structures could be an innovative application of these molecules.

2.4.2 Surface functionalization

The electrostatic nature of silica supports does not favor the direct interaction with biosurfactants. Thus, the interaction between siliceous materials with organic molecules can be enhanced by the functionalization of siliceous material surfaces through adsorption and chemical bonding of the desired molecules. The surface functionalization will depend on the desired interaction, being amine-containing (NH_2) molecules such as diethanolamine (DEA), tetraethylenepentamine (TEPA), methyl-diethanolamine (MDEA), and 3-Aminopropyltriethoxysilane (APTES), the most used molecules for interaction with naturally derived organic molecules (RATH; RANA; PARIDA, 2014; RIBEIRO *et al.*, 2019).

Between the amine-containing molecules, APTES is the most used for the functionalization of siliceous materials, where the silane termination, present in its structure, allows a covalent bonding between silica and APTES (CHANG *et al.*, 2003). However, for molecules without silane termination, the impregnation onto the surface of siliceous materials is accomplished through evaporation methods, which do not covalently bind these molecules to the surface, being easily removed by solvents (RIBEIRO *et al.*, 2019).

Siliceous materials normally present high surface areas and large pore volumes, and adjustable pore size, being attractive materials for amino functionalization, allowing it application in many different fields, such as stationary phase for chromatography, protein retainer, coatings, and gas adsorption (BUSZEWSKI; JEZIERSKA-ŚWITAŁA; KOWALSKA, 2003; CHEN *et al.*, 2017; SHAH *et al.*, 2008; VANDENBERG *et al.*, 1991).

Amine-silica materials could be prepared through post-synthetic treatments or through direct synthesis. The post-synthetic treatment is widely used, achieving the desired structure

formation, and then the amine species are subsequently incorporated into the structure (CHEN *et al.*, 2017). Direct synthesis occurs via the hydrolysis and co-condensation of organo-silanes with amino-silanes, where the material structure is determined by an organic template through acid/basic catalysis (TANG; LANDSKRON, 2010).

The synthesis of these amino-silica materials takes place on nonpolar solvents such as toluene or hexane, being an environmental problem and is not in agreement with green chemistry (CUOQ *et al.*, 2013; HARLICK; SAYARI, 2007; HUANG *et al.*, 2003). The use of nonpolar environments is due to the hydrolyzation of the APTES molecule in contact with hydroxyl groups in aqueous conditions, whereas in a nonpolar environment, the hydrolyzation will only occur when the APTES molecule reaches the hydroxyl groups in the surface of the siliceous material, attaching covalently with the material structure (CUOQ *et al.*, 2013). In the last years, researchers have been trying to use aqueous environments for the preparation of amino-siliceous materials (CUOQ *et al.*, 2013; DU; HE, 2012). Many studies claim that the functionalization of siliceous materials with amine-based molecules leads to lower and unstable surface loading. However, Cuoq *et al.* (2013) compared the grafting of APTES on the surface of siliceous material in two different environments (anhydrous and hydrous) where for the anhydrous environment the grafting was more efficient because of the formation of multilayers of APTES molecules. However, when rinsed with water for several hours, only the APTES monolayer was left on the surface, yielding results analogous to those obtained in the hydrous environment.

Therefore, the use of molecular linkers, as APTES, in the synthesis of siliceous materials, could improve the interaction between anionic/non-ionic biosurfactants self-aggregation structures and silica species, leading to materials with porous properties, originated by biosurfactants.

CHAPTER III – SYNTHESIS OF HIERARCHICAL ZEOLITES USING RHAMNOLIPIDS AND SOPHOROLIPIDS AS STRUCTURES DIRECTING AGENTS

Chapter III accomplishes the materials synthesis methodologies and characterization results of the obtained materials. From which, an article will be written and submitted to a Journal that comprehends the scope of the work, since few articles are found in the literature regarding the use of biosurfactants as structure-directing agents in the synthesis of conventional and hierarchical zeolites.

3 INTRODUCTION

The limitations imposed by zeolites microporous structure is a crucial factor for the development of materials with mesopores systems. Since the discovery of low ordered mesoporous silicas, such as M41s and SBA families, these materials were applied as catalysts and adsorbents in oil industry, due to their crystalline portion with pore openings larger than 2 nm (SCHAWANKE; BALZER; PERGHER, 2017). However, the lack of crystallinity on ordered mesoporous silicas leads to low acidity and hydro-thermal resistance, restricting their use (VERMEIREN; GILSON, 2009).

To overcome pure mesoporous silicas application problems in the zeolite field, hierarchical zeolites become an alternative since the zeolite microporous structure is maintained, and a second level of porosity is added to their structure, enhancing the material mass transportation. To achieve hierarchical zeolite structures, synthetic cationic surfactants are used as SDAs, guaranteeing a better interaction with zeolite building blocks and allowing to control the material formation by adjusting the surfactant molecular parameters. The substitution of synthetic surfactants for biosurfactants becomes a greener way to achieve hierarchical zeolite structures. However, biosurfactants are mainly composed of sulfate, phosphonate, or carboxylate polar functions, leading to molecules with anionic/non-ionic nature, which hinders their interaction with zeolite building blocks (GÉRARDIN *et al.*, 2013).

To improve the interaction between biosurfactants and zeolite building blocks, their molecules could be modified to give biosurfactants a cationic nature, normally to the attachment of molecules with amino groups, with strongly interacts with different functional groups found in biosurfactant molecules (RAMOS DA SILVA *et al.*, 2019; THOMAS *et al.*, 2014). Another attempt to improve biosurfactant interactions could be made by controlling the synthesis pH,

inducing the formation of cationic inorganic species, which will better interact with biosurfactants (BOFFA *et al.*, 2010).

Therefore, this chapter aims to synthesize mesoporous silicas and hierarchical Y zeolites using pure rhamnolipids and sophorolipids and their combination with APTES molecules as structure-directing agents.

3.1 MATERIAL AND METHODS

3.1.1 Material

Sophorolipid (S) surfactant REWOFERM SL ONE® (Evonik), Rhamnolipid (R) RHEANCE ONE® (Evonik), ammonium hydroxide (synth), sodium hydroxide (Neon), hydrochloric acid (Synth), toluene (Neon), Sodium Aluminate, sodium silicate C-325 (MQB chemicals), (Sigma Aldrich), Ethyl Alcohol (Synth), tetraethyl orthosilicate (Sigma Aldrich), 3-aminopropyl-triethoxysilane (Sigma Aldrich).

3.1.2 Silica Materials

3.1.2.1 Synthesis of Biosurfactant-APTES compound

The methodology for the functionalization of the R and S biosurfactant with the APTES molecule was based on the work of THOMAS *et al.* (2014). Initially, 0.456 g of the biosurfactant (R or S) were added to 10 mL of Milli-Q water, adjusted to pH = 5, and then the system was stirred until total dissolution of the biosurfactant. The following step consisted in the addition of 0.121 g of APTES, and the system was left under static conditions for 12 h at 60 °C. The obtained material was named as Bios-APTES.

3.1.2.2 Synthesis of amino-functionalized silicas

The chemical grafting of the APTES molecule into the silica surface followed the procedure of Cuoq *et al.* (2013), using water environment. Initially, 2.0 g of the Pure Silica (PS) material were added to 40 mL of Milli-Q water, followed by 0.002 M of APTES, the final

mixture was left under stirring at room temperature for 18 h. The obtained material was vacuum filtered and washed with 300 mL of Milli-Q water and dried at 40 °C overnight.

The obtained material was dispersed in 150 mL of a pH = 3 solution and left under agitation for 24 h for the removal of the APTES which doesn't covalently bound to the silica surface. After that, the material was vacuum filtered and dried overnight at 40 °C, being the material named Amino Pure Silica (APS).

3.1.2.3 Biosurfactant bonding onto amino-functionalized silicas

For biosurfactant bonding, initially, 0.456 g of the biosurfactant (R or S) was added to 20 mL of Milli-Q water, and the pH was adjusted to 6 with sodium hydroxide. Then, the system was stirred until total dissolution, followed by heating the system to 60 °C and adding 2.0 g of the APS material. The system was left under magnetic stirring for 12 h at 60 °C, and the obtained material was washed with 100 mL of Milli-Q water and dried overnight at 60 °C. The methodology used for the grafting of biosurfactants in the silica material is presented in Figure 7.

Figure 7 – Grafting of biosurfactants in amino-functionalized silicas

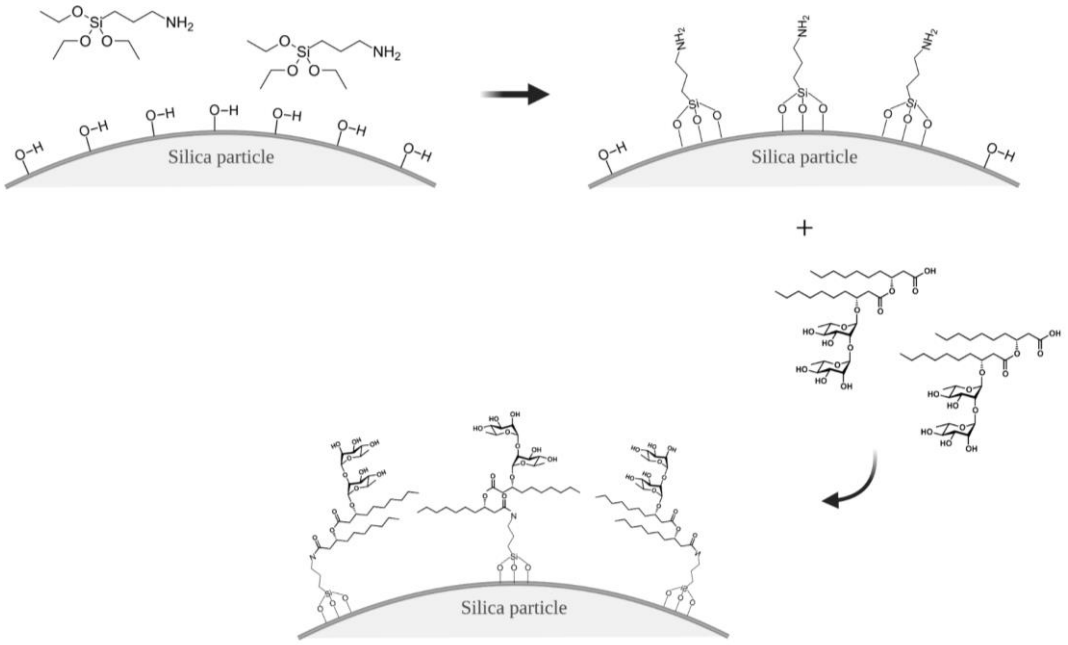

Source: elaborated by the author, using Biorender software (2023)

3.1.3 Synthesis of mesoporous silicas using biosurfactants as SDAs

For silica materials synthesis, the sol-gel method was used, consisting of a low-temperature inorganic polymerization process of silicon alkoxides (HENCH; WEST, 1990). Polymerization occurs through hydrolyzation and condensation of silicon alkoxides through alkaline or acid catalysis leading to gel formation. The use of acid or basic environments in the synthesis process will influence the obtained material, where for acid catalysis the oxygen atom bounded to the silicon (Si-O or Si-OR) is removed, allowing a nucleophilic attack of water molecules to the Si atom, leading to condensation of Si-OH and the formation of a compact silica structure with low pore volume and size. For polymerization in alkaline media, the nucleophilic attack occurs directly to the Si atom without the previous interaction with the oxygen, inducing condensation and spheres aggregates formation in the gel, leading to a silica matrix with higher porosity (BENVENUTTI; MORO; GALLAS, 2009). The hydrolysis and condensation reactions occur as follows:

$$Si(OR)_4 + H_2O \rightarrow (RO)_3Si\text{-}OH + R\text{-}OH \qquad \textit{Hydrolysis}$$

$$\equiv Si\text{-}OH + OH\text{-}Si\equiv \rightarrow \equiv Si\text{-}O\text{-}Si\equiv + H_2O$$

$$\equiv Si\text{-}OH + R\text{-}O\text{-}Si\equiv \rightarrow \equiv Si\text{-}O\text{-}Si\equiv + R\text{-}OH \qquad \textit{Condensation}$$

For the synthesis of mesoporous silicas using biosurfactants and the Bios-APTES compound as mesoporous inducers, the sol-gel method was used. For the material synthesis, 0.6 mmol of the biosurfactant was solubilized in 50 mL of distilled and the solution pH adjusted to ~ 2 and left under agitation until total dissolution. A second solution was made to induce the TEOS pre-hydrolysis, where 10.35 g were dispersed in 10.0 mL of HCl ethanolic solution (pH ≈ 2) until total dissolution, been this solution added to the former one and the final solution put into a horizontal shaker and left under agitation at 80 °C, which was left under agitation for 24 h. The obtained material was submitted to vacuum filtration, washed with 100 mL of deionized water, and dried overnight at 60 °C. The obtained materials were identified as Rhamnolipid – Mesoporous Silica (R-MS) and Sophorolipid – Mesoporous Silica (S-MS). A schematic figure of the procedure is shown in Figure 8 (HENCH; WEST, 1990).

Figure 8 – Mesoporous silica formation

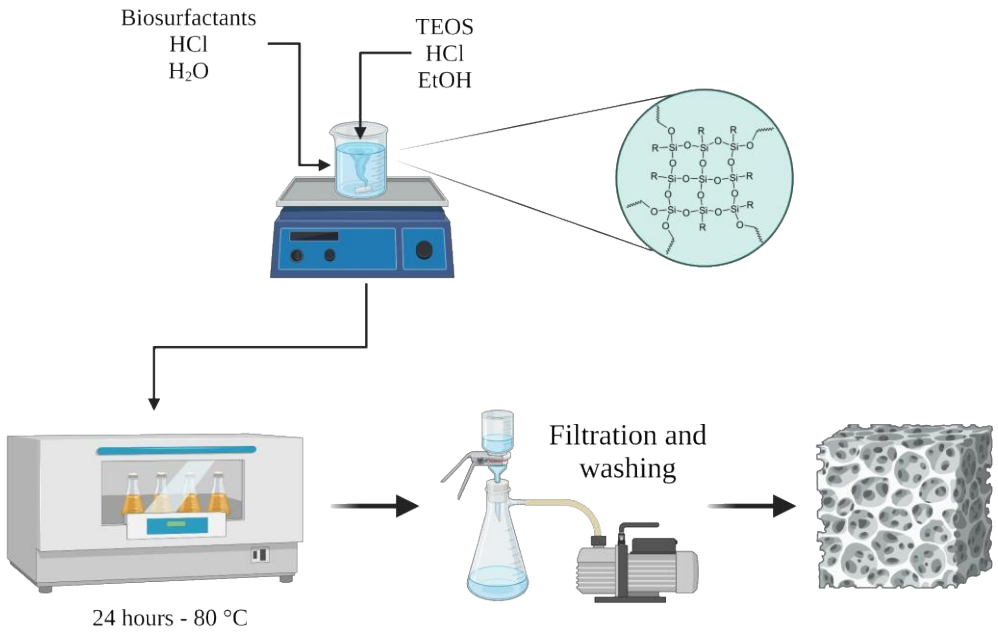

Source: elaborated by the author, using Biorender software (2023)

3.1.4 Synthesis of Y zeolite

For the synthesis of the Y zeolite, different molar ratios between reactants were tested, aiming to synthesize the microporous phase without the use of SDA. The range of molar ratios for each of the reactants is given as: SiO_2 (4.0 – 6.0 – 7.0) and Na_2O (3.2 – 3.5 – 10.6), where the Al_2O_3 and H_2O molar ratios were kept constant at 1.0 and 220, respectively. The crystallization time of the synthesis gel was also tested, aiming to achieve a highly crystalline material.

For all different molar ratios, the procedure parameters were the same. Initially, sodium hydroxide [77.5% Na_2O; 22.5% H_2O] (wt.%) and sodium aluminate [55.0% Al_2O_3; 44.5% Na_2O; 0.5% impurities] (wt.%) were added to the beaker, followed by the addition deionized water, and the solution was mechanically stirred until total dissolution. In the next step, sodium silicate [27.7% SiO_2; 8.6% Na_2O; 63.7% H_2O] (wt.%) was added to the solution under vigorous stirring, where after a few seconds, the silica and alumina molecules started to condensate, forming a white gel, with pH values between 12 – 13. For the crystallization step, the synthesis gel was added to an oven in Teflon-lined stainless-steel autoclaves at 100 °C under autogenous pressure for 36 h, where samples were taken every 6 h of the experiment. After the

crystallization time was finished, the obtained material was washed with distilled water under vacuum until pH ≤ 8 and dried overnight at 60 °C (CONATO *et al.*, 2015).

3.1.5 Synthesis hierarchical Y zeolite

Regarding the synthesis of hierarchical pore zeolites, pure biosurfactants, and biosurfactant functionalized with APTES molecule were used as SDA during the zeolite crystallization step. The methodology was similar to the procedure used in the synthesis of Y zeolite, where the SDAs were added to the solution before the crystallization step.

Initially, sodium hydroxide [77.5% Na_2O; 22.5% H_2O] (wt.%) and sodium aluminate [55.0% Al_2O_3; 44.5% Na_2O; 0.5% impurities] (wt.%) were added to the beaker and dissolved in deionized water. After dissolution, sodium silicate [27.7% SiO_2; 8.6% Na_2O; 63.7% H_2O] (wt.%) was added to the solution under vigorous stirring. After a few seconds, the silica and alumina molecules started to condensate, forming a white gel, with molar composition of $4SiO_2$:$1Al_2O_3$:$10.6Na_2O$:$220H_2O$. The SDA was added during the gel condensation, where for the pure biosurfactant pathway 0.423g was added, and for the biosurfactant-APTES complex pathway 5 mL was added. The gel with the SDA was transferred to a Teflon-lined stainless-steel autoclaves which were placed in an oven at 100 °C under autogenous pressure and left for 24 h to induce zeolite crystallization. After the crystallization time was finished, the obtained material was washed with distilled water under vacuum until pH ≤ 8 and dried overnight at 60 °C. The synthesis procedure is represented in Figure 9.

Figure 9 – Synthesis of hierarchical materials using biosurfactants

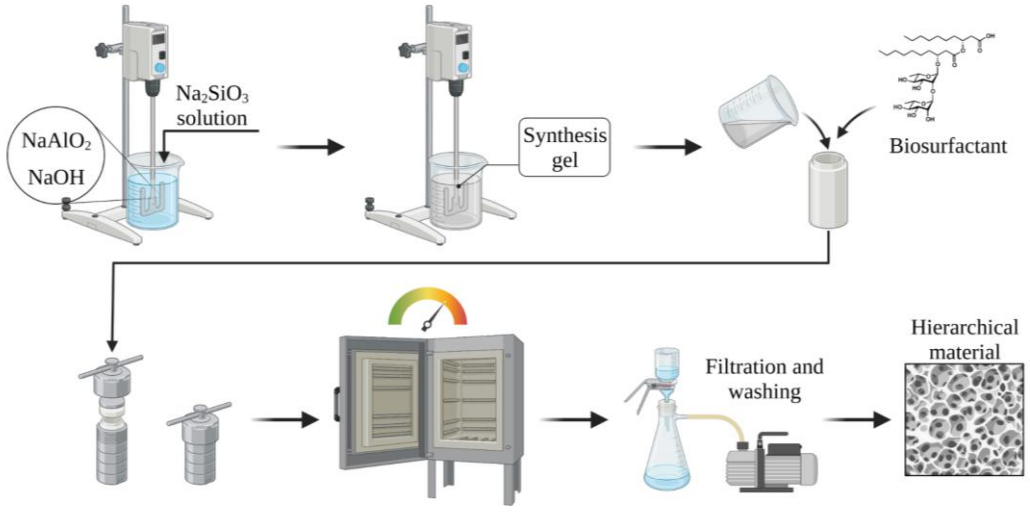

Source: elaborated by the author, using Biorender software (2023)

The obtained hierarchical materials synthesized with pure biosurfactants were identified as Rhamnolipid – Hierarchical Y Zeolite (R-HYZ) and Sophorolipid – Hierarchical Y Zeolite (S-HYZ). As for the materials synthesized with the bio-APTES compounds, identified as Rhamnolipid-APTES – Hierarchical Y Zeolite (RA-HYZ) and Sophorolipid-APTES – Hierarchical Y Zeolite (SA-HYZ).

3.1.6 Characterization of the obtained materials

3.1.6.1 X-Ray Diffraction (XRD)

The X-ray diffraction profiles of the materials were obtained by the Rigaku MiniFlex600 DRX equipment under Cu-Kα radiation (λ = 0.154 nm) in the 2θ angle range from 2˚ to 60˚. From the XRD diffraction pattern, it is possible to evaluate the material crystallinity and identify the Y zeolite formation by comparison with the calculated pattern of Y zeolite found in the Inorganic Crystal Structure Database (ICSD), identified as ICSD_#416357.

All the XRD measurements were conducted in the Interdisciplinary Laboratory for the Development of Nanostructures (LINDEN) of the Department of Chemical Engineering and Food Engineering at the Federal University of Santa Catarina - UFSC.

3.1.6.2 Fourier-Transform Infrared Spectroscopy (FT-IR)

The functional groups of the samples were identified by spectroscopy in the infrared region by Fourier transform using the model equipment Agilent Technologies – Cary 660 FT-IR, using a KBr wafer for the materials analysis, in a range between 400 cm^{-1} – 4000 cm^{-1}. The FT-IR analysis also aimed to verify the functionalization of the silica materials with the APTES and biosurfactant molecules (BRANDENBURG; SEYDEL, 1998). The FT-IR measurements were carried out at the Analysis Center of the Chemical Engineering and Food Engineering Department at the Federal University of Santa Catarina – UFSC.

3.1.6.3 Nitrogen adsorption-desorption experiments

The nitrogen adsorption-desorption experiment - specific surface areas and pore systems, such as pore size, volume, and shape. was carried out using Quantachrome Autosorb-

1. The specific area of the synthesized samples was determined through the BET (Brunauer, Emmett, and Teller) method using the multipoint data of nitrogen adsorption isotherms at 77 K in vapor pressures between 0.01 to 1.0. The pore information was determined by BJH (Barrett, Joyner, and Halenda), and t-plot methods, which calculates porosity parameters from experimental isotherms based on the Kelvin equation of pore filling applied to mesopore and small macropore size ranges and surface N_2 film thickness by gas condensation (LOWELL *et al.*, 2004).

Prior to analysis, the samples were calcined and kept for 24 h at 300 °C under vacuum to promote the volatilization of water vapors and the desorption of possible adsorbed molecules. This analysis was carried out at the Analysis Center of the Department of Chemical Engineering and Food Engineering at Federal University of Santa Catarina - UFSC.

3.1.6.4 Scanning Electron Microscopy (SEM)

SEM micrographs were obtained using a High-Resolution Scanning Microscope (JEOL model JSM-6390LV) at the Central Laboratory of Electronic Microscopy (LCME) at the Federal University of Santa Catarina - UFSC. Scanning electron microscopy was used to verify the morphology of the mesoporous silicas and zeolite crystals obtained in the synthesis process. The samples were coated with a gold layer to avoid the accumulation of electrons on the sample surface that could lead to image distortion (PANEK; WDOWIN; FRANUS, 2014).

3.1.6.5 Transmission Electron Microscopy (TEM)

The sample preparation was carried out by dispersing the material powder in ethanol to deagglomeration in an ultrasonic bath for 60 min or more, where the supernatant was dripped onto copper grids covered with amorphous carbon film (WAN *et al.*, 2018). The TEM images were obtained using a 100 kV JEM-1011 electronic microscope at the Central Laboratory of Electronic Microscopy (LCME) at the Federal University of Santa Catarina - UFSC.

3.2 RESULTS AND DISCUSSION

3.2.1 Silica materials

The weak interaction between anionic and nonionic surfactants with silica species makes its application difficult as SDAs. Different synthesis routes were tested in order to improve the interactions between biosurfactants and silica materials.

3.2.1.1 Synthesis of Biosurfactant-APTES complex

The APTES bonding in the biosurfactant could improve the molecule interaction capability with silica species, allowing the direct the formation of mesoporous during the silica condensation step. The APTES molecule interaction with biosurfactants can occur through covalent bonding or electrostatic interactions between the biosurfactant carboxylic acid moieties and the APTES amino functional group. The covalent bonding interaction between these molecules induces the formation of secondary amides, where electrostatic interactions are the charged forms of the carboxylic acids (COO^-) and amine (NH_3^+) functional groups. The sophorolipid and rhamnolipid interaction with APTES was evaluated through FT-IR analysis. The obtained FT-IR patterns are shown in Figure 10 and
Figure 11.

Figure 10 – FT-IR pattern of (A) R-APTES modified and (B) Pure R-biosurfactant

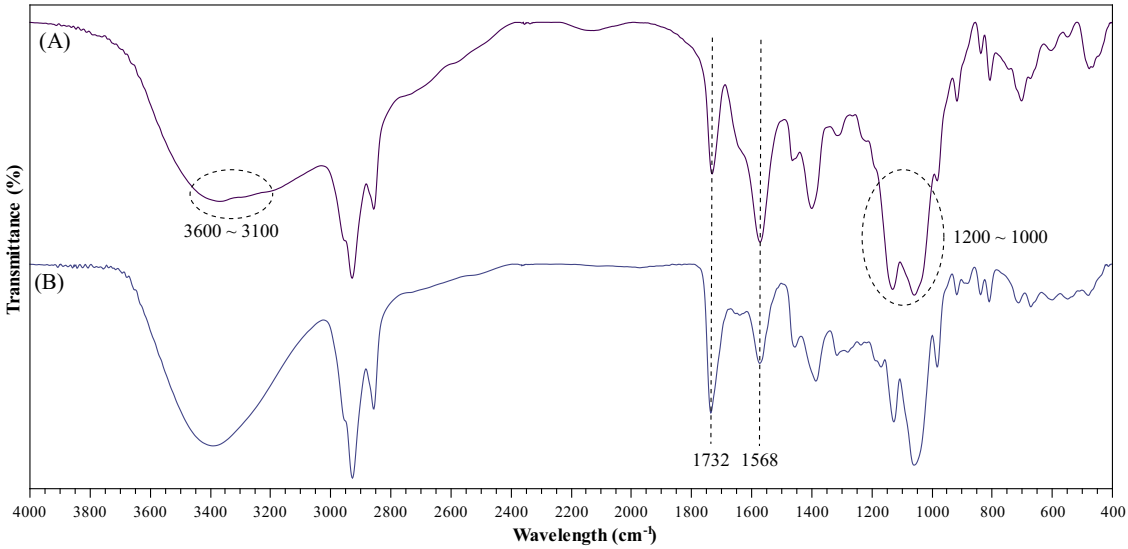

Source: elaborated by the author (2023)

Figure 11 – FT-IR pattern of (A) S-APTES modified and (B) Pure S-biosurfactant

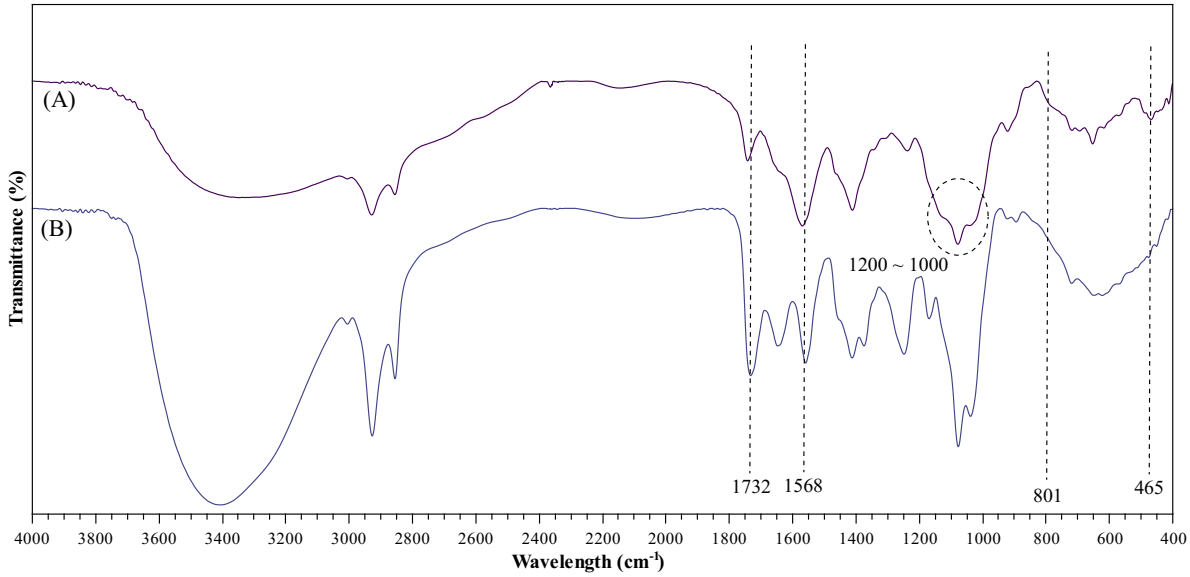

Source: elaborated by the author (2023)

To better understand the different transmittance signals generated in the FT-IR analysis, Table 2 present the functional groups and their respective transmittance signals, found in the free biosurfactants.

Table 2 – transmittance signals of functional groups found in biosurfactant, APTES molecules, and derivatives

Free biosurfactants					
Alcohols	O-H stretch	3700-3000 cm^{-1}	*Carboxylic acid*	O-H stretch	3300-2500 cm^{-1}
	O-H folding	1420-1330 cm^{-1}		C=O stretch	1760 cm^{-1}
Ether	C-O stretch	1150-1085 cm^{-1}		C=O stretch	1720-1706 cm^{-1}
Alkanes	C-H stretch	3100-2841 cm^{-1}		O-H folding	1440-1395 cm^{-1}
	C-H stretch	1450-1465 cm^{-1}	*Alkenes*	C=C stretch	1650-1600 cm^{-1}
	C-C rocking	1145 cm^{-1}	*Ester*	C=O stretch	1730-1715 cm^{-1}
Aromatic	C-H folding	2000-1650 cm^{-1}		C-O stretch	1210-1163 cm^{-1}
	C-O stretch	1310-1250 cm^{-1}	*Ether*	C-O stretch	1150-1085 cm^{-1}
Free APTES					
Amine	N-H stretch	1650-1580 cm^{-1}	*Primary amine*	N-H stretch	3400-3500 cm^{-1}
	C-N stretch	1250-1020 cm^{-1}		C-N stretch	1000-1250 cm^{-1}
	N-H (salt)	3000-2800 cm^{-1}		NH_2 vibration	1550-1650 cm^{-1}

Silicates	Si-O stretch	1000-1250 cm^{-1}	*Secondary amine*	N-H stretch	3350-3310 cm^{-1}
	Si-OH stretch	950-1130 cm^{-1}		C-N stretch	1000-1250 cm^{-1}
	Si-C stretch	1015-1180 cm^{-1}		NH_2 vibration	1500-1600 cm^{-1}
	Si-O-Si symmetric	440-480 cm^{-1}			
	Si-O-Si asymmetric	790-820 cm^{-1}			
Amides					
Primary amide	C=O stretch	1590-1690 cm^{-1}	*Secondary amide*	C=O stretch	1500-1650 cm^{-1}
	N-H stretch	3170-3500 cm^{-1}		N-H stretch	3170-3500 cm^{-1}
	C-N stretch	1410-1450 cm^{-1}		C-N stretch	1410-1450 cm^{-1}

Source: elaborated by the author (2023)

Through Figure 10 and
Figure 11, it was possible to notice that both electrostatic and covalent interactions occurred in the synthesis process. The bands at 1568 cm^{-1} and 1732 cm^{-1} are related to the C=O stretch. A decrease in the magnitude of the 1732 cm^{-1} band could be observed, which is related to the C=O stretch in the carboxylic functional group, linked to an increase in the 1568 cm^{-1} band, which is related to the C=O stretch in the amide functional group (DARDOURI *et al.*, 2021; THOMAS *et al.*, 2014). The presence of these two signals indicates the formation of an amide functional group which intensifies the 1568 cm^{-1} band. At the same time, the band at 1732 cm^{-1} is still present with lower intensity indicating the presence of carboxylic acid groups. This pattern occurs for APTES interaction with both rhamnolipid and sophorolipid.

The rhamnolipid interaction with the APTES molecule presents bands related to the primary amine moieties (N-H), observed in the 3100 – 3600 cm^{-1} regions, which probably is related to the electrostatic interaction between the molecules (SARAVANAN *et al.*, 2018). Bands related to the silica interactions could be seen for both FT-IR, where for the rhamnolipid surfactant (Figure 10), it is possible to observe the signal widening in the region of 1000 – 1200 cm^{-1}, probably related to the covalent Si-O bond found in the APTES molecule (WIDJONARKO *et al.*, 2014). This signal is also observed in

Figure 11, along with more distinct signs of the presence of Si-X groups which could interact with other APTES molecules through silica polymerization, leading to 465 cm^{-1} and

801 cm^{-1} bands related to symmetric and asymmetric Si-O-Si bounds(SARAVANAN *et al.*, 2018; WIDJONARKO *et al.*, 2014).

From the FT-IR analysis, it is possible to notice that both electrostatic and covalent interactions have occurred. In the rhamnolipid, the electrostatic interaction is more evident, and in the sophorolipid, the APTES presence is more visible, which may indicate the presence of amide formation.

3.2.1.2 Synthesis of functionalized silicas

To a better understanding of the interaction between biosurfactants and silica materials, silica with a high surface area (> 800 m^2/g) was used as supporting material for biosurfactants using the APTES molecule as a linker between the silica surface and the biosurfactants. To confirm the formation of the bonds, the materials were submitted to FT-IR analysis, which is shown in Figure 12.

Figure 12 – FT-IR analysis of (A) PS; (B) APTES-modified silica; (C) R-APTES-modified silica; (D) S-APTES-modified silica

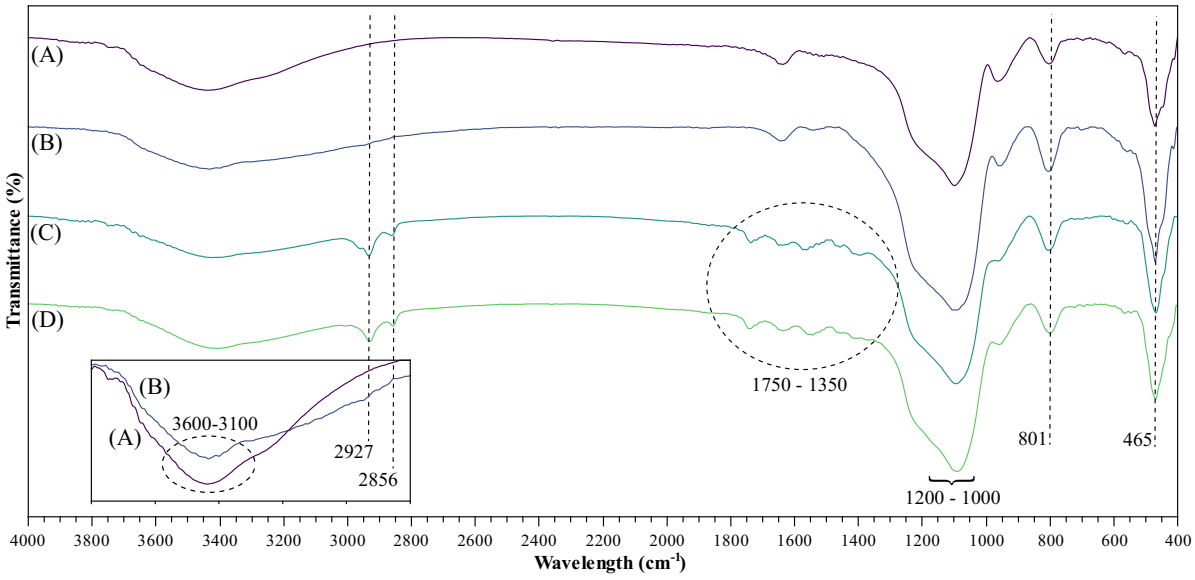

Source: elaborated by the author (2023)

The obtained FT-IR spectra for the APTES functionalization of PS, (A) and (B) spectra, indicates that the APTES molecule was successfully incorporated into the pure silica material by the two disturbances in the 3600 – 3100 cm^{-1} region, related to the N-H stretch of

primary and secondary amines and by the bands in 2927 cm^{-1} and 2856 cm^{-1}, related to symmetric and asymmetric vibration of the C-H group (SARAVANAN *et al.*, 2018).

The binding of the rhamnolipid and sophorolipid biosurfactants to the amino-functionalized silica surface was also indicated by the (C) and (D) FT-IR spectra (Figure 12), related to the rhamnolipid and sophorolipid, respectively. It is possible to notice the intensification of the C-H vibration bands at 2927 cm^{-1} and 2856 cm^{-1}, due to the concentration increase of the C-H groups found in the biosurfactants molecules (DARDOURI *et al.*, 2021; DAVEREY; PAKSHIRAJAN, 2009). Both rhamnolipid and sophorolipid biosurfactants present similar organic functional groups, in which FT-IR bands can be seen in the region of 1350 to 1750 cm^{-1} related to C-O, C=O, C-C, C-H, and among other organic groups, being these bands the identification of both rhamnolipid and sophorolipid (DARDOURI *et al.*, 2021; THOMAS *et al.*, 2014). However, the low intensity of FT-IR bands in the functionalized silica materials is due to the small concentration of both APTES and biosurfactants molecules on the silica surface.

From the FT-IR results it is also possible to identify the FT-IR spectra bands related to the silica material, in the wavenumber region of 1000 to 1200 cm^{-1}, related to Si-O stretch, and the bands at 465 cm^{-1} and 801 cm^{-1} refereed to symmetric and asymmetric Si-O-Si bonds vibrations (WIDJONARKO *et al.*, 2014).

3.2.2 Synthesis of mesoporous silicas using biosurfactants as SDAs

The utilization of synthetic surfactants in the synthesis of silica materials directs the formation of ordered micro and mesoporous systems in the obtained material (WAN; ZHAO, 2007). Alternatively, to direct the formation of mesopores in silica materials R and S biosurfactants were used as SDAs through acid sol-gel method, by adding the pure biosurfactant or the functionalized biosurfactant in the silica condensation step. The obtained materials were evaluated through N_2 adsorption and desorption isotherms, using BET/BJH methods and through TEM images. The results obtained by textural analysis are shown in Figure 13.

Figure 13 – N_2 adsorption and desorption isotherms and pore size distributions of S-MS R-MS PS

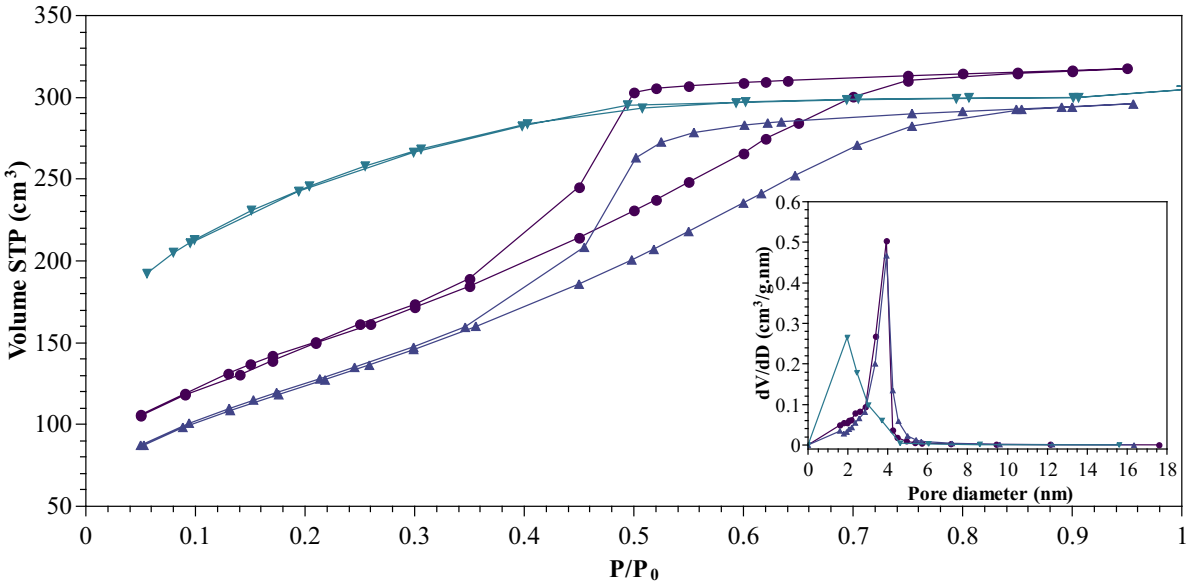

Source: elaborated by the author (2023)

The obtained adsorption and desorption isotherm for the pure silica material is typical for this class of materials (THOMMES *et al.*, 2015). The pure silica shows a type I isotherm without hysteresis loops, showing a high surface area of 852.00 m^2/g. The porous properties of the obtained material are related to narrow pores presenting an average pore size of 2.217 nm. The sample did not show the formation of mesoporous (absence of hysteresis loop) and presented low micropore formation.

To attribute larger pores sizes to the silica materials, rhamnolipids, and sophorolipids were used as SDAs in the synthesis process. The obtained isotherms show a behavior characteristic of organically templated mesoporous networks, where a type IV isotherm with an H2 hysteresis loop can be seen for both R-MS and S-MS materials, being characteristic of a complex network of interconnected pores of different sizes and shapes. When a type IV isotherm, accompanied by a hysteresis loop, is obtained from a porous material under N_2 adsorption/desorption process at 77 K, the hysteresis loop indicates that the material pore diameter exceeds a certain critical diameter (larger than ~ 4 nm) (THOMMES *et al.*, 2015).

Hysteresis loops are generally associated with different mechanisms occurring in the material pores during the adsorption and desorption processes, where during the adsorption process, the pores are filled through capillary condensation by the formation of multiple layers of adsorbate molecules in the pore wall until it is completely filled, on the other hand, in the desorption process a reversible liquid-vapor mechanism occurs, reaching a thermodynamic

equilibrium during the desorption process. These different mechanisms provide important information on the type and shape of the pores in the material under analysis. The hysteresis observed in the R-MS and S-MS materials is related to H2 type hysteresis, which is characterized by complex pore structures in which network effects are important, being attributed to pore-blocking/percolation in a narrow range of pore necks or to cavitation-induced evaporation, being found in many silica gels, as well as some ordered mesoporous materials (e.g., SBA-16 and KIT-5 silicas) (THOMMES *et al.*, 2015).

The textural data obtained from the adsorption and desorption of N_2 isotherms using BET, BJH and t-plot methods for pure silica material and modified silicas are shown in Table 3, allowing the properties comparison among these materials.

Table 3 – Surface and porosity parameters for the materials obtained through biosurfactant modification

Sample	S_{BET} (m^2/g)	Average P_{Size} (nm)	High occurrence P_{Size} (nm)	V_{total} (mL/g)	V_{meso} (mL/g)
PS	852.000	2.217	1.957	0.471	0.460
R-MS	462.200	3.955	3.940	0.458	0.437
S-MS	514.200	3.609	3.930	0.491	0.480

Source: elaborated by the author (2023)

From the analysis of data obtained from N_2 adsorption and desorption isotherms, it is possible to observe an increase in the pore size of the material synthesized in the presence of rhamnolipid and sophorolipid biosurfactants. When an SDA was used to synthesize a determined material, one could expect that the porous property of the synthesized material shows sizes and shapes analogous to the self-aggregation forms - SDA. Considering that the size of rhamnolipids and sophorolipids are lower than 2.5 nm, and the corresponding self-aggregation form diameters lower than 5 nm, the obtained results for the materials synthesized using the biosurfactants as SDAs show pore diameters in the expected range. The specific surface area (S_{BET}) of MS-R and MS-S materials decreased for both materials, together with an increase in the pore size (P_{size}). Comparing the R-MS and S-MS materials, a higher average pore size could be seen for the MS-R material, which is probably related to the large molecule of di-rhamnolipid when compared to the sophorolipid molecule since the used reagent presented a mixture of both mono and di-rhamnolipid biosurfactants. The mesopore volume (V_{meso}) of R-MS material presented a smaller value when compared to the PS and S-MS materials. However,

both R-MS and S-MS materials presented the highest pore occurrence in the range of 3.940 and 3.930 nm, respectively, showing no significant difference in the use of rhamnolipid and sophorolipid as mesoporous inducers. To support the formation of complex pore structures, a TEM images of the synthesized materials were obtained, and the results shown in Figure 14.

Figure 14 – TEM images of the synthesized mesoporous materials

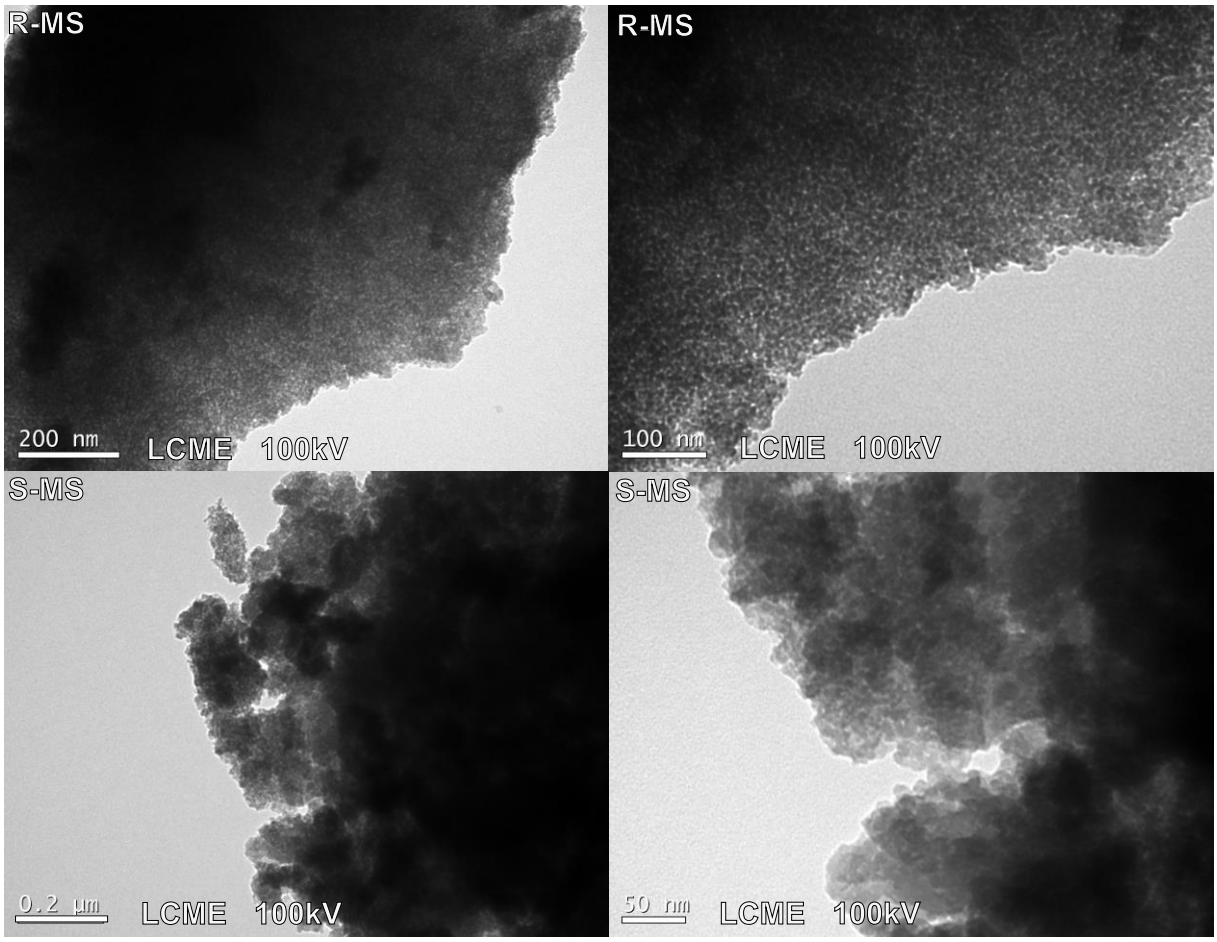

Source: elaborated by the author (2023)

From TEM images, it is possible to observe that a sponge-like morphology with randomly oriented mesopores was obtained, guaranteeing accessible porosity over the whole particle. The obtained images are aligned with Enterría *et al.* (2014) and Thomas *et al.* (2014) mesoporous silica materials which synthesis of mesoporous silicas. It is worth noting that Thomas *et al.* (2014) used sophorolipids biosurfactants as mesopore inducer.

3.2.3 Synthesis of Y zeolite

As a first step, the Y zeolite was synthesized without the use of SDAs to achieve the microporous zeolite structure, aiming the use of the rhamnolipid and sophorolipid biosurfactants as mesopores inducers. For the zeolite synthesis, sodium silicate (Na_2SiO_3) was used as a silica source, sodium aluminate ($NaAlO_2$) as an alumina source, and sodium hydroxide (NaOH) as a mineralizing agent. The reagent molar ratios were varied, and their impact on the obtained material was evaluated, being the obtained results shown in Figure 15.

Figure 15 – XRD of different gel molar rations in the synthesis of pure Y zeolite

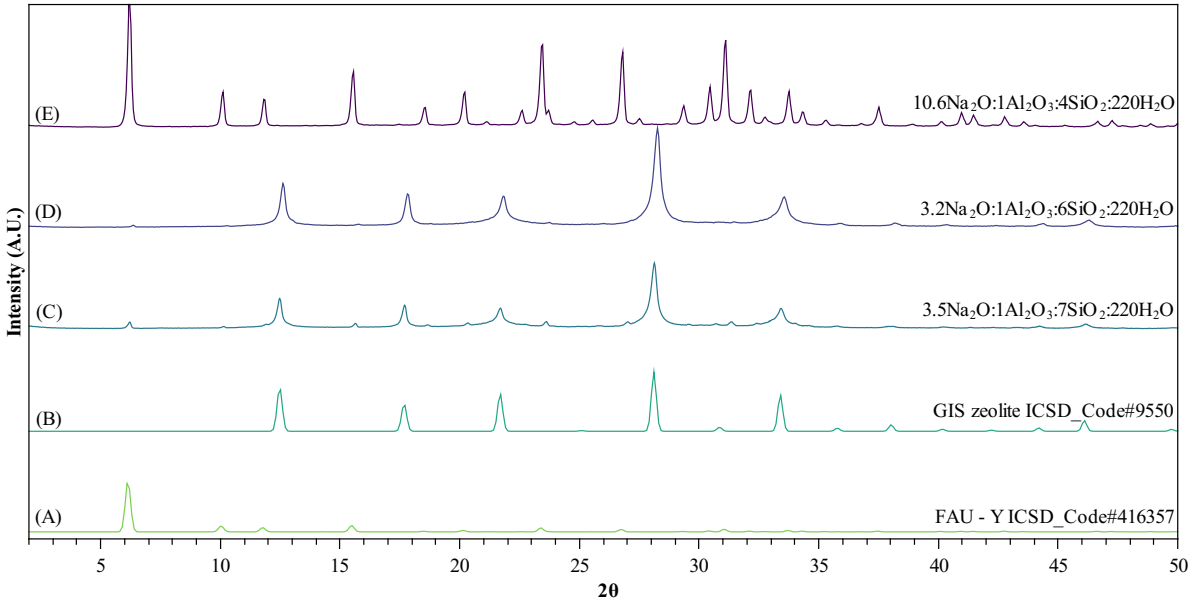

Source: elaborated by the author (2023)

Through the analysis of Figure 15, it is possible to notice the formation of faujasite (FAU – Y) and gismondine (GIS) zeolites from the initial synthesis gel, being these phases identified by comparison with crystallographic patterns of these phases, found in the Inorganic Crystal Structure Database (ICSD) of FIZ Karlsruhe – Leibniz Institute for Information Infrastructure. The FAU-Y pattern is related to the ICSD code #416357, and the GIS pattern is related to the ICSD code #9550. The pure Y zeolite pattern was just observed in the (E) diffraction pattern, where peaks related to the GIS phase could not be observed. The zeolite crystallization during the synthesis process depends on the starting gel building units, which will favor the formation of the more thermodynamically metastable structure, being this process described by the Ostwald rule of stages, where the use of SDAs during the synthesis process

provides kinetic pathways to synthesize less thermodynamically stable structures (MALDONADO *et al.*, 2013). Usually, the crystallization of more than one structure during the synthesis process will occur when both zeolitic structures share the same building unit. However, in some cases, the crystalized zeolites present no apparent structural similarity, being the case of the co-crystallization of FAU (Y zeolite) and GIS (gismondine) zeolites in temperatures close to 100 °C (CONATO *et al.*, 2015; MALLETTE *et al.*, 2022).

The FAU-type zeolites form their structures from sod and d6r building units, and GIS-type zeolites crystalize from gis and dcc building units. The FAU and GIS building have no similarities between them. Therefore, possibly both building units are formed in the initial synthesis gel, leading to the co-crystallization of these two phases. As the Si/Al ratio decreases in the synthesis gel, the formation of more closely packed and thermodynamically metastable phase is formed, being the case of the FAU type zeolites, which presents a cubic F d -3 m structure with packing parameter of 0.74, a value higher than GIS zeolites, which presents a tetragonal I 41/a m d structure with packing parameter of 0.52 (MALLETTE *et al.*, 2022).

The gel molar ratio required to achieve microporous Y zeolite through the synthesis process is $10.6Na_2O{:}1Al_2O_3{:}4SiO_2{:}220H_2O$. In order to evaluate the optimal synthesis conditions, a crystallization kinetics procedure was conducted, and the results are shown in Figure 16.

Figure 16 – Crystallization kinetics of pure Y zeolite

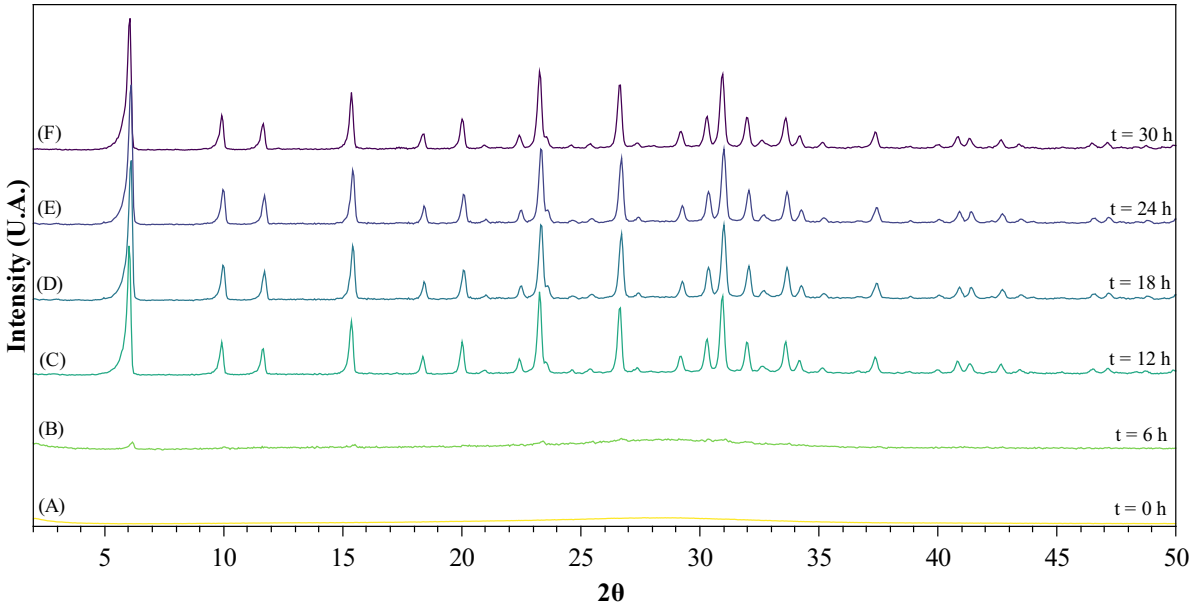

Source: elaborated by the author (2023)

From Figure 16, it is possible to notice that the Y zeolite structure is formed within 12h under hydrothermal conditions no significative changes could be seen from higher crystallization times. Using the Scherrer equation, which relates the width at half height of the peaks in 2θ of the diffraction pattern, it is possible to qualitatively measure the particle size of the synthesized material obtained after 12 and 30 hours of hydrothermal crystallization, noticing a decrease in the crystal size as the synthesis time increases, where for the 12 h of crystallization time, the crystallite size was 41.78 nm and for the material after 30 h of hydrothermal crystallization the crystallite size was of 39.62 nm, being the obtained crystallites in the nanosized range. Zeolites with crystallite sizes in the range of 10 – 100 nm have already been reported in literature, obtained by using SDAs in the synthesis process and for SDA free synthesis with low Si/Al ratios at temperatures close to 100 °C (MASTROPIETRO; DRIOLI; POERIO, 2014; MORALES-PACHECO *et al.*, 2009).

3.2.4 Synthesis of hierarchical Y zeolite

After achieving both microporous and mesoporous structures, the hierarchical Y zeolite structure was synthesized using the biosurfactants molecules as mesoporous inducers, proved in the synthesis of mesoporous silicas. For the synthesis of hierarchical materials, pure rhamnolipids and sophorolipids biosurfactants, and APTES-biosurfactants compounds were used as mesopores inducers for materials synthesis. Initially an XRD of the obtained materials was conducted to prove the microporous Y zeolite formation, being the results shown in Figure 17.

Figure 17 – XRD of pure Y zeolite and Y zeolites modified with rhamnolipids and sophorolipids

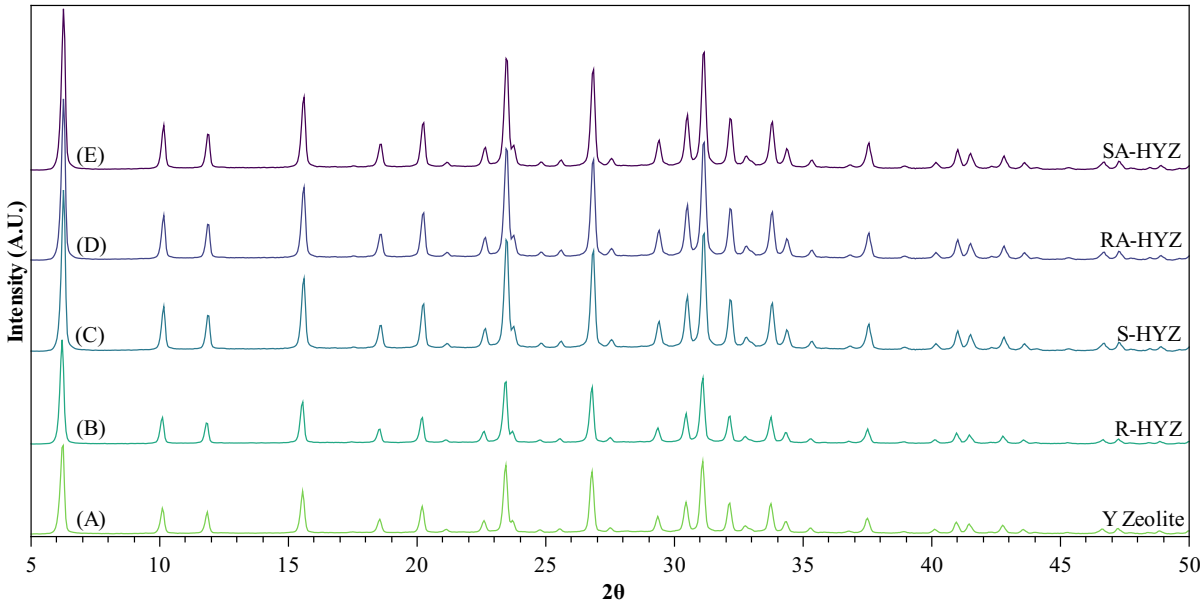

Source: elaborated by the author (2023)

From Figure 17, no significant changes could be seen from XRD patterns of the materials modified with pure biosurfactants and with Bio-APTES compounds. Taking into consideration the Y zeolite crystallinity, the addition of biosurfactants subtly decreased the crystallinity, on the other hand the R-HYZ sample did not show a decrease in the material crystallinity. The reason for no visible changes in the XRD patterns was due to the use of the biosurfactants SDAs just as mesopore inducers, which are characterized as a non-ordered or low-ordered phase, leading to no apparent changes in XRD patterns. For a better understanding of biosurfactants, and compounds influence on hierarchical Y zeolite synthesis, scanning electron microscopy (SEM) was carried out on the materials modified with biosurfactants, and for the pure Y zeolite, the results are shown in Figure 18.

Figure 18 – SEM image of I(a) Pure Y zeolite; I(b) Pure Y zeolite; (II) R-HYZ; (III) S-HYZ; (IV) RA-HYZ and (V) SA-HYZ

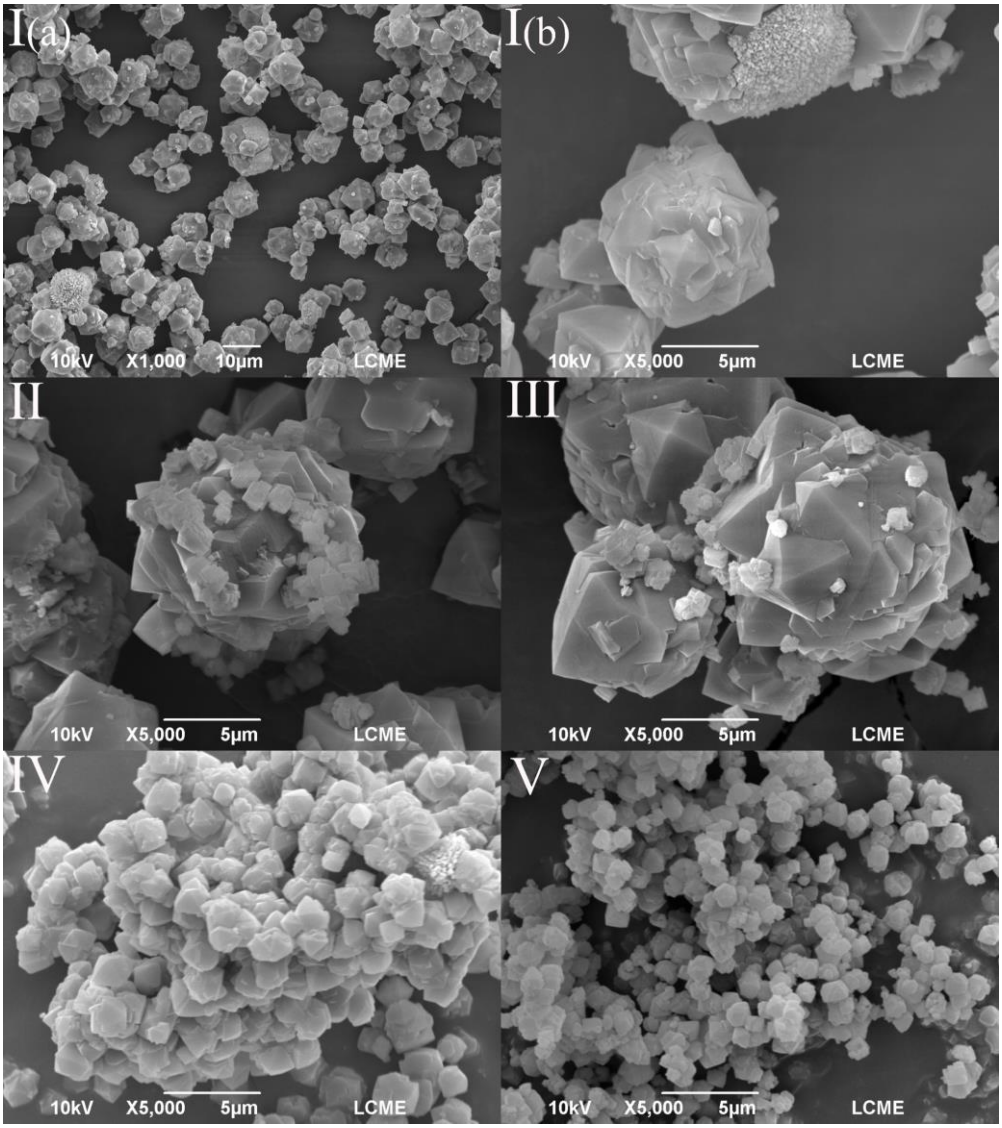

Source: elaborated by the author (2023)

From SEM images, it is possible to confirm the formation of the Y zeolite material by the formation of cubic-octahedrally shaped particles for all samples, characteristic morphology for this type of material (DABBAWALA *et al.*, 2020). The pure Y zeolite material presented particles in the micrometer level with an average particle size distribution of 4.851±1.688 μm.

Even though all samples show the same morphology, a clear decrease in particle size could be seen when biosurfactant compounds are applied to the synthesis process. For the materials synthesized with the pure rhamnolipid and sophorolipids biosurfactants (R-HYZ and S-HYZ), a co-existence of big-sized particles and small-sized particles is seen, where the overall particle size distribution for R-HYZ and S-HYZ materials are 1.603±2.865 and

1.474±3.084 µm, respectively. The co-existence of both degrees of particle sizes leads to high values of particle size standard deviation, as the obtained values in this case. Therefore, when the biosurfactant-APTES compounds were used in the synthesis process, it was possible to observe an extinction of the larger particles for both RA-HYZ and SA-HYZ materials, leading to uniform micrometer-sized particles. The particle size distribution for these materials is 1.859±0.265 for RA-HYZ and 1.117±0.317 µm for SA-HYZ.

These results are similar to Kannangara *et al.* (2020), where the authors used sodium dodecyl sulfate (SDS), an anionic surfactant, as a particle size-controlling agent, showing that this surfactant induces fast nucleation and formation of smaller crystals with a narrow particle size distribution, also decreasing the agglomeration between the precursor and crystalline particles. Contributing with the morphological analysis of the synthesized materials, TEM images of the obtained hierarchical materials were shown in Figure 19

Figure 19 – TEM images of synthesized hierarchical materials.

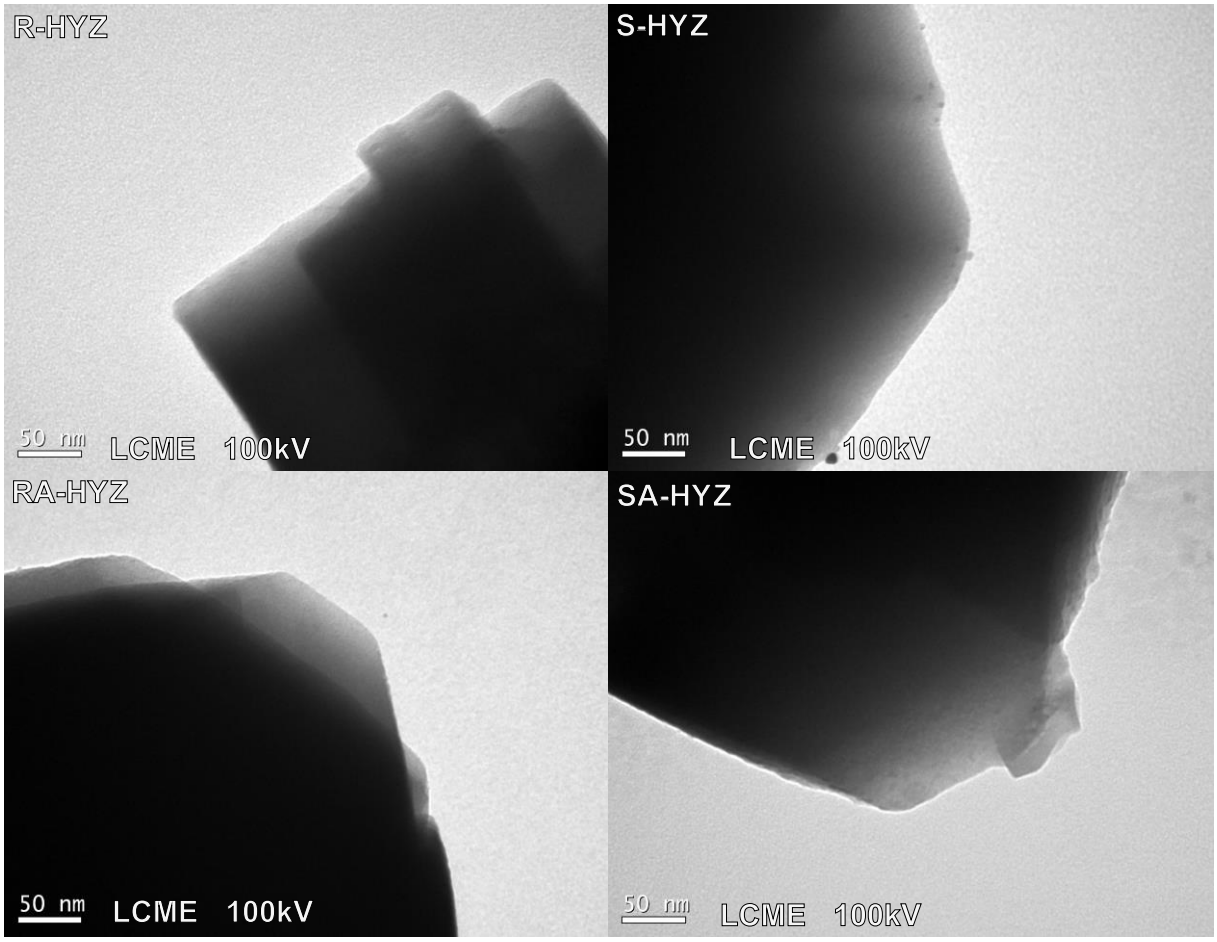

Source: elaborated by the author (2023)

From TEM images, it is clear that the Y zeolite material was obtained, presenting characteristic particles morphologies for these material type (INAYAT *et al.*, 2012). However, the microporous structures of the synthesized materials were not seen from the obtained images, been a High-Resolution Transmission Electron Microscopy (HRTEM) necessary to access microporosity.

The nitrogen adsorption/desorption analysis of the materials obtained using biosurfactants and APTES-biosurfactants compounds as SDAs, will elucidate the assumptions made by SEM and TEM images analysis on the materials' structural properties. The obtained results are shown in Figure 20.

Figure 20 – N_2 adsorption/desorption isotherms of the synthesized materials SA-HYZ RA-HYZ S-HYZ R-HYZ Y zeolite

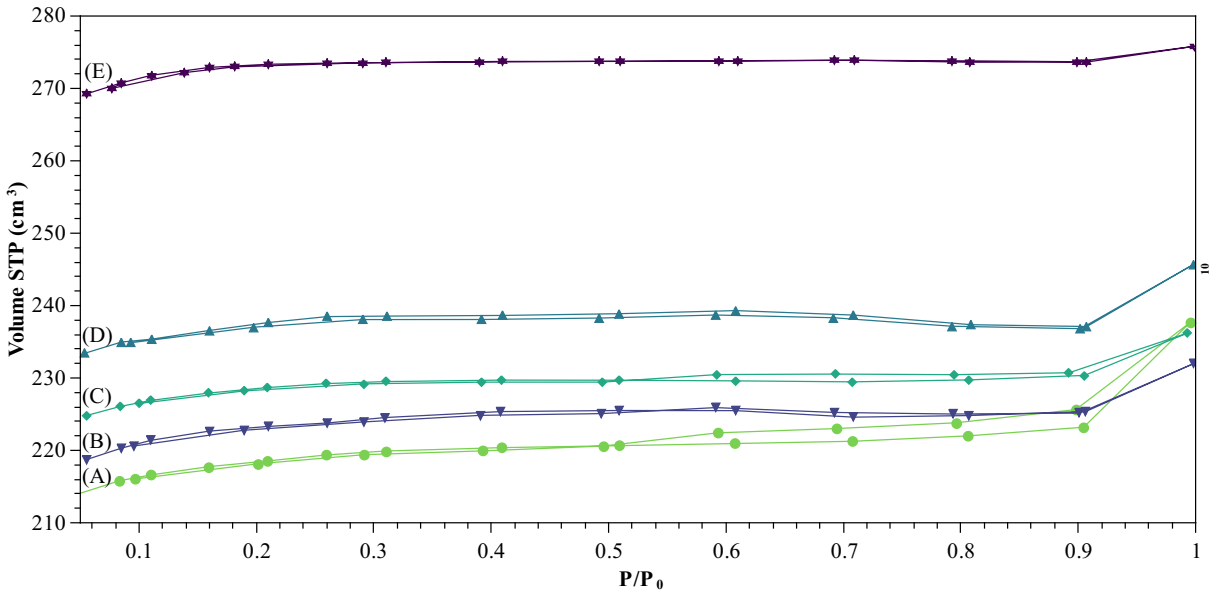

Source: elaborated by the author (2023)

From nitrogen adsorption/desorption analysis, it could be seen that for all samples, mixtures of type I(b) and II isotherms were obtained, presented by uptake at a low relative pressure range with an increase in the thickness of the N_2 multilayer at relative pressure close to ~1 (THOMMES *et al.*, 2015). The pure biosurfactants and the APTES-Biosurfactants compounds modified the porous properties of the synthesized materials and their influence in the synthesis process seen from the formation of hysteresis loops in the microporous Y zeolite. The absence of hysteresis loops on microporous materials is characteristic when N_2 molecules fill the micropores at low relative pressures (< 0.1), showing no influence in the desorption

procedure. However, in materials with pore diameters greater than 2.0 nm, the pore filling occurs at higher relative pressures, leading to different adsorption and desorption mechanisms inside the pores. In this case, H4 hysteresis loops are formed during the desorption process, which is characterized by a sharp step-down of the desorption branch in a narrow range of P/P_0, where for N_2 adsorption/desorption at 77 K, the relative pressure range is between 0.4 – 0.5. The H4 hysteresis loop is a common feature of type I and II isotherms, when larger pore systems are attributed to the material under analysis (VU; HARTH; WILDE, 2018).

To better understand the pore properties of the synthesized materials, a Pore Size Distribution (PSD) was obtained through the BJH method based on the desorption branch of the N_2 adsorption/desorption analysis. The results are shown in Figure 21.

Figure 21 – Pore size distribution of the synthesized materials; Y zeolite R-HYZ S-HYZ RA-HYZ SA-HYZ

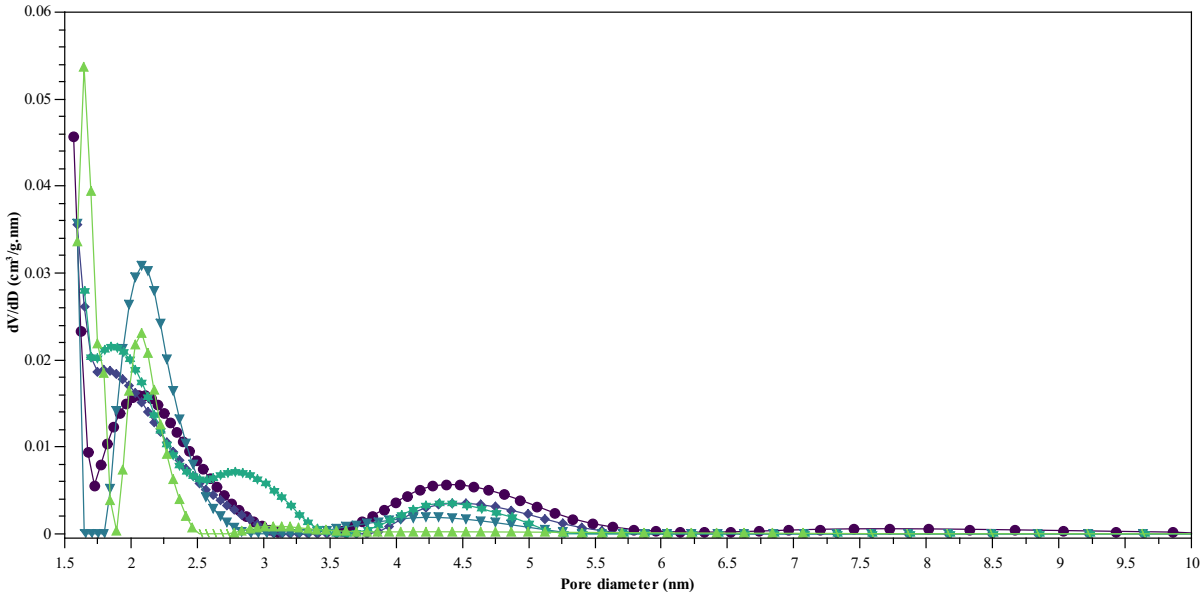

Source: elaborated by the author (2023)

The textural properties of the synthesized materials were evaluated from N_2 adsorption and desorption data using BET, BJH, and the t-plot methods. To estimate the specific surface area (S_{BET}) of the synthesized material the BET theory was applied, based on monolayer surface coverage, which is obtained from relative pressure (P/P_0) in the range between 0.05 – 0.35 of adsorption isotherm, where a linear region takes place, which will depend on adsorbate and adsorbent types, as well as the physisorption temperature (LOWELL *et al.*, 2004).

To estimate the porous properties of the synthesized materials, the pore shape was considered cylindrical, and mechanisms occurring inside the pores result from both the pore wall physical adsorption and capillary condensation. This assumption allows the application of the BJH method, considering the N_2 desorption branch, which is based on the Kelvin equation, considering the pore radius as the sum of the multilayer thickness and the meniscus radius. The changes in the layer thickness from the decrease of relative pressure are related to the evacuation of the largest pores through capillary condensation (BARDESTANI; PATIENCE; KALIAGUINE, 2019).

For microporous and mesoporous volumes, the t-plot method was used, which considers the use of standard adsorption isotherms, relating the statistical film thickness on a flat surface as a function of pressure for the same adsorbate and temperature. The micropore and mesopore volumes are related to the t-plot behavior, where all linear regimes provide evidence that adsorption, for that specific pressure range, is taking place similarly as on a flat surface, and any departure from that indicates the presence of a porosity getting filled. The pore volumes are related to the corresponding pressure at which this departure is observed (GALARNEAU *et al.*, 2014). The results obtained from the BET, BJH, and t-plot methods are summarized in Table 4.

Table 4 – Textural properties of the synthesized samples

Sample	**S_{BET} (m^2/g)**	**Average P_{Size} (nm)**	**V_{Micro} (cm^3/g)**	**V_{Meso} (cm^3/g)**	**Mesopore (%)**
Y zeolite	853.80	1.949	0.426	---	---
HYZ-R	699.40	2.058	0.315	0.033	9.50
HYZ-S	745.50	2.044	0.344	0.025	6.78
HYZ-APTES-R	716.50	2.044	0.329	0.025	7.06
HYZ-APTES-S	688.40	2.141	0.312	0.029	8.50

Source: elaborated by the author (2023)

From the obtained data, the materials S_{BET} decreased when the biosurfactants were used in the synthesis process, which could be related to the mesopores formation in the material structure, where micropores ensure greater use of the surface area of material when compared to mesopores. The materials with higher values of average pore size (P_{size}) and mesoporous volume (V_{meso}) were the materials that showed the lowest surface area values, agreeing with the assumption that the mesopores formation leads to a decrease in the specific surface area. The

SA-HYZ material showed the higher mesopore formation, related to P_{size} and V_{meso} values, and consequently the lowest specific surface area, a result that is in agreement with the obtained by Vu, Harth and Wilde (2018) in the syntheses of hierarchical Y zeolites for aqueous-phase hydrogenation.

From Figure 21 it is possible to notice three main regions of pores, where the first region is related to micropores, showing a concentration of pores bellow 2.0 nm. The second region is related to narrow mesopores, being in the range of 2.0 – 3.0 nm, and the third region, which is related to mesopores formation, covering the range of 3.0 – 5.5 nm. The pure Y zeolite showed a concentration of pores just in the first and second regions of the PSD, indicating the presence of micropores and narrow mesopores on its structure. For all the samples synthesized with biosurfactants compounds, the three regions are present in the PSD graph (Figure 21), proving that the use of rhamnolipids and sophorolipids, as well as their combination with the APTES molecule, leads to the formation of mesopores in the material structure.

For samples synthesized with pure rhamnolipids and sophorolipids, major differences from pure Y zeolite were observed. In the narrow mesopores range, the presence of rhamnolipid biosurfactant showed a higher concentration of pores in the narrow mesopores range, leading to pores with larger diameters in this region. Therefore, for the sophorolipid biosurfactant, a higher concentration of narrow mesopores, when compared with pure Y zeolite, was observed with a high concentration of pores with ~ 2.1 nm. Regarding the mesoporous range, a slight concentration of pores could be observed for both biosurfactants.

Materials synthesized with the APTES-Biosurfactant compounds showed a different behavior when compared to the materials synthesized with the pure biosurfactants, and the pure Y zeolite. For both RA-HYZ and SA-HYZ materials, a decrease in the concentration of pores in the narrow mesopore size region (2.0 – 3.0 nm) and an increase in the mesoporous region (3.0 – 5.5 nm) could be observed. This behavior is probably related to the increase in the molecule structure due to the interaction with the APTES molecule, favoring the formation of larger pores and disfavoring the formation of pores in the narrow mesopore range.

To calculate mesopore and micropores volumes, the t-plot method was applied. Plotting the amount of adsorbed volume (V_{ads}) vs. the monolayer thickness (t), a t-curve is obtained, giving information about microporous and mesoporous volumes. Classically, the behavior of the t-curve indicates the volume of mesoporous and microporous materials. For mesoporous materials, the t-curve has a straight regime going through the origin, and the y-intercept of the linear regime after condensation gives the mesopore volume. Microporous

materials also present two linear regimes in the t-plot curve. However, the first regime doesn't go through the origin, indicating the presence of microporosity, being the micropore volume related to the y-intercept of the first linear region of the t-curve (LOWELL *et al.*, 2004). Therefore, for materials with both microporous and mesoporous structures, a correction of this method needs to be done, as evidenced by Galarneau *et al.* (2014) in the validity of the t-plot method to assess microporosity in hierarchical materials, due to the fact that this method does not capture the effect of curvature on the thickness of the adsorbed film. Using the linear correction suggested by the authors, the obtained values for the hierarchical materials are shown in Table 4.

The pure Y zeolite exhibited higher values of microporous volumes and, consequently, higher values of S_{BET}. When biosurfactants were used in the synthesis process, a decrease in the microporous volume and the formation of mesopores could be observed. The highest values of mesopores were observed for R-HYZ and SA-HYZ materials, with values of 9.50% and 8.50%, respectively. The obtained results indicate that rhamnolipid generates a higher formation of mesopores than sophorolipid when pure biosurfactants are used. For the materials synthesized with the biosurfactant-APTES compounds, a higher value of mesopore formation was observed when the APTES-sophorolipid compound was used, probably due to a better interaction between the acid form of sophorolipid and the APTES molecule.

The bottom-up technique is widely used in the research field to generate mesoporosity on zeolites, where different compounds are used as SDAs in this process. Dabbawala *et al.* (2020) used a bi-functional cationic polymer (polydiallyldimethyl ammonium chloride) as SDA in the synthesis of mesoporous Y zeolite leading to an average pore size ranging from 3.6 – 3.8 nm, where the amount of mesopores increase as the SDA concentration increased, going from 6.6% to 33.0% of mesopores, but a decrease in the zeolite was also observed when the SDA concentration increased. The same behavior was observed by Zhao and colaborators (2016) in the use of pluronic F127 block co-polymers as SDA, where the increase on SDA concentration also decreases the crystallinity and increases the mesopore volumes of obtained materials, leading to a high concentration of pores in the range of 3.0 – 5.0 nm and mesopores volumes ranging from 30 to 50 %. When synthetic surfactants were used as SDAs, lower mesopores volumes were observed, probably due to the smaller molecular size, as demonstrated by Martins *et al.* (2021), who used CTAB (cetyltrimethylammonium bromide) and DTAB (dodecyltrimethylammonium bromide) as SDAs, leading to mesoporous volumes close to 17%

for CTAB and 20% for DTAB with the highest concentration of pores in the size range of 3.0 – 8.0 nm.

When comparing the results obtained using biosurfactants compounds as SDAs in the synthesis of hierarchical zeolites with the ones obtained by using polymers and synthetic surfactants, the mesopore sizes are similar for both cases, leading to the formation of pores in the range of 3.0 to 8.0 nm. However, the concentration of mesopores in the materials obtained through polymers and synthetic surfactants is higher than the ones obtained from biosurfactants, probably due to the weaker interaction between non-ionic/anionic biosurfactant with silica and alumina species, when compared to classically used synthetic cationic compounds as SDAs in the synthesis process.

CHAPTER IV

This chapter presents a general conclusion of the dissertation in addition to future outlooks to continue this research project.

4 CONCLUSION

Biosurfactants as structure-directing agents in porous materials synthesis is an important step forward toward green chemistry, in addition to applying the unique self-aggregation structures induced by biosurfactants, which could lead to different porous shapes and organizations in the synthesized materials. The main challenge in the application of biosurfactants is their anionic/nonionic nature, which hinders their direct interaction with silica species. The application of biosurfactants as mesopores inducers has been proved through acid sol-gel synthesis, resulting in materials with type I isotherms and H4 hysteresis loops, indicating mesopore formation.

Regarding hierarchical Y zeolite synthesis, the pure biosurfactants and their combination with APTES molecules used as SDAs proved to act as a mesopore inducers, where the combination of APTES molecules to the biosurfactants contributed increase the formation of mesopores in the range of 3.0 nm to 5.5 nm, and pure biosurfactants lead to higher concentration of mesopores in the narrow mesopore range between 2.0 nm – 3.0 nm. A major influence of biosurfactants in hierarchical zeolite synthesis was in the particle size, where a significant decrease was observed being the addition of APTES to the biosurfactant molecules a crucial factor in decreasing the material particle size.

Therefore, the use of rhamnolipids and sophorolipids in hierarchical Y zeolite synthesis was accomplished. Both biosurfactants proved to induce the formation of mesopores, becoming a green alternative to the classical synthesis routes and opening a new application field for rhamnolipids and sophorolipids biosurfactants.

4.1 FUTURE OUTLOOKS

The synthesis of hierarchical zeolites using biosurfactants as structure-directing agents is still in its beginning. Biosurfactant production is increasing over time, and different biosurfactants are isolated and available for use in various applications, material synthesis is

one of them, where future efforts should be applied in this field, aiming to evaluate the influence of the biosurfactant self-aggregation structures in their induced porous structures, and suggests nucleation and crystal growth mechanisms, induced by biosurfactants micelles in the synthesis process, since the results obtained in this study showed a major influence of biosurfactants in particles sizes, leading to believe that nucleation and crystal growth mechanisms are affected by biosurfactant molecules. Regarding pore formation, different techniques could be applied, looking to improve the interaction between biosurfactants and zeolites building blocks (e. g. silica and alumina), which will lead to different pore structure organization and possibly direct the formation of different types of zeolites.

Hierarchical zeolites could be applied in different fields and have been studied by researchers around the world. bringing benefits regarding mass transportation inside zeolite pores. Regarding oil industry, hierarchical zeolites could be applied as improved catalysts on fluid catalytic cracking processes, being also able to act as adsorbents, and ion exchangers, where the pore interconnectivity induced by the utilization of biosurfactants as structure-directing agents could improve mass transport diffusivity on hierarchical zeolite materials and, therefore, longer deactivation times enable the utilization of green synthesis routes for obtaining these materials.

REFERENCES

ABBASI, Habib *et al.* Physicochemical characterization of a monorhamnolipid secreted by Pseudomonas aeruginosa MA01 in aqueous media. An experimental and molecular dynamics study. **Colloids and Surfaces B: Biointerfaces**, v. 101, p. 256–265, 2013. Disponível em: http://dx.doi.org/10.1016/j.colsurfb.2012.06.035.

ABELLÓ, Sònia; BONILLA, Adriana; PÉREZ-RAMÍREZ, Javier. Mesoporous ZSM-5 zeolite catalysts prepared by desilication with organic hydroxides and comparison with NaOH leaching. **Applied Catalysis A: General**, v. 364, n. 1–2, p. 191–198, 2009.

AL-JUBOURI, Sama M. Synthesis of hierarchically porous ZSM-5 zeolite by self-assembly induced by aging in the absence of seeding-assistance. **Microporous and Mesoporous Materials**, v. 303, n. April, p. 110296, 2020. Disponível em: https://doi.org/10.1016/j.micromeso.2020.110296.

ANTONELLI, David M.; YING, Jackie Y. Synthesis of Hexagonally Packed Mesoporous TiO2 by a Modified Sol–Gel Method. **Angewandte Chemie International Edition in English**, v. 34, n. 18, p. 2014–2017, 1995.

ARAÚJO, Hélvia W.C. *et al.* Sustainable biosurfactant produced by Serratia marcescens UCP 1549 and its suitability for agricultural and marine bioremediation applications. **Microbial Cell Factories**, v. 18, n. 1, p. 1–13, 2019. Disponível em: https://doi.org/10.1186/s12934-018-1046-0.

ATTARD, George S.; GLYDE, Joanna C.; GOLTNER G., Christine. Liquid_crystalline phases as templates or the synthesis of mesoporous silicas. **Nature**, v. 378, n. 7, p. 603–605, 1995.

BAGSHAW, Stephen A.; PINNAVAIA, Thomas J. Mesoporous Alumina Molecular Sieves. **Angewandte Chemie (International Edition in English)**, v. 35, n. 10, p. 1102–1105, 1996.

BAHRI, Mohamed A. *et al.* Investigation of SDS, DTAB and CTAB micelle microviscosities by electron spin resonance. **Colloids and Surfaces A: Physicochemical and Engineering Aspects**, v. 290, n. 1–3, p. 206–212, 2006.

BANAT, I. M. Characterization of biosurfactants and their use in pollution removal – State of the Art. (Review). **Acta Biotechnologica**, v. 15, n. 3, p. 251–267, 1995.

BANAT, Ibrahim M. *et al.* Cost effective technologies and renewable substrates for biosurfactants' production. **Frontiers in Microbiology**, v. 5, n. DEC, p. 1–18, 2014.

BARDESTANI, Raoof; PATIENCE, Gregory S.; KALIAGUINE, Serge. Experimental methods in chemical engineering: specific surface area and pore size distribution measurements—BET, BJH, and DFT. **Canadian Journal of Chemical Engineering**, v. 97, n. 11, p. 2781–2791, 2019.

BENVENUTTI, Edilson V; MORO, Celso C; GALLAS, Marcia R. MATERIAIS HÍBRIDOS À BASE DE SÍLICA OBTIDOS PELO MÉTODO SOL-GEL. **Química Nova**, v. 32, n. 7, p. 1926–1933, 2009.

BOFFA, Vittorio *et al.* A Waste-Derived Biosurfactant for the Preparation of Templated Silica Powders. **ChemSusChem**, v. 3, p. 445–452, 2010.

BOFFA, Vittorio *et al.* Role of a waste-derived polymeric biosurfactant in the sol – gel synthesis of nanocrystalline titanium dioxide. **Ceramics International**, v. 40, p. 12161–12169, 2014.

BOGNOLO, G. Biosurfactants as emulsifying agents for hydrocarbons. **Colloids and Surfaces A: Physicochemical and Engineering Aspects**, v. 152, n. 1–2, p. 41–52, 1999.

BORDOLOI, N. K.; KONWAR, B. K. Microbial surfactant-enhanced mineral oil recovery under laboratory conditions. **Colloids and Surfaces B: Biointerfaces**, v. 63, n. 1, p. 73–82, 2008.

BOTELLA, Pablo; CORMA, Avelino; QUESADA, Manuel. Synthesis of ordered mesoporous silica templated with biocompatible surfactants and applications in controlled release of drugs. **Journal of Materials Chemistry**, v. 22, n. 13, p. 6394–6401, 2012.

BRANDENBURG, Klaus; SEYDEL, Ulrich. Infrared spectroscopy of glycolipids. **Chemistry and Physics of Lipids**, v. 96, n. 1–2, p. 23–40, 1998.

BUSZEWSKI, B.; JEZIERSKA-ŚWITAŁA, M.; KOWALSKA, S. Stationary phase with specific surface properties for the separation of estradiol diastereoisomers. **Journal of Chromatography B: Analytical Technologies in the Biomedical and Life Sciences**, v. 792, n. 2, p. 279–286, 2003.

CANLAS, Christian P.; PINNAVAIA, Thomas J. Bio-derived oleyl surfactants as porogens for the sustainable synthesis of micelle-templated mesoporous silica. **RSC Advances**, v. 2, n. 19, p. 7449–7455, 2012.

CHAIKITTISILP, Watcharop *et al.* Formation of Hierarchically Organized Zeolites by Sequential Intergrowth. **Angewandte Chemie**, v. 125, n. 12, p. 3439–3443, 2013.

CHAL, Robin *et al.* Pseudomorphic synthesis of mesoporous zeolite y crystals. **Chemical Communications**, v. 46, n. 41, p. 7840–7842, 2010.

CHANG, Alex C C *et al.* In-Situ Infrared Study of CO 2 Adsorption on SBA-15 Grafted with. **Energy and Fuels**, v. 17, n. 11, p. 468–473, 2003.

CHEN, Chao *et al.* Amine–silica composites for CO2 capture: A short review. **Journal of Energy Chemistry**, v. 26, n. 5, p. 868–880, 2017. Disponível em: https://doi.org/10.1016/j.jechem.2017.07.001.

CHEN, Li Hua *et al.* Hierarchically structured zeolites: Synthesis, mass transport properties and applications. **Journal of Materials Chemistry**, v. 22, n. 34, p. 17381–17403, 2012.

CHOI, Minkee *et al.* Amphiphilic organosilane-directed synthesis of crystalline zeolite with tunable mesoporosity. **Nature Materials**, v. 5, n. 9, p. 718–723, 2006.

CHOI, Sunho *et al.* Layered silicates by swelling of AMH-3 and nanocomposite membranes. **Angewandte Chemie - International Edition**, v. 47, n. 3, p. 552–555, 2008.

CHOI, Minkee *et al.* Stable single-unit-cell nanosheets of zeolite MFI as active and long-lived catalysts. **Nature**, v. 461, n. 7261, p. 246–249, 2009.

CHONG, Huiqing; LI, Qingxin. Microbial production of rhamnolipids: Opportunities, challenges and strategies. **Microbial Cell Factories**, v. 16, n. 1, p. 1–12, 2017.

CHRISTENSEN, Claus Hviid *et al.* Mesoporous zeolite single crystal catalysts: Diffusion and catalysis in hierarchical zeolites. **Catalysis Today**, v. 128, n. 3-4 SPEC. ISS., p. 117–122, 2007.

CONATO, Marlon T. *et al.* Framework stabilization of Si-rich LTA zeolite prepared in organic-free media. **Chemical Communications**, v. 51, n. 2, p. 269–272, 2015.

COOPER, D. G.; PADDOCK, D. A. Production of a biosurfactant from Torulopsis bombicola. **Applied and Environmental Microbiology**, v. 47, n. 1, p. 173–176, 1984.

CORMA, A. *et al.* Delaminated zeolites: Combining the benefits of zeolites and mesoporous materials for catalytic uses. **Journal of Catalysis**, v. 186, n. 1, p. 57–63, 1999.

CORMA, Avelino. State of the art and future challenges of zeolites as catalysts. **Journal of Catalysis**, v. 216, n. 1–2, p. 298–312, 2003.

CUOQ, Fabrice *et al.* Preparation of amino-functionalized silica in aqueous conditions. **Applied Surface Science**, v. 266, p. 155–160, 2013. Disponível em: http://dx.doi.org/10.1016/j.apsusc.2012.11.120.

DA ROCHA JUNIOR, Rivaldo B. *et al.* Application of a low-cost biosurfactant in heavy metal remediation processes. **Biodegradation**, v. 30, n. 4, p. 215–233, 2019. Disponível em: https://doi.org/10.1007/s10532-018-9833-1.

DABBAWALA, Aasif A *et al.* Synthesis of hierarchical porous Zeolite-Y for enhanced CO 2 capture. **Microporous and Mesoporous Materials**, v. 303, n. April, p. 110261, 2020. Disponível em: https://doi.org/10.1016/j.micromeso.2020.110261.

DARDOURI, Maïssa *et al.* Using plasma-mediated covalent functionalization of rhamnolipids on polydimethylsiloxane towards the antimicrobial improvement of catheter surfaces. **Materials Science and Engineering C**, v. 134, p. 112563, 2021. Disponível em: https://doi.org/10.1016/j.msec.2021.112563.

DARVISHI, Parviz *et al.* Biosurfactant production under extreme environmental conditions by an efficient microbial consortium, ERCPPI-2. **Colloids and Surfaces B: Biointerfaces**, v. 84, n. 2, p. 292–300, 2011. Disponível em: http://dx.doi.org/10.1016/j.colsurfb.2011.01.011.

DATTA, Poulami; TIWARI, Pankaj; PANDEY, Lalit M. Isolation and characterization of biosurfactant producing and oil degrading Bacillus subtilis MG495086 from formation water of Assam oil reservoir and its suitability for enhanced oil recovery. **Bioresource Technology**, v. 270, n. September, p. 439–448, 2018. Disponível em: https://doi.org/10.1016/j.biortech.2018.09.047.

DAVEREY, Achlesh; PAKSHIRAJAN, Kannan. Production, characterization, and properties of sophorolipids from the yeast Candida bombicola using a low-cost fermentative medium. **Applied Biochemistry and Biotechnology**, v. 158, n. 3, p. 663–674, 2009.

DE ALMEIDA, Darne G. *et al.* Biosurfactants: Promising molecules for petroleum biotechnology advances. **Frontiers in Microbiology**, v. 7, n. OCT, p. 1–14, 2016.

DÉJUGNAT, Christophe; DIAT, Olivier; ZEMB, Thomas. Surfactin self-assembles into direct and reverse aggregates in equilibrium and performs selective metal cation extraction. **ChemPhysChem**, v. 12, n. 11, p. 2138–2144, 2011.

DELEU, Magali *et al.* Effects of surfactin on membrane models displaying lipid phase separation. **Biochimica et Biophysica Acta - Biomembranes**, v. 1828, n. 2, p. 801–815, 2013. Disponível em: http://dx.doi.org/10.1016/j.bbamem.2012.11.007.

DESAI, J D; BANAT, I M. Microbial production of surfactants and their commercial potential. **Microbiology and Molecular Biology Reviews**, v. 61, n. 1, p. 47–64, 1997.

DING, Kunlun *et al.* Constructing Hierarchical Porous Zeolites via Kinetic Regulation. **Journal of the American Chemical Society**, v. 137, n. 35, p. 11238–11241, 2015.

DOMÍNGUEZ RIVERA, Ángeles; MARTÍNEZ URBINA, Miguel Ángel; LÓPEZ Y LÓPEZ, Víctor Eric. Advances on research in the use of agro-industrial waste in biosurfactant

production. **World Journal of Microbiology and Biotechnology**, v. 35, n. 10, p. 1–18, 2019. Disponível em: https://doi.org/10.1007/s11274-019-2729-3.

DU, Xin; HE, Junhui. Amino-functionalized silica nanoparticles with center-radially hierarchical mesopores as ideal catalyst carriers. **Nanoscale**, v. 4, n. 3, p. 852–859, 2012.

DUBEY, Kirti V.; JUWARKAR, Asha A.; SINGH, S. K. Adsorption-desorption process using wood-based activated carbon for recovery of biosurfactant from fermented distillery wastewater. **Biotechnology Progress**, v. 21, n. 3, p. 860–867, 2005.

DUNPHY, Darren R. *et al.* Characterization of lipid-templated silica and hybrid thin film mesophases by grazing incidence small-angle X-ray scattering. **Langmuir**, v. 25, n. 16, p. 9500–9509, 2009.

DUTTA, Saikat; BHAUMIK, Asim; WU, Kevin C. Hierarchically porous carbon derived from polymers and biomass: effect of interconnected pores on energy applications. **Energy & Environmental Science**, v. 7, n. 11, p. 3445–3816, 2014.

EGLIN, David *et al.* Type I collagen, a versatile liquid crystal biological template for silica structuration from nano- to microscopic scales. **Soft Matter**, v. 1, n. 2, p. 129–131, 2005.

EJKA, Jiří; MORRIS, Russell E; NACHTIGALL, Petr. **Zeolites in Catalysis: Properties and Applications**. Royal Society of Chemistry, 2017.

ENTERRÍA, Marina *et al.* Preparation of hierarchical micro-mesoporous aluminosilicate composites by simple Y zeolite / MCM-48 silica assembly. **Journal of Alloys and Compounds**, v. 583, p. 60–69, 2014.

FELICZAK-GUZIK, Agnieszka. Hierarchical zeolites: Synthesis and catalytic properties. **Microporous and Mesoporous Materials**, v. 259, p. 33–45, 2018. Disponível em: https://doi.org/10.1016/j.micromeso.2017.09.030.

FLASZ, A. *et al.* comparative study of the toxicity of a synthetic surfactant and one produced by Pseudomonas aeruginosa ATCC 55925. **Medical Science Research**, v. 26, n. 3, p. 181–185, 1998.

FUKUOKA, Tokuma *et al.* The diastereomers of mannosylerythritol lipids have different interfacial properties and aqueous phase behavior, reflecting the erythritol configuration. **Carbohydrate Research**, v. 351, p. 81–86, 2012. Disponível em: http://dx.doi.org/10.1016/j.carres.2012.01.019.

GALARNEAU, Anne *et al.* Validity of the t - plot Method to Assess Microporosity in Hierarchical Micro / Mesoporous Materials. **Langmuir**, v. 30, p. 13266–13274, 2014.

GARCÍA-MARTÍNEZ, Javier *et al.* Mesostructured zeolite Y — high hydrothermal

stability and superior FCC catalytic performance w. **Catalysis Science & Technology**, v. 2, p. 987–994, 2012.

GÉRARDIN, Corine *et al.* Ecodesign of ordered mesoporous silica materials. **Chemical Society Reviews**,v. 42, n. 9, p. 4217–4255, 2013.

GIL, Barbara *et al.* High acidity unilamellar zeolite MCM-56 and its pillared and delaminated derivatives. **Journal of the Chemical Society. Dalton Transactions**, v. 43, n. 27, p. 10501–10511, 2014.

GOOSSENS, Eliane *et al.* Enhanced separation and analysis procedure reveals production of tri-acylated mannosylerythritol lipids by Pseudozyma aphidis. **Journal of Industrial Microbiology and Biotechnology**, v. 43, n. 11, p. 1537–1550, 2016.

GROEN, Johan C.; PEFFER, Louk A.A.; PÉREZ-RAMÍREZ, Javier. Pore size determination in modified micro- and mesoporous materials. Pitfalls and limitations in gas adsorption data analysis. **Microporous and Mesoporous Materials**, v. 60, n. 1–3, p. 1–17, 2003.

GU, Fang Na *et al.* New strategy to synthesis of hierarchical mesoporous zeolites. **Chemistry of Materials**, v. 22, n. 8, p. 2442–2450, 2010.

GUDIÑA, Eduardo J. *et al.* Biosurfactant production by Bacillus subtilis using corn steep liquor as culture medium. **Frontiers in Microbiology**, v. 6, n. FEB, p. 1–7, 2015.

HARLICK, Peter J.E.; SAYARI, Abdelhamid. Applications of pore-expanded mesoporous silica. 5. triamine grafted material with exceptional CO2 dynamic and equilibrium adsorption performance. **Industrial and Engineering Chemistry Research**, v. 46, n. 2, p. 446–458, 2007.

HARTMANN, Martin; MACHOKE, Albert Gonche; SCHWIEGER, Wilhelm. Catalytic test reactions for the evaluation of hierarchical zeolites. **Chemical Society Reviews**, v. 45, n. 12, p. 3313–3330, 2016. Disponível em: http://dx.doi.org/10.1039/C5CS00935A.

HATO, Masakatsu. Synthetic glycolipid/water systems. **Current Opinion in Colloid and Interface Science**, v. 6, n. 3, p. 268–276, 2001.

HAZRA, Chinmay *et al.* Ultrasonics Sonochemistry of nano-calcium sulfate with controllable crystal morphology. **Ultrasonics - Sonochemistry**, v. 21, n. 3, p. 1117–1131, 2014. Disponível em: http://dx.doi.org/10.1016/j.ultsonch.2013.12.020.

HENCH, Larry L.; WEST, Jon K. The sol-gel process. **Chemical Reviews**, v. 90, n. 1, p. 33–72, 1990. Disponível em: http://pubs.acs.org/doi/abs/10.1021/cr00099a003.

HOLLAND, Brian T.; ABRAMS, Lloyd; STEIN, Andreas. Dual templating of

macroporous silicates with zeolitic microporous frameworks. **Journal of the American Chemical Society**, v. 121, n. 17, p. 4308–4309, 1999.

HOLM, Martin Spangsberg; HANSEN, Martin Kalniar; CHRISTENSEN, Claus Hviid. "One-pot" Ion-exchange and mesopore formation during desilication. **European Journal of Inorganic Chemistry**, n. 9, p. 1194–1198, 2009.

HOLMBERG, K. *et al.* **Surfactants and polymers in aqueous solutions**. John Wiley ed.1, 2002-. ISSN 08837554.v. 2

HUANG, Helen Y. *et al.* Amine-grafted MCM-48 and silica xerogel as superior sorbents for acidic gas removal from natural gas. **Industrial and Engineering Chemistry Research**, v. 42, n. 12, p. 2427–2433, 2003.

HUO, Qisheng *et al.* Generalized synthesis of periodic surfactant/inorganic composite materials. **Nature**, v. 368, n. 6469, p. 317–321, 1994.

IMURA, Tomohiro *et al.* Aqueous-phase behavior of natural glycolipid biosurfactant mannosylerythritol lipid A: Sponge, cubic, and lamellar phases. **Langmuir**, v. 23, n. 4, p. 1659–1663, 2007.

INAYAT, Alexandra *et al.* Assemblies of mesoporous FAU-type zeolite nanosheets. **Angewandte Chemie - International Edition**, v. 51, n. 8, p. 1962–1965, 2012.

ISMAIL, A. A. *et al.* Synthesis of nanosized ZSM-5 using different alumina sources. **Crystal Research and Technology**, v. 41, n. 2, p. 145–149, 2006.

IVANOVA, Irina I. *et al.* Mechanistic study of zeolites recrystallization into micro-mesoporous materials. **Microporous and Mesoporous Materials**, v. 189, p. 163–172, 2014. Disponível em: http://dx.doi.org/10.1016/j.micromeso.2013.11.001.

IVANOVA, Irina I.; KNYAZEVA, Elena E. Micro-mesoporous materials obtained by zeolite recrystallization: Synthesis, characterization and catalytic applications. **Chemical Society Reviews**, v. 42, n. 9, p. 3671–3688, 2013.

JAHAN, Ruksana *et al.* Biosurfactants, natural alternatives to synthetic surfactants: Physicochemical properties and applications. **Advances in Colloid and Interface Science**, v. 275, p. 102061, 2020. Disponível em: https://doi.org/10.1016/j.cis.2019.102061.

JHA, Sujata S.; JOSHI, Sanket J.; GEETHA, S. J. Lipopeptide production by Bacillus subtilis R1 and its possible applications. **Brazilian Journal of Microbiology**, v. 47, n. 4, p. 955–964, 2016. Disponível em: http://dx.doi.org/10.1016/j.bjm.2016.07.006.

JIA, Xicheng *et al.* Modern synthesis strategies for hierarchical zeolites : Bottom-up versus top-down strategies. **Advanced Powder Technology**, v. 30, p. 467–484, 2019.

Disponível em: https://doi.org/10.1016/j.apt.2018.12.014.

JIMOH, Abdullahi Adekilekun; LIN, Johnson. Biosurfactant: A new frontier for greener technology and environmental sustainability. **Ecotoxicology and Environmental Safety**, v. 184, n. June, p. 109607, 2019. Disponível em: https://doi.org/10.1016/j.ecoenv.2019.109607.

JIN, Lei *et al.* Interaction of a biosurfactant, Surfactin with a cationic Gemini surfactant in aqueous solution. **Journal of Colloid and Interface Science**, v. 481, p. 201–209, 2016. Disponível em: http://dx.doi.org/10.1016/j.jcis.2016.07.044.

JOSHI, Sanket *et al.* Biosurfactant production using molasses and whey under thermophilic conditions. **Bioresource Technology**, v. 99, n. 1, p. 195–199, 2008.

KANNANGARA, Ishara *et al.* Synthesis and characterization of nano zeolite-A with aid of sodium dodecyl sulfate (SDS) as particle size-controlling agent. **Colloids and Surfaces A: Physicochemical and Engineering Aspects**, v. 589, n. January, p. 124427, 2020. Disponível em: https://doi.org/10.1016/j.colsurfa.2020.124427.

KHAN, Ali; MARQUES, Eduardo F. Synergism and polymorphism in mixed surfactant systems. **Current Opinion in Colloid and Interface Science**, v. 4, n. 6, p. 402–410, 1999.

KHOPADE, A. *et al.* Production and stability studies of the biosurfactant isolated from marine Nocardiopsis sp. B4. **Desalination**, v. 285, p. 198–204, 2012. Disponível em: http://dx.doi.org/10.1016/j.desal.2011.10.002.

KITAMOTO, Dai *et al.* Self-assembling properties of glycolipid biosurfactants and their potential applications. **Current Opinion in Colloid and Interface Science**, v. 14, n. 5, p. 315–328, 2009. Disponível em: http://dx.doi.org/10.1016/j.cocis.2009.05.009.

KULAKOVSKAYA, Ekaterina; KULAKOVSKAYA, Tatiana. Physicochemical Properties of Yeast Extracellular Glycolipids. *In*: EXTRACELLULAR GLYCOLIPIDS OF YEASTS. MA, USA: Academic Press, 2014. p. 29–34.

LEBRÓN-PALER, Ariel *et al.* Determination of the acid dissociation constant of the biosurfactant monorhamnolipid in aqueous solution by potentiometric and spectroscopic methods. **Analytical Chemistry**, v. 78, n. 22, p. 7649–7658, 2006.

LEE, Seungju; SHANTZ, Daniel F. Zeolite growth in nonionic microemulsions: Synthesis of hierarchically structured zeolite particles. **Chemistry of Materials**, v. 17, n. 2, p. 409–417, 2005.

LI, Kunhao; VALLA, Julia; GARCIA-MARTINEZ, Javier. Realizing the commercial

potential of hierarchical zeolites: New opportunities in catalytic cracking. **ChemCatChem**, v. 6, n. 1, p. 46–66, 2014.

LOWELL, S. *et al.* **Characterization of Porous Solids and Powders: Surface Area, Pore Size and Density**. 1st. ed. Dordrecht, Netherlands: Kluwer Academic Publishers, P.O. Box 17,3300 AA Dordrecht, The Netherlands., 2004.

LV, Kaihe *et al.* Modified Biosurfactant Cationic Alkyl Polyglycoside as an Effective Additive for Inhibition of Highly Reactive Shale. **Energy and Fuels**, v. 34, n. 2, p. 1680–1687, 2020.

MACHOKE, Albert G. *et al.* Micro/macroporous system: MFI-type zeolite crystals with embedded macropores. **Advanced Materials**, v. 27, n. 6, p. 1066–1070, 2015.

MAKKAR, Randhir S.; CAMEOTRA, Swaranjit S.; BANAT, Ibrahim M. Advances in utilization of renewable substrates for biosurfactant production. **AMB Express**, v. 1, n. 1, p. 1–19, 2011.

MALDONADO, Miguel *et al.* Controlling Crystal Polymorphism in Organic-Free Synthesis of Na- Zeolites. **Journal of the American Chemical Society**, v. 135, p. 2641–2652, 2013.

MALLETTE, Adam J *et al.* Heteroatom Manipulation of Zeolite Crystallization: Stabilizing Zn- FAU against Interzeolite Transformation. **Journal of the American Chemical Society**, v. 2, p. 2295–2306, 2022.

MARCELINO, Paulo Ricardo Franco *et al.* Biosurfactants produced by Scheffersomyces stipitis cultured in sugarcane bagasse hydrolysate as new green larvicides for the control of Aedes aegypti, a vector of neglected tropical diseases. **PLoS ONE**, p. 1–16, 2017.

MARKANDE, A R; ACHARYA, S R; NERURKAR, A S. Physicochemical characterization of a thermostable glycoprotein bioemulsifier from Solibacillus silvestris AM1. **Process Biochemistry**, v. 48, n. 11, p. 1800–1808, 2013. Disponível em: http://dx.doi.org/10.1016/j.procbio.2013.08.017.

MARTINS, Angela *et al.* Friedel-Crafts acylation reaction over hierarchical Y zeolite modified through surfactant mediated technology. **Microporous and Mesoporous Materials**, v. 323, n. April, p. 1–8, 2021.

MASTROPIETRO, T. F.; DRIOLI, E.; POERIO, T. Low temperature synthesis of nanosized NaY zeolite crystals from organic-free gel by using supported seeds. **RSC Advances**, v. 4, n. 42, p. 21951–21957, 2014.

MEI, Jinlin; DUAN, Aijun; WANG, Xilong. A brief review on solvent-free synthesis

of zeolites. **Materials**, v. 14, n. 4, p. 1–13, 2021.

MEYNEN, V.; COOL, P.; VANSANT, E. F. Verified syntheses of mesoporous materials. **Microporous and Mesoporous Materials**, v. 125, n. 3, p. 170–223, 2009. Disponível em: http://dx.doi.org/10.1016/j.micromeso.2009.03.046.

MIAO, Zhenjiang *et al.* Fabrication of 3D-networks of native starch and their application to produce porous inorganic oxide networks through a supercritical route. **Microporous and Mesoporous Materials**, v. 111, n. 1–3, p. 104–109, 2008.

MOLINER, Manuel; MARTÍNEZ, Cristina; CORMA, Avelino. Multipore zeolites: Synthesis and catalytic applications. **Angewandte Chemie - International Edition**, v. 54, n. 12, p. 3560–3579, 2015.

MONTONERI, Enzo *et al.* Biosurfactants from Urban Green Waste. **Chemsuschem**, v. 2, p. 239–247, 2009.

MORALES-PACHECO, P. *et al.* Synthesis and structural properties of zeolitic nanocrystals II: FAU-type zeolites. **Journal of Physical Chemistry,** v. 113, n. 6, p. 2247–2255, 2009.

MULLIGAN, Catherine N. Environmental applications for biosurfactants. **Environmental Pollution**, v. 133, n. 2, p. 183–198, 2005.

MULLIGAN, C. N.; GIBBS, B. F. Correlation of nitrogen metabolism with biosurfactant production by Pseudomonas aeruginosa. **Applied and Environmental Microbiology**, v. 55, n. 11, p. 3016–3019, 1989.

NIE, Pengfei *et al.* Quaternary ammonium cellulose promoted synthesis of hollow nano-sized ZSM-5 zeolite as stable catalyst for benzene alkylation with ethanol. **Journal of Materials Science**, v. 56, n. 14, p. 8461–8478, 2021. Disponível em: https://doi.org/10.1007/s10853-021-05856-8.

NITSCHKE, Marcia; COSTA, Siddhartha G.V.A.O.; CONTIERO, Jonas. Rhamnolipid surfactants: An update on the general aspects of these remarkable biomolecules. **Biotechnology Progress**, v. 21, n. 6, p. 1593–1600, 2005.

NITSCHKE, Marcia; COSTA, Siddhartha G.V.A.O.; CONTIERO, Jonas. Structure and applications of a rhamnolipid surfactant produced in soybean oil waste. **Applied Biochemistry and Biotechnology**, v. 160, n. 7, p. 2066–2074, 2010.

NITSCHKE, Marcia; PASTORE, Gláucia Maria. Biossurfactantes: Propriedades e aplicações. **Quimica Nova**, v. 25, n. 5, p. 772–776, 2002.

NUMATA, Munenori *et al.* Sol–Gel Reaction Using DNA as a Template: An Attempt

Toward Transcription of DNA into Inorganic Materials. **Angewandte Chemie**, v. 116, n. 25, p. 3341–3345, 2004.

ONBASLI, D.; ASLIM, B. Determination of rhamnolipid biosurfactant production in molasses by some Pseudomonas spp. **New Biotechnology**, v. 25, p. S255, 2009.

OSMAN, M.; HØILAND, H.; HOLMSEN, H. Micropolarity and microviscosity in the micelles of the heptapeptide biosurfactant "surfactin". **Colloids and Surfaces B: Biointerfaces**, [*s. l.*], v. 11, n. 4, p. 167–175, 1998.

PACWA-PŁOCINICZAK, Magdalena *et al.* Environmental applications of biosurfactants: Recent advances. **International Journal of Molecular Sciences**, v. 12, n. 1, p. 633–654, 2011.

PANEK, Rafal; WDOWIN, Magdalena; FRANUS, Wojciech. The Use of Scanning Electron Microscopy to Identify Zeolite Minerals. *In*: POLYCHRONIADIS, Efstathios K.; ORAL, Ahmet Yavuz; OZER, Mehmet (org.). **Springer Proceedings in Physics**. Springer International Publishing, 2014. v. 154, p. 45–50.

PAQUIN, Francis *et al.* Multi-phase semicrystalline microstructures drive exciton dissociation in neat plastic semiconductors. **J. Mater. Chem. C**, v. 3, p. 10715–10722, 2015. Disponível em: http://xlink.rsc.org/?DOI=C5TC02043C.

PARK, Woojin *et al.* Hierarchically structure-directing effect of multi-ammonium surfactants for the generation of MFI zeolite nanosheets. **Chemistry of Materials**, v. 23, n. 23, p. 5131–5137, 2011.

PAWOLSKI, Damian *et al.* Reconstituting the formation of hierarchically porous silica patterns using diatom biomolecules. **Journal of Structural Biology**, v. 204, n. 1, p. 64–74, 2018. Disponível em: https://doi.org/10.1016/j.jsb.2018.07.005.

PEDOTT, Victor De Aguiar *et al.* Biosurfactants as structure directing agents of porous siliceous materials. **Microporous and Mesoporous Materials**, v. 345, n. October, p. 112279, 2022. Disponível em: https://doi.org/10.1016/j.micromeso.2022.112279.

PERFUMO, A. *et al.* Production and Roles of Biosurfactants and Bioemulsifiers in Accessing Hydrophobic Substrates. *In*: TIMMIS, Kenneth N. (org.). **Handbook of Hydrocarbon and Lipid Microbiology**. 1. ed. Springer Berlin Heidelberg, 2010. p. 4699.

PORNSUNTHORNTAWEE, Orathai; CHAVADEJ, Sumaeth; RUJIRAVANIT, Ratana. Solution properties and vesicle formation of rhamnolipid biosurfactants produced by Pseudomonas aeruginosa SP4. **Colloids and Surfaces B: Biointerfaces**, v. 72, n. 1, p. 6–15, 2009.

PRASOMSRI, Teerawit *et al.* Mesostructured zeolites: Bridging the gap between zeolites and MCM-41. **Chemical Communications**, v. 51, n. 43, p. 8900–8911, 2015.

RAMOS DA SILVA, Anderson *et al.* Rhamnolipids functionalized with basic amino acids: Synthesis, aggregation behavior, antibacterial activity and biodegradation studies. **Colloids and Surfaces B: Biointerfaces**, v. 181, n. May, p. 234–243, 2019. Disponível em: https://doi.org/10.1016/j.colsurfb.2019.05.037.

RASHEDI, H. *et al.* Isolation and production of biosurfactant from Pseudomonas aeruginosa isolated from Iranian southern wells oil. **Int. J. Environ. Sci. Tech.**, v. 2, n. 5, p. 121–127, 2005.

RATH, Dharitri; RANA, Surjyakanta; PARIDA, K. M. Organic amine-functionalized silica-based mesoporous materials: An update of syntheses and catalytic applications. **RSC Advances**, v. 4, n. 100, p. 57111–57124, 2014.

RAZA, Zulfiqar A.; KHALID, Zafar M.; BANAT, Ibrahim M. Characterization of rhamnolipids produced by a Pseudomonas aeruginosa mutant strain grown on waste oils. **Journal of Environmental Science and Health - Part A Toxic/Hazardous Substances and Environmental Engineering**, v. 44, n. 13, p. 1367–1373, 2009.

RAZA, Zulfiqar A.; KHAN, Muhammad S.; KHALID, Zafar M. Physicochemical and surface-active properties of biosurfactant produced using molasses by a Pseudomonas aeruginosa mutant. **Journal of Environmental Science and Health - Part A Toxic/Hazardous Substances and Environmental Engineering**, v. 42, n. 1, p. 73–80, 2007.

RIBEIRO, Jéssicade O. N. *et al.* Role of the type of grafting solvent and its removal process on APTES functionalization onto SBA-15 silica for CO2 adsorption. **Journal of Porous Materials**, v. 26, n. 6, p. 1581–1591, 2019. Disponível em: https://doi.org/10.1007/s10934-019-00754-6.

ROBAK, Maryann T.; HERBAGE, Melissa A.; ELLMAN, Jonathan A. Synthesis and applications of tert -butanesulfinamide. **Chemical Reviews**, v. 110, n. 6, p. 3600–3740, 2010.

ROTH, Wieslaw J. *et al.* Layer like porous materials with hierarchical structure. **Chemical Society Reviews**, v. 45, n. 12, p. 3400–3438, 2016.

ROTH, W. J. *et al.* MCM-36: The first pillared molecular sieve with zeoliteproperties. **Studies in Surface Science and Catalysis**, v. 94, n. C, p. 301–308, 1995.

ROTH, Wieslaw J. *et al.* Swelling and Interlayer Chemistry of Layered MWW Zeolites MCM-22 and MCM-56 with High Al Content. **Chemistry of Materials**, v. 27, n. 13, p. 4620–4629, 2015.

SACHSE, Alexander; GARCÍA-MARTÍNEZ, Javier. Surfactant-Templating of Zeolites: From Design to Application. **Chemistry of Materials**, v. 29, n. 9, p. 3827–3853, 2017.

SANTOS, Danyelle Khadydja F. *et al.* Biosurfactants: Multifunctional biomolecules of the 21st century. **International Journal of Molecular Sciences**, v. 17, n. 3, p. 1–31, 2016.

SARAVANAN, P. *et al.* Twin Applications of Tetra-Functional Epoxy Monomers for Anticorrosion and Antifouling Studies. **Silicon**, v. 10, n. 2, p. 555–565, 2018. Disponível em: http://dx.doi.org/10.1007/s12633-016-9489-6.

SARAVANAN, Varadharajan; VIJAYAKUMAR, Subramaniyan. Malaysian Journal of Microbiology. **Malaysian Journal of Microbiology**, v. 9, n. 2, p. 166–175, 2013. Disponível em: http://web.usm.my/mjm/issues/vol9no4/Short 2.pdf.

SATPUTE, Surekha K. *et al.* Biosurfactants, bioemulsifiers and exopolysaccharides from marine microorganisms. **Biotechnology Advances**, v. 28, n. 4, p. 436–450, 2010. Disponível em: http://dx.doi.org/10.1016/j.biotechadv.2010.02.006.

SCHAWANKE, Anderson Joel; BALZER, Rosana; PERGHER, Sibele. Microporous and Mesoporous Materials from Natural and Inexpensive Sources. **Handbook of Ecomaterials**, v. 1, p. 1–3773, 2017.

SCHWANKE, Anderson Joel; PERGHER, Sibele. Handbook of Ecomaterials. **Handbook of Ecomaterials**, n. February 2018, 2020.

SELVAM, Thangaraj; INAYAT, Alexandra; SCHWIEGER, Wilhelm. Reactivity and applications of layered silicates and layered double hydroxides. **Dalton Transactions**, v. 43, n. 27, p. 10365–10387, 2014.

SHAH, Pallavi *et al.* Structural features of Penicillin acylase adsorption on APTES functionalized SBA-15. **Microporous and Mesoporous Materials**, v. 116, n. 1–3, p. 157–165, 2008. Disponível em: http://dx.doi.org/10.1016/j.micromeso.2008.03.030.

SHARMA, Raju Kumar *et al.* A novel BMSN (biologically synthesized mesoporous silica nanoparticles) material: Synthesis using a bacteria-mediated biosurfactant and characterization. **RSC Advances**, v. 11, n. 52, p. 32906–32916, 2021.

SHI, Yifeng; WAN, Ying; ZHAO, Dongyuan. Ordered mesoporous non-oxide materials. **Chemical Society Reviews**, v. 40, n. 7, p. 3854–3878, 2011.

SHVETS, O. V.; KONYSHEVA, K. M.; KURMACH, M. M. Morphology and Catalytic Properties of Hierarchical Zeolites with MOR, BEA, MFI, and MTW Topology. **Theoretical and Experimental Chemistry**, v. 54, n. 2, p. 138–145, 2018.

SILVA, S. N.R.L. *et al.* Glycerol as substrate for the production of biosurfactant by Pseudomonas aeruginosa UCP0992. **Colloids and Surfaces B: Biointerfaces**, v. 79, n. 1, p. 174–183, 2010. Disponível em: http://dx.doi.org/10.1016/j.colsurfb.2010.03.050.

SÖDERMAN, Olle; JOHANSSON, Ingegärd. Polyhydroxyl-based surfactants and their physico-chemical properties and applications. **Current Opinion in Colloid and Interface Science**, v. 4, n. 6, p. 391–401, 1999.

SOLER-ILLIA, Galo J.De A.A. *et al.* Chemical strategies to design textured materials: From microporous and mesoporous oxides to nanonetworks and hierarchical structures. **Chemical Reviews**, v. 102, n. 11, p. 4093–4138, 2002.

SOUZA, Ellen Cristina; VESSONI-PENNA, Thereza Christina; DE SOUZA OLIVEIRA, Ricardo Pinheiro. Biosurfactant-enhanced hydrocarbon bioremediation: An overview. **International Biodeterioration and Biodegradation**, v. 89, p. 88–94, 2014. Disponível em: http://dx.doi.org/10.1016/j.ibiod.2014.01.007.

STOJKOVIC, S. R.; ADNADJEVIC, B. Investigation of the NaA zeolite crystallization mechanism by i.r. spectroscopy. **Zeolites**, v. 8, n. 6, p. 523–525, 1988.

SULIKOWSKI, Bogdan. The fractal dimension in molecular sieves: Synthetic faujasite and related solids. **Journal of Physical Chemistry**, v. 97, n. 7, p. 1420–1425, 1993.

SUN, Qiming; XIE, Zaiku; YU, Jihong. The state-of-the-art synthetic strategies for SAPO-34 zeolite catalysts in methanol-to-olefin conversion. **National Science Review**, v. 5, n. 4, p. 542–558, 2018.

TANEV, Peter T.; PINNAVAIA, Thomas J. A Neutral Templating Route to Mesoporous Molecular Sieves. **Science**, v. 267, n. 5, p. 1–6, 1995.

TANG, Yadan; LANDSKRON, Kai. CO2-sorption properties of organosilicas with bridging amine functionalities inside the framework. **Journal of Physical Chemistry C**, v. 114, n. 6, p. 2494–2498, 2010.

THOMAS, Bejoy *et al.* Mesostructured silica from amino acid-based surfactant formulations and sodium silicate at neutral pH. **Journal of Sol-Gel Science and Technology**, v. 58, n. 1, p. 170–174, 2011.

THOMAS, Bejoy *et al.* One-Step Introduction of Broad-Band Mesoporosity in Silica Particles Using a Stimuli-Responsive Bioderived Glycolipid. **ACS Sustainable Chemistry and Engineering**, v. 2, p. 512–522, 2014.

THOMMES, Matthias *et al.* Physisorption of gases, with special reference to the evaluation of surface area and pore size distribution (IUPAC Technical Report). **Pure and**

Applied Chemistry, v. 87, n. 9–10, p. 1051–1069, 2015.

TONDRE, Christian; CAILLET, Céline. Properties of the amphiphilic films in mixed cationic/anionic vesicles: A comprehensive view from a literature analysis. **Advances in Colloid and Interface Science**, v. 93, n. 1–3, p. 115–134, 2001.

UAD, I *et al.* Biodegradative potential and characterization of bioemulsi fi ers of marine bacteria isolated from samples of seawater , sediment and fuel extracted at 4000 m of depth (Prestige wreck). **International Biodeterioration & Biodegradation**, v. 64, n. 6, p. 511–518, 2010. Disponível em: http://dx.doi.org/10.1016/j.ibiod.2010.06.005.

VAN OERS, C. J. *et al.* Formation of a combined micro- and mesoporous material using zeolite Beta nanoparticles. **Microporous and Mesoporous Materials**, v. 120, n. 1–2, p. 29–34, 2009. Disponível em: http://dx.doi.org/10.1016/j.micromeso.2008.08.056.

VANDENBERG, Elaine T. *et al.* Structure of 3-aminopropyl triethoxy silane on silicon oxide. **Journal of Colloid And Interface Science**, v. 147, n. 1, p. 103–118, 1991.

VARJANI, Sunita J; UPASANI, Vivek N. Critical review on biosurfactant analysis, purification and characterization using rhamnolipid as a model biosurfactant. **Bioresource Technology**, v. 232, p. 389–397, 2017.

VERBOEKEND, Danny; MITCHELL, Sharon; PÉREZ-RAMÍREZ, Javier. Hierarchical Zeolites Overcome all Obstacles : Next Stop Industrial Implementation. **Chimia**, v. 67, n. 5, p. 327–332, 2013.

VERMEIREN, W; GILSON, J. P. Impact of Zeolites on the Petroleum and Petrochemical Industry. **Topics in Catalysis**, v. 52, p. 1131–1161, 2009.

VU, Hue-tong; HARTH, Florian M; WILDE, Nicole. Silylated Zeolites With Enhanced Hydrothermal Stability for the Aqueous-Phase Hydrogenation of Levulinic Acid to γ -Valerolactone. **Frontiers in Chemistry**, v. 6, n. 143, p. 1–9, 2018.

WAN, W. *et al.* Transmission electron microscopy as an important tool for characterization of zeolite structures. **Inorganic Chemistry Frontiers**, v. 5, n. 11, p. 2836–2855, 2018.

WAN, Ying; ZHAO, Dongyuan. On the Controllable Soft-Templating Approach to Mesoporous Silicates. **Chemical Reviews**, v. 107, n. 7, p. 2821–2860, 2007.

WANG, Chunfeng *et al.* Evaluation of zeolites synthesized from fly ash as potential adsorbents for wastewater containing heavy metals. **Journal of Environmental Sciences**, v. 21, n. 1, p. 127–136, 2009. Disponível em: http://dx.doi.org/10.1016/S1001-0742(09)60022-X.

WANG, Tongwen *et al.* Templating behavior of a long-chain ionic liquid in the

hydrothermal synthesis of mesoporous silica. **Langmuir**, v. 23, n. 3, p. 1489–1495, 2007.

WHANG, Liang-ming *et al.* Application of biosurfactants , rhamnolipid , and surfactin , for enhanced biodegradation of diesel-contaminated water and soil. **Journal of Hazardous Materials**, v. 151, p. 155–163, 2008.

WIDJONARKO, Dian Maruto *et al.* Phosphonate modified silica for adsorption of Co(II), Ni(II), Cu(II), and Zn(II). **Indonesian Journal of Chemistry**, v. 14, n. 2, p. 143–151, 2014.

WU, Yuan Seng *et al.* Anticancer activities of surfactin potential application of nanotechnology assisted surfactin delivery. **Frontiers in Pharmacology**, v. 8, n. OCT, p. 1–22, 2017.

XU, Ruren *et al.* **Chemistry of Zeolites and Related Porous Materials: Synthesis and Structure**. John Wiley & Sons, 2009.

YAN, Ping *et al.* Bioresource Technology Oil recovery from refinery oily sludge using a rhamnolipid biosurfactant-producing Pseudomonas. **Bioresource Technology**, v. 116, p. 24–28, 2012. Disponível em: http://dx.doi.org/10.1016/j.biortech.2012.04.024.

ZANOTTO, Aline Wasem *et al.* New sustainable alternatives to reduce the production costs for surfactin 50 years after the discovery. **Applied Microbiology and Biotechnology**, v. 103, n. 21–22, p. 8647–8656, 2019.

ZHANG, Lei *et al.* Synthesis and interfacial properties of sophorolipid derivatives. **Colloids and Surfaces A: Physicochemical and Engineering Aspects**, v. 240, n. 1–3, p. 75–82, 2004.

ZHANG, Baojian; DAVIS, Sean A.; MANN, Stephen. Starch gel templating of spongelike macroporous silicalite monoliths and mesoporous films. **Chemistry of Materials**, v. 14, n. 3, p. 1369–1375, 2002.

ZHAO, Jun *et al.* Synthesis and characterization of mesoporous zeolite Y by using block copolymers as templates. **Chemical Engineering Journal**, v. 284, p. 405–411, 2016. Disponível em: http://dx.doi.org/10.1016/j.cej.2015.08.143.

ZHU, Haibo *et al.* Nanosized CaCO3 as hard template for creation of intracrystal pores within silicalite-1 crystal. **Chemistry of Materials**, v. 20, n. 3, p. 1134–1139, 2008.

ZHU, Kake; EGEBLAD, Kresten; CHRISTENSEN, Claus Hviid. Mesoporous carbon prepared from carbohydrate as hard template for hierarchical zeolites. **European Journal of Inorganic Chemistry**, n. 25, p. 3955–3960, 2007.